An International Journal of Analytical Chemistry

ταλαντα

talanta

PERGAMON PRESS
OXFORD • LONDON • NEW YORK • PARIS

1971 VOLUME 18, NO. 2 FEBRUARY

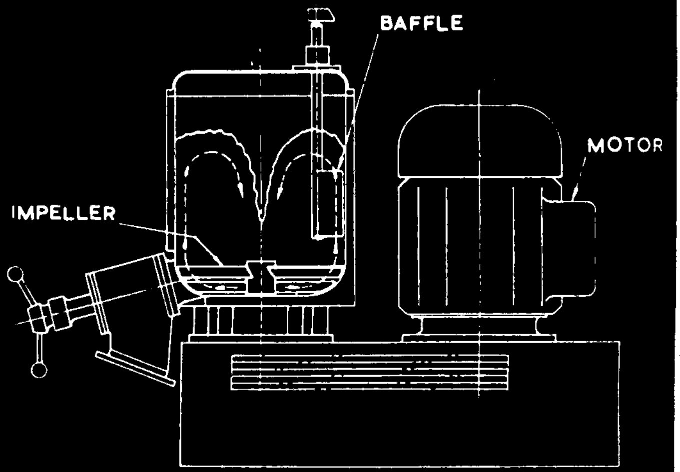
BAFFLE
MOTOR
IMPELLER

Talanta

An International Journal of Analytical Chemistry

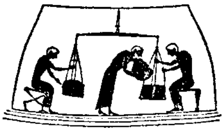

The illustration of a Greek balance from one of the Hope Vases is reproduced here by kind permi
of Cambridge University Press

Editor-in-Chief

DR.R.A.CHALMERS, Department of Chemistry, University of Aberdeen, Old Aberdeen, Scotland

Assistant Editors

DR.D.BETTERIDGE, University College, Swansea, Wales
DR.J.R.MAJER, University of Birmingham, England
DR.I.L.MARR, University of Aberdeen, Scotland

Regional Editors

PROFESSOR I.P.ALIMARIN, Vernadsky Institute of Geochemistry and Analytical Chemistry, U.S.S.
Academy of Sciences, Vorobievskoe Shosse 47a, Moscow V-334, U.S.S.R.

PROFESSOR E.BLASIUS, Institut für Analytische Chemie und Radiochemie der Universität des Saa
66 Saarbrücken 15, Bundesrepublik Deutschland

MR.H.J.FRANCIS, JR., Pennwalt Corporation, 900 First Avenue, King of Prussia, Pennsylvania 19406,

PROFESSOR J.S.FRITZ, Department of Chemistry, Iowa State University, Ames, Iowa 50010, U.S.A.

DR.M.PESEZ, Roussel-Uclaf, 102 et 111 route de Noisy, Romainville (Seine), France

DR.R.PŘIBIL, Laboratory of Analytical Chemistry, Polarographic Institute of J. Heyrovský, Czech
Academy of Sciences, Prague 1, Jilská 16, Czechoslovakia

Consulting Editors

DR.M.WILLIAMS, Oxford, England
PROFESSOR C.L.WILSON, Belfast, N. Ireland

Editorial Board

Chairman: PROFESSOR R.BELCHER, *representing Advisory Board*
DR.R.A.CHALMERS, *Editor-in-Chief*
DR.M.WILLIAMS, *Consulting Editor*
PROFESSOR C.L.WILSON, *Consulting Editor*
DR.D.BETTERIDGE, *Assistant Editor*
DR.J.R.MAJER, *Assistant Editor*
MR.H.J.FRANCIS, JR., *representing Regional*
MR.G.F.RICHARDS, *Director, Pergamon Pr*

Annual Subscription Rates (including postage)

Published monthly—1 volume per annum
$10(£3.50)—For *bona fide* students, who place their orders with the publisher together with a no
their professor or tutor certifying their status
Private individuals whose departmental libraries subscribe, may obtain this Journal for their perso
at the reduced rate of $25(£8) per annum
$90(£36)—For libraries, government laboratories, research establishments, manufacturing houses an
multiple-reader institutions
Payments must be made in advance
Back numbers are available—write for Back Issues Price List

Publishing and Advertising Offices

American Continent: Pergamon Press Inc., Maxwell House, Fairview Park, Elmsford, New York 10523,
Rest of the World: Pergamon Press Ltd., Headington Hill Hall, Oxford OX3 0BW, England

Copyright © 1971 Pergamon Press Ltd.

ห้องสมุด กรมวิทยาศาสตร

Advisory Board

Aims and Scope

Established as a medium for the rapid publication of papers dealing with all aspects of analytical chemistry, *Talanta* is the natural vehicle for the international communication of progress in this field. As an international journal, its papers are expected to be of a very high standard and to make definite contributions to the subject: they must be new publications. Papers may be written in English, French or German; all papers have abstracts in these three languages and also in Russian. Special importan is attached to work dealing with the principles of analytical chemistry in which experimental material is critically evaluated, and to similar fundamental studies. Reviews in rapidly expanding fields or of hitherto widely scattered material are considered for publication, but should be critical. Original pape short communications and reviews are refereed in the normal manner. Preliminary communications a refereed urgently and accorded priority in publication. Correspondence of interest to analytical chemis is welcomed by the Editor-in-Chief, at whose discretion it is published. A new feature is Annotations, which are critical commentaries on some aspect of analytical chemistry and deal with topics such as sources of error, or the scope and limitations of methods and techniques; these commentaries are refereed.

Allied Journals

Other Pergamon Journals which are of interest to readers of *Talanta:*

Annals of Occupational Hygiene
Applied Radiation and Isotopes
Atmospheric Environment
Carbon
Chemical Engineering Science
Corrosion Science
Electrochimica Acta
European Polymer Journal
Food and Cosmetics Toxicology
Geochimica et Cosmochimica Acta
Inorganic and Nuclear Chemistry
Inorganic and Nuclear Chemistry Letters
Materials Research Bulletin
Petroleum Chemistry
Photochemistry and Photobiology
Physics and Chemistry of Solids
Phytochemistry
Polymer Science USSR
Society of Cosmetic Chemists Journal
Spectrochimica Acta, Part A: Molecular Spectrosco
Spectrochimica Acta, Part B: Atomic Spectroscopy
Tetrahedron
Tetrahedron Letters
Water Research

Each journal has an individual Information and Index Leaflet giving full details. Write now for any these leaflets which interest you.

ADVISORY BOARD OF TALANTA

The Editorial Board and Publishers of *Talanta* take pleasure in welcoming the following new members to the Advisory Board of the journal.

Adam Hulanicki
Candin C. Liteanu
J. Růžička

Adam Hulanicki, Dozent of Analytical Chemistry in the Institute of Basic Problems in Chemistry at Warsaw University, was born in 1929. He studied chemistry at Warsaw University, receiving his doctorate in 1961 under Professor W. Kemula. He became Dozent in 1968. His teaching activity is connected with fundamentals of chemical analysis and instrumental methods. The field of his research interest is mainly connected with electroanalytical methods of analysis (potentiometry, amperometry, coulometry), ionic equilibria, and organic reagents for trace analysis.

Candin C. Liteanu is Professor of Analytical Chemistry at the University of Cluj, Romania. He received his B.S. (1941), Ph.D. (1945) and D.Sc. (1964) from the same University. Since 1964 he has been the head of the Department of Analytical Chemistry. His research interests include temperature-gradient chromatography with open columns (also on paper and thin layers), ion-selective membrane-electrodes (made with precipitates and polymers), fundamentals of analytical determinations in the concentration range below the detection level and statistical methods for the estimation of the sensitivity of analytical reactions. He is the author of a book entitled "Volumetric Analysis" which has appeared in five editions.

Dr. J. Růžička, docent in Analytical Chemistry, The Technical University of Denmark, Lyngby by Copenhagen, was born in Prague, Czechoslovakia in 1934. He graduated in 1957 at the Department of Analytical Chemistry of the Faculty of Sciences, Charles University, Prague, and worked at the Faculty of Technical and Nuclear Physics, Technical University of Prague, for a number of years. During that time he obtained his CSc degree (in 1963) and also the degree of Doctor of Natural Sciences at the Charles University in 1967. For his work in radioanalytical chemistry he was awarded the State Prize in 1965. He spent a short time at the Moscow State University in 1960, studying radiochemistry, and five years later one year at the University of Aston at Birmingham as a lecturer, where he helped to start research in radioanalytical chemistry. He is now a member of the Danish Chemical Society and secretary of the Danish Analytical Society.

He is co-author of a monograph on substoichiometry—a method which he suggested and developed with J. Starý. J. Růžička has also contributed to two other monographs and published over 60 papers. His interests are trace analysis, radiochemical analysis, automation and recently also ion-selective electrodes.

Talanta, 1971, Vol. 18, pp. 127 to 137. Pergamon Press. Printed in Northern Ireland

ROLE OF SOLUTION EQUILIBRIA IN ATOMIC-ABSORPTION SPECTROSCOPY

P. E. THOMAS* and W. F. PICKERING
Department of Chemistry, University of Newcastle, N.S.W. 2308

(*Received* 4 *May* 1970. *Accepted* 3 *June* 1970)

Summary—The interference effects observed in a series of absorption studies using nitrous oxide/acetylene or air/acetylene flames are interpreted in terms of the nature of the chemical species present in solution. The elements studied include Nb, Ta, Ti, Y, V, W and Ni, and species shown to influence the atomic absorption include hydrofluoric, phosphoric and sulphuric acids, the ions of Ca, K, Al, Fe and Mn, and compounds such as EDTA and ammonium acetate.

THE PHENOMENON of "chemical" interference has been widely quoted in emission flame photometry studies and Alkemade[1] has made a systematic classification of such interferences. Numerous workers have reported chemical interference effects in atomic-absorption spectroscopy. For example, in detailed studies of the determination of calcium and magnesium,[2–4] it has been shown that the absorption is reduced by the presence of a wide range of both anions and cations. Other studies[5–7] involving species known to form refractory oxides (for example, the hydrous oxide group and alkaline earths), have indicated marked mutual interference when pairs of elements from this category are present in the same solution.

Theoretical treatments of chemical interferences have been rather meagre, largely because of the difficulty in assigning the effects to any single cause. Interference is normally attributed to processes which occur in the flame. However, the nature of the species entering the flame may be determined by the composition of the test solution and the object of this paper is to indicate the possible roles of solution equilibria in atomic-absorption spectroscopy. A necessary preliminary to any such discussion, however, is a brief review of relevant flame processes or reactions.

FLAME PROCESSES ASSOCIATED WITH INTERFERENCE EFFECTS

It is well known that the object of atomic-absorption spectroscopy is to measure the amount of characteristic resonance radiation absorbed by a population of atoms in their electronic ground-state and placed in the path of the radiation. These atoms are usually produced in a flame. The primary role of the flame is thus to convert, efficiently, fine droplets of analyte solution into gaseous metal atoms. The actual concentration of atoms achieved is controlled by the concentration of the element of interest in the test solution; by the rate of delivery of the solution to the flame; by the rate of volatilization of the solvent; and by the ease of atom formation.

Chemical interference effects are concerned primarily with the last-mentioned aspect, since the ease of atom formation is related to the chemical composition of the minute specks of solute in the flame and to the environment surrounding the solid.

When heated in a flame, the salts of many elements tend to form metal oxides of low volatility (*e.g.*, the alkaline earths, iron, aluminium, chromium, titanium, zirconium)

---

* Present address: Varian Techtron, Baarerstrasse 77, Switzerland.

and there is both circumstantial[7] and direct evidence[5] that mixtures of different salts form spinels (*e.g.*, $MgO{\cdot}Al_2O_3$) of even lower volatility or tendency to dissociate into atoms.

This problem of oxide formation has been partially solved by increasing thermal decomposition through the use of hotter flames. The effect of thermal decomposition can also be enhanced by reactions involving radicals or other species present in the flame.

For example, it has been proposed[4] that the production of magnesium atoms in an air/propane flame might involve a reaction such as

$$MgO_{(s)} + H^{\cdot}_{(g)} \rightleftharpoons Mg_{(g)} + OH^{\cdot}_{(g)}$$

In this system, the absorption increases in the presence of calcium salts, possibly owing to a reaction in the flame such as

$$MgO_{(s)} + Ca_{(g)} \rightleftharpoons CaO_{(s)} + Mg_{(g)}$$

Amos and Thomas[8] attributed their ability to determine low concentrations of aluminium, using a premixed flame which burnt acetylene in a 1:1 mixture of nitrogen and oxygen, to a combination of higher temperature and the availability of free carbon.

$$AlO_{(s)} + C \rightleftharpoons Al_{(g)} + CO_{(g)}$$

Willis[9] subsequently proposed nitrous oxide as a substitute for the oxygen/nitrogen mixture and development work by Amos and Willis[10] added some 25 elements to the list of elements which could be determined by atomic-absorption spectroscopy.

The nitrous oxide/acetylene flame is almost as hot as oxygen/acetylene (*ca.* 3100°) and possesses reducing properties which inhibit oxide formation. Studies using a separated flame[11] have confirmed emissions corresponding to molecular band systems of C_2, CH, NH and CN, and the unique reducing properties of a fuel-rich flame are attributed primarily to the high concentration of CN.

A consequence of the use of higher-temperature flames is a marked increase in the degree of ionization of some elements. A number of workers have minimized this effect by adding an element of low ionization potential (*e.g.*, K) to the test solution. Fleming,[12] on the other hand, developed a means of producing flames of any desired temperature within the limits of 2300° and 2950° by using mixed air/nitrous oxide/acetylene flames.

The determination of a number of refractory metals has also been achieved through the use of organic solvents and fuel-rich oxy-acetylene flames. The effect of mixed organic solvents on the atomic-absorption spectrophotometry of vanadium has been investigated in some detail[13] and it was found that absorption increased as the concentration of organic solvent increased. Further studies indicated that the addition of compounds with high boiling point and relatively long carbon chain (*e.g.*, oleic acid) increased the absorption signal even though the aspiration rate into the flame was reduced. The enhancement may be due to a decrease in the droplet size of the spray, although it was considered that other factors such as the heat of combustion of the solvent and better reducing conditions established in the flame could also play a significant role.

Several of these aspects are discussed in some detail in recent articles by Willis.[14,15]

EXPERIMENTAL

Reagents

Analytical-reagent grade metal salts or pure metals dissolved in chemically pure acids.

Apparatus

A Techtron AA-4 was used in conjunction with either a Techtron AB-50 grooved nitrous oxide/acetylene burner or an AB-40 type burner. Standard hollow-cathode tubes were used for all the elements. Monochromator slitwidth 100 μm.

The conditions used in the various studies are summarized in Table I.

TABLE I.—EXPERIMENTAL CONDITIONS

Element and line, *nm*	Flame type	Lamp current, *mA*	Solution conditions	Additive studied
Ti 364·3	$N_2O—C_2H_2$	20	8% HNO_3	HF, Fe, Na
Ta 271·5	$N_2O—C_2H_2$	15	8% HNO_3	HF, Na
Nb 334·9	$N_2O—C_2H_2$	20	8% HNO_3	HF, Na
Hf 307·3	$N_2O—C_2H_2$	15	8% HNO_3	HF, Na, Fe
Y 410·2	$N_2O—C_2H_2$	15	10% HNO_3	HF, Al
Be 234·8	$N_2O—C_2H_2$	5	5% HCl	Na, Si
Al 309·2	$N_2O—C_2H_2$	12	8% HCl	Cl^-, PO_4^{3-}, Mg SO_4^{2-}, Fe
W 400·8	$N_2O—C_2H_2$	20	Sulphuric, phosphoric or hydrofluoric acid solns	SO_4^{2-}, PO_4^{3-}, HF, K, Fe, Si
Ni 232·0	$N_2O—C_3H_8$ Air–C_3H_8 Air–C_2H_2	10	H_2O	Fe, ammonium acetate, Mn
Co 240·7	$N_2O—C_3H_8$ Air–C_3H_8 Air–C_2H_2	10	H_2O	Mn
Cr 357·9	$N_2O—C_2H_2$ Air–C_2H_2	5	20% HCl	K, Mg
Ca 422·7	Air–C_2H_2	5		La, SO_4^{2-}, H_2EDTA^{2-}, Mg, Sr, Al, PO_4^{3-}
Mg 285·2	Air–C_2H_2 $N_2O—C_2H_2$ $N_2O—C_3H_8$	4	5% HNO_3	Al, PO_4^{3-}, Ca, Sn, H_2EDTA^{2-}, Si, tartaric acid, K, Fe

RESULTS AND DISCUSSION

With the exception of the tungsten study, which was used to develop a method for the determination of this element in wolframite,[16] the experiments were concerned primarily with elucidating the nature and magnitude of specific interference problems. It was previously noted by Amos and Willis[10] that the absorption by metals which exist in solution as oxy or hydroxy species is enhanced by the addition of small amounts of fluoride, and the enhancement effect associated with zirconium and titanium salts has recently been used for the determination of fluoride concentrations.[17]

Subsequent studies involving the metals nickel, tin, titanium, zirconium, hafnium,

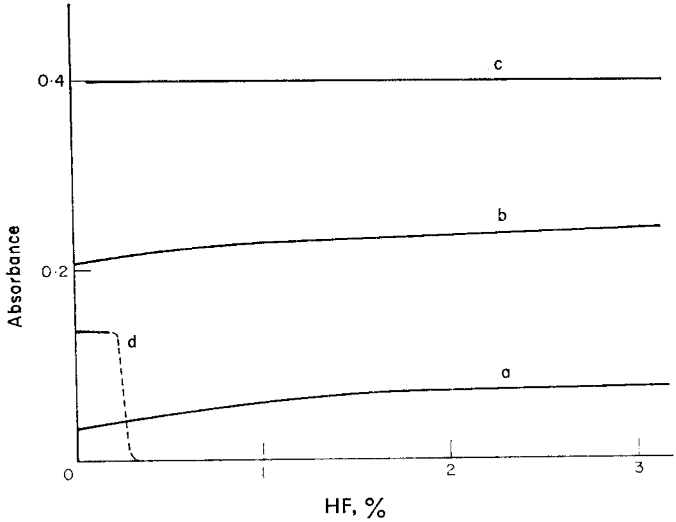

FIG. 1.—Effect of hydrofluoric acid on the absorbance of solutions containing metallic ions. (*a*) 400 ppm Ta; (*b*) 400 ppm Ti; (*c*) 500 ppm W + 1 % K; (*d*) Y, which forms a sparingly soluble fluoride. Nitrous oxide/acetylene flame.

niobium and tantalum, showed[6] that in the case of metals which form oxides of high lattice energy, sensitivity is enhanced if the metals in solution are not bonded to oxygen, as in metallocenes or fluoro-complexes.

When fluoride ions are added to solutions containing the nitrates of elements from Groups IVB and VB, oxy-fluoro complexes tend to form as discrete entities. In the flame the species formed by tantalum, titanium and vanadium volatilize readily, atomization occurs more easily, and the absorption is enhanced. Conversely, as the concentration of fluoride ions increases, yttrium solutions form a precipitate and yield zero absorbance values, and hafnium solutions show a continual decrease in absorbance. Niobium and zirconium solutions pass through a point of maximum absorption which is indicative of competing processes. The effect of acid concentration is clearly shown in Figs. 1 and 2.

Some of these elements are known[18] to form a variety of crystalline products when alkali and alkali metal fluorides are added to solutions of the hydrous oxide in aqueous hydrofluoric acid. Typical examples are the commercially important materials $K_2NbOF_5 \cdot H_2O$ and K_2TaF_7.

The tendency of these species to form in solution has a marked effect on the ease of atom formation, as shown by the large decrease in absorption caused by the addition of sodium ions to hydrofluoric acid solutions of these metals (Fig. 3).

With titanium, zirconium and hafnium solutions, a high concentration of sodium ions (>1:1 sodium:metal) has a marked inhibiting effect; this effect is only slightly influenced by the presence of hydrofluoric acid and is greatest with zirconium and hafnium. With tungsten solutions, absorption is independent of the acid concentration but the addition of potassium ions enhances the signal (reaching a limiting value when $K/W > 4$; most probably attributable to minimization of the extent of tungsten ionization in the flame).

The tungsten system provides further confirmation of the statement by Sastri *et al.*[7]

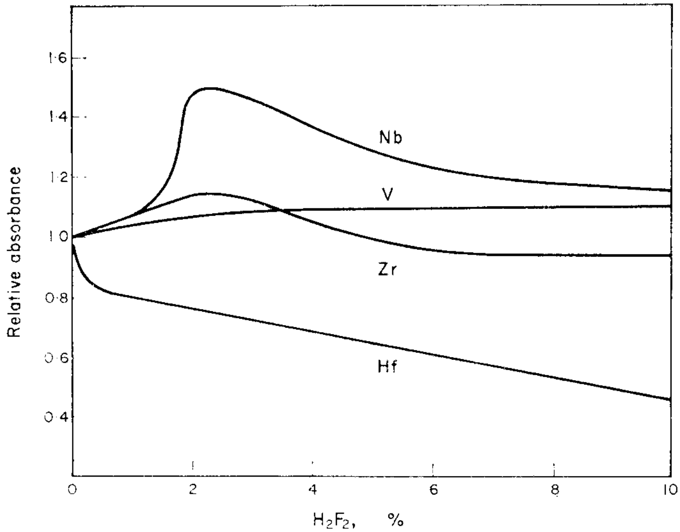

FIG. 2.—Effect of hydrofluoric acid on the absorbance of solutions containing the nitrates of metals from Group IVB and VB. Nitrous oxide/acetylene flame.

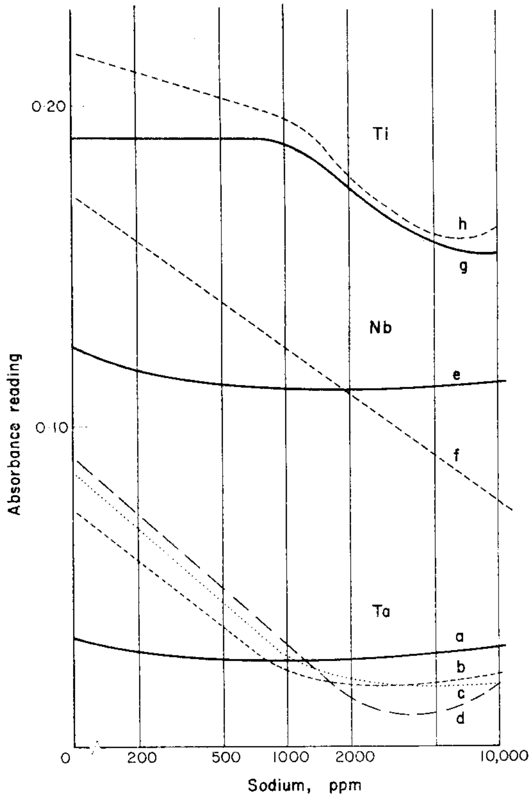

FIG. 3.—Effect of added sodium ions on the absorbance of rare earth atoms, in the presence and absence of hydrofluoric acid. Nitrous oxide/acetylene flame.
Ta, 400 ppm in 8% HNO_3. (*a*) 0% HF; (*b*) 2% HF; (*c*) 5% HF; (*d*) 10% HF. Nb, 800 ppm in 8% HNO_3. (*e*) 0% HF; (*f*) 2% HF. Ti, 400 ppm. (*g*) 0% HF; (*h*) 2% HF.

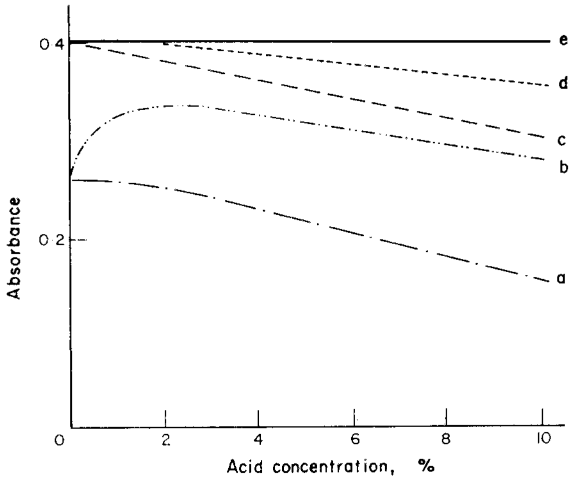

FIG. 4.—Effect of acid concentration on the absorbance (at 400·8 nm) of a solution containing 500 ppm tungsten.
(*a*) sulphuric acid; (*b*) phosphoric acid; (*c*) phosphoric acid plus 10000 ppm potassium salt; (*d*) sulphuric acid plus 10000 ppm potassium salt; (*e*) hydrofluoric acid plus 10000 ppm potassium salt.

that sensitivity is enhanced if the metals in solution are not bonded to oxygen. Reference to Fig. 4 clearly shows the difference in response when hydrofluoric, sulphuric or phosphoric acid is used to complex the tungsten(VI) and so prevent hydrolysis in solution.

In the presence of excess of potassium ions, the sensitivity achieved with low sulphuric acid concentrations approaches that observed when hydrofluoric acid is used. However, as the sulphuric acid concentration is increased, there is a decrease in absorption. This effect may be attributed in part to a change in viscosity, in part to the additional energy required for volatilization of the solvent droplets entering the flame, and in part to the presence of increasing proportions of protonated polynuclear tungstic oxide species which in solid form can exist as $H_8W_{12}O_{40}$, $Ce_2W_{12}O_{40}$ *etc.*

In the absence of the radiation buffer (K^+), increasing the phosphoric acid concentration in the analyte initially increases the absorption, by formation of a complex which is either less readily ionized, or conversely, more readily dissociated into free atoms than the tungstate ion. The nature of the species is easy to predict, since the ability of tungsten to form heteropoly acids is well established (*e.g.*, $H_3[P(W_3O_{10})_4]\cdot$ or $H_4[Si(W_3O_{10})_4]$. The decrease in absorption signal observed when the acid concentration exceeded 2% can be attributed to stabilization of protonated species, thermal effects associated with solvent evaporation, or physical effects such as changes in droplet size and flow-rate.

In sulphuric acid solutions absorbance decreased when the concentration of added silicon approached that of the tungsten present. This can be attributed to the formation of a silicotungstate heteropoly acid. In the presence of phosphoric acid this effect was not observed, owing to the preponderance of the competing phosphate ions (Fig. 5).

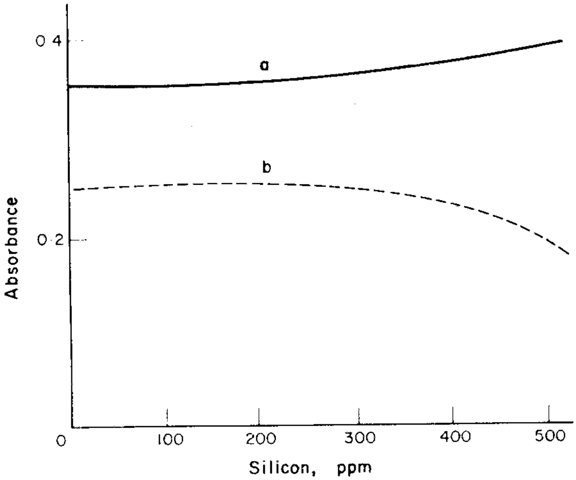

FIG. 5.—Effect of adding a salt containing silicon on the absorbance at 400·8 nm of a solution containing 500 ppm tungsten, 10000 ppm potassium, and (*a*) 5% phosphoric acid or (*b*) 5% sulphuric acid. Nitrous oxide/acetylene flame.

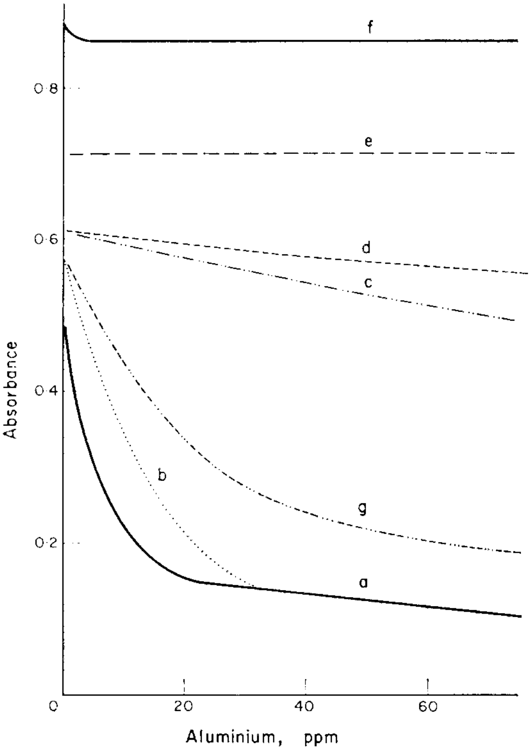

FIG. 6.—The effect of calcium on the interference effect of aluminium in the determination of magnesium. Absorbance measured at 285·2 nm, air/acetylene flame, 2 ppm magnesium.
(*a*) Inhibiting effect of aluminium; (*b*) 10 ppm Ca present; (*c*) 50 ppm Ca present; (*d*) 100 ppm Ca; (*e*) 500 ppm Ca; (*f*) 1000 ppm Ca; (*g*) 1000 ppm EDTA present.

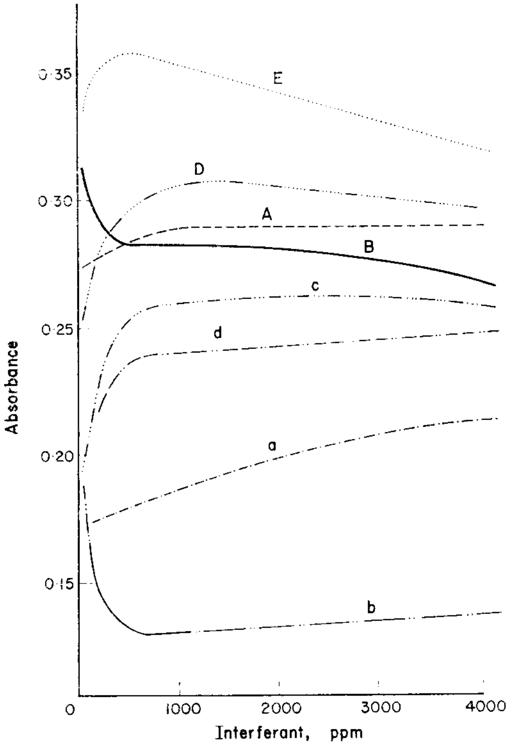

FIG. 7.—The effect of time of standing and presence of ammonium acetate on the absorption of the 232·0 nm line by a 3-ppm nickel solution, an air/propane flame.

A—3 ppm Ni plus added Fe;
a—same solutions after standing 11 days;
B—3 ppm Ni plus 2% ammonium acetate plus added Fe;
b—Ni + Fe + acetate solutions after standing 11 days;
c—3 ppm Ni plus added Mn, after standing 13 days;
D—3 ppm Ni plus 2% ammonium acetate plus added Mn.
d—Ni + Mn + acetate solutions after standing 13 days;
E—3 ppm Co plus added Mn.

The addition of iron to a tungstate solution reduces the absorption signal, probably through the formation of metal tungstate anions (*e.g.*, $FeW_{12}O_{40}^{5-}$) which presumably give a mixed oxide of limited volatility and reactivity in the flame.

The mutual interference effects of other metals which form refractory oxides has been explained[7] in terms of preliminary co-ordination in solution. In the determination of a metal ion (M_1) which co-ordinates through oxygen atoms, the presence of another metal (M_2) as an oxy-salt may lead to a loose —M_2—O—M_1—O—M_2— type of framework. On dehydration this leads to a three-dimensional framework in the solid state, and if the metal-oxygen bond energies are high, the crystal is likely to be involatile and few free metal atoms are likely to be formed in a low-temperature flame.

The best-documented example of mixed oxide formation involves the metals magnesium and aluminium, although there are many other systems where interference has been attributed to mixed oxide formation. Among these may be listed Mg–Fe, Mg–Si, Mg–Cr, Mg–Ti, Mg–Zr, Ti–Fe, Ca–Fe, Ca–Ti, Ca–Zr, Ba–Ti, Sr–Ti, Sr–Zr, Sr–Hf, Cr–Zr, Cr–Ti, Cr–Hf, Cr–Mg and Fe–Ni. The inhibiting effect attributable to mixed oxide formation is most marked in cooler flames, the magnitude being indicated by the examples shown in Figs. 6 and 7.

In most practical systems this type of interference has been overcome by using nitrous oxide in the flame system. With cooler flames, the interference has occasionally been overcome by adding "sacrificial ions" to the test solution or by adding complexing agents to this solution. Figure 6 shows how the addition of calcium ions to the analyte affects the interaction between aluminium and magnesium. In this case it may be suggested that the excess of calcium in the solutions causes the aluminium to be predominantly associated with this species. In addition, calcium atoms in the flame may hasten the decomposition of MgO as previously suggested.

Current evidence suggests that the role of many complexing agents is merely to increase the reducing power of the flame. For example, it was noted in this study that the addition of tartaric acid to a magnesium solution reduced the inhibiting effect of iron, aluminium, and to a lesser extent, silicon. Since the test solution contained 5% nitric acid, complex formation in solution would be virtually nil and the enhancement effect must be attributed to the formation of tiny globules of organic matter and carbon char in the flame. A similar explanation has previously been proposed to explain the beneficial effect of oxine. In addition, the work by Sastri *et al.*[6,7] clearly indicates that the formation of complexes using oxygen-donor type ligands does not necessarily inhibit oxide formation. EDTA forms stable complexes in solution with both magnesium and aluminium ions, yet it can be seen from Fig. 6 that a large excess of this ligand (containing both oxygen and nitrogen donor atoms) does not significantly overcome the interference of aluminium in magnesium studies.

In air/acetylene flames, absorption by calcium solutions is markedly reduced in the presence of sulphate and phosphate ions and aluminium salts. As in the magnesium study, the effect of these interferences is not eliminated by the addition of the complexing agent EDTA but it can be overcome by adding an excess of a cation (*e.g.*, La, Sr) which reacts preferentially in solution with the interfering species.

A significant indication of the role played by the formation of mixed hydroxy-bonded polymers in solution was provided by the study of the interference of iron in nickel determinations. The temperature of the air/acetylene and nitrous oxide/propane flame was sufficient to decompose any mixed oxide formed, and when these flames were used the addition of up to 5000 ppm of Fe to 3 ppm of Ni had no effect on the absorption signal. With air/propane flames, however, there was appreciable interference when the solutions were allowed to stand. In simple aqueous solution iron(III) salts hydrolyse slowly, yielding colloidal matter which can adsorb or coprecipitate measurable amounts of nickel. Thus the extent of nickel absorption decreases as hydrolysis proceeds. Adding ammonium acetate to the solution provides a medium which favours the formation of nickel acetate complex ions which should not be so readily incorporated into an oxygen-bonded polymeric complex in solution. Countering this effect is the buffer action of the added salt, which gives a pH of about 7. At this pH, hydrolysis of the iron proceeds rapidly and nickel species must be trapped in the resultant hydroxy-acetate species as evidenced by the large inhibitory effects shown in Fig. 7. In the absence of iron, acetate ions enhance the extent of absorption.

In contrast to this, the addition of 2% of ammonium acetate to freshly prepared nickel solutions eliminated the usual effects of added manganese(II) salts, although on standing (Fig. 7) the signal from the acetate solution was less than from the control solution. The tendency of added manganese salts to enhance signals when present in small amounts and inhibit them when in larger amounts (in an air/propane flame) is illustrated in Fig. 7 by a cobalt calibration curve. As with the nickel system, this interference is overcome by using a hotter flame.

The role of solution equilibria

With cool flames, chemical interactions in the solution can significantly influence the concentration of ground-state radiation-absorbing atoms in the flame.

The extent of any solution interaction is determined by the magnitude of the appropriate equilibrium constants, and the types of equilibria to be considered include the following.

(1) Solute–solvent interaction, *i.e.*, hydrolysis of multivalent cations.

(2) Ion-pairing, *e.g.*, selective association of phosphate with lanthanum or strontium

(3) Complex formation.

(4) Precipitation, *e.g.*, loss of absorption due to formation of a sparingly soluble compound such as yttrium fluoride.

(5) Adsorption on the surface of colloidal precipitates, *e.g.*, the nickel, iron, ammonium acetate system.

(6) Polymerization, *i.e.*, the formation of the mixed, oxygen-bonded, three-dimensional lattices discussed by Sastri.[7]

The situation is complicated by the fact that several equilibria may be operating simultaneously and generally only some of the relevant data is available in the literature.

To date, conclusions as to the role of the various equilibria are in general empirical and are derived from studies designed to overcome interference effects rather than to examine the basic causes. A possible exception is the work of Sastri, Chakrabarti and Willis,[6,7] who showed that efficiency in atom formation is enhanced if the metal ion is bonded to groups other than those containing oxygen atoms.

The force of this argument is reduced by the results of Hartlage[19] who studied the effect of various added amines on the atomic absorption or iron, cobalt, nickel, chromium and copper solutions, both an air/acetylene and a nitrous oxide/acetylene flame being used. In each case, the addition of the amine resulted in a lower absorption figure, and the author concluded that the interference appears to be caused by metal-amine complexes which do not dissociate at the temperature of the flame.

Acknowledgements—The authors wish to thank the management of Varian-Techtron for granting permission to publish this material and gratefully acknowledge the assistance of J. Sanders, A. Copley and H. Chumnong in some of the experimental studies.

Zusammenfassung—Die bei einer Reihe von Absorptionsuntersuchungen mit Lachgas/Acetylen- oder Luft/Acetylen-Flammen beobachteten Störeffekte werden auf die Natur der in Lösung vorliegenden chemischen Spezies zurückgeführt. Die untersuchten Elemente umfassen Nb, Ta, Ti, Y, V, W und Ni; die Atomabsorption wird beeinflußt durch Flußsäure, Phosphor- und Schwefelsäure, die Ionen von Ca, K, Al, Fe und Mn sowie Verbindungen wie EDTA und Ammoniumacetat.

Résumé—On interprète les effets d'interférences observés dans une série d'études d'absorption utilisant les flammes protoxyde d'azote-acétylène ou air-acétylène en fonction de la nature de l'espèce chimique présente en solution. Les éléments étudiés comprennent Nb, Ta, Ti, Y, V, W et Ni, et les espèces dont on a montré qu'elles influencent l'absorption atomique comprennent les acides fluorhydrique, phosphorique et sulfurique, les ions de Ca, K, Al, Fe et Mn, et les composés tels que l'EDTA et l'acétate d'ammonium.

REFERENCES

1. C. Th. J. Alkemade, *Anal. Chem.*, 1966, **38,** 1252.
2. T. V. Ramakrishna, J. W. Robinson and P. W. West, *Anal. Chim. Acta*, 1966, **36,** 57.
3. D. J. Halls and A. Townshend, *ibid.*, 1966, **36,** 278.
4. C. Rocchiccioli and A. Townshend, *ibid.*, 1968, **41,** 93.
5. I. Rubeska and B. Moldan, *ibid.*, 1967, **37,** 421.
6. V. S. Sastri, C. L. Chakrabarti, and D. E. Willis, *Can. J. Chem.*, 1969, **47,** 587.
7. V. S. Sastri, C. L. Chakrabarti, and D. E. Willis, *Talanta*, 1969, **16,** 1093.
8. M. D. Amos and P. E. Thomas, *Anal. Chim. Acta*, 1965, **32,** 139.
9. J. B. Willis, *Nature*, 1965, **207,** 715.
10. M. D. Amos and J. B. Willis, *Spectrochim. Acta*, 1966, **22,** 1325.
11. G. F. Kirkbright, A. Semb and T. S. West, *Talanta*, 1968, **15,** 441.
12. H. D. Fleming, *Spectrochim. Acta*, 1967, **22B,** 207.
13. S. L. Sachdev, J. W. Robinson and P. W. West, *Anal. Chim. Acta*, 1967, **37,** 156.
14. J. B. Willis, *Appl. Opt.*, 1968, **7,** 1295.
15. J. B. Willis, *Spectrochim. Acta*, 1967, **23A,** 811.
16. P. E. Thomas, J. B. Sanders and H. Chumnong, *Resonance Lines*, 1969, **1, 3.**
17. A. M. Bond and T. A. O'Donnell, *Anal. Chem.*, 1968, **40,** 560.
18. F. Fairbrother, *The Chemistry of Niobium and Tantalum*, Elsevier, Amsterdam, 1967.
19. F. R. Hartlage, *Anal. Chim. Acta*, 1967, **39,** 273.

Talanta, 1971, Vol. 18, pp. 139 to 146. Pergamon Press. Printed in Northern Ireland

REAKTIONSSTUFEN-COULOMETRIE—I

THEORETISCHE PRINZIPIEN

PETER GRÜNDLER und HEINZ HOLZAPFEL
Sektion Chemie der Karl-Marx-Universität, 701 Leipzig, D.D.R.

(*Eingegangen am* 22. *Januar* 1970. *Angenommen am* 12. *Juni* 1970)

Zusammenfassung—Unterschiedliche kinetische Eigenschaften zweier Substanzen in Lösung werden ausgenutzt um beide Substanzen mit einem coulometrisch erzeugten Titrationsmittel separat zu titrieren. Die zwei Konzentrationen lassen sich aus den während der Titration auftretenden Konzentrations-Zeit-Kurven ablesen. Für zwei oxydierende Stoffe werden die entstehenden Konzentration-Zeit-Kurven theoretisch abgeleitet. Für die analytische Anwendung müssen die Reaktionsgeschwindigkeitskonstanten bestimmte Bedingungen einhalten. Der Einfluß der amperometrischen Indikation auf die Form der experimentell meßbaren Kurven wird diskutiert.

DER ABLAUF einer chemischen Reaktion wird bestimmt von zwei fundamentalen Größen, nämlich von den Triebkräften (thermodynamische Faktoren) und von der Summe der Reaktionshemmungen (kinetische Faktoren). Unterschiedliche thermodynamische Eigenschaften verschiedener Stoffe in einem Gemisch dienen häufig als unterscheidende, trennende Kriterien bei der Ausführung von Analysen. Beispiele dafür sind die Redoxpotentiale. Es sollte möglich sein, für den gleichen Zweck der Trennung und Unterscheidung auch kinetische Faktoren heranzuziehen. Dies ist besonders dann von Interesse, wenn sich mehrere Stoffe trotz gleicher thermodynamischer Eigenschaften kinetisch verschieden verhalten.

Zur Erreichung dieses Zieles wählen wir folgende Methode: Zwei Stoffe reagieren unterschiedlich schnell mit einem gemeinsamen Titrationsmittel. Dieses wird mit konstanter Geschwindigkeit zugeführt (durch Coulometrie bei konstantem Strom). Die in der Lösung eintretenden Konzentrationsänderungen werden mit fortschreitender Zeit registriert (durch Messung des konzentrationsproportionalen amperometrischen Grenzstroms). Die resultierenden Konzentrations–Zeit-Kurven enthalten die gewünschten Informationen über Art und Menge der zu bestimmenden Stoffe. Im vorliegenden Falle werden Redoxreaktionen untersucht. Das Verfahren ist jedoch für alle Arten von Reaktionen anwendbar. Es muß lediglich ein Titrationsmittel mit konstanter Geschwindigkeit zugeführt und eine konzentrationsproportionale Größe zeitlich registriert werden.

Zeitliche Konzentrationsänderungen während einer coulometrischen Titration

Die beiden Oxydationsmittel A_{O_1} und A_{O_2} reagieren gemeinsam mit dem reduzierenden Titrationsmittel B_R:

$$A_O + B_R \xrightarrow{k} A_R + B_O \tag{1}$$

Zur Vereinfachung wird ein "elektrisches Konzentrationsmaß" $\bar{c}$ eingeführt:

$$\bar{c} = nFk \tag{2}$$

n ist die Anzahl umgesetzter Elektronen pro Mol,
F die Faraday-Konstante,
k die Geschwindigkeitskonstante 2. Ordnung.
$\bar{c}$ hat die Maßeinheit Coulomb pro Liter (Strommenge pro Volumen).

Wenn die Reaktion nach einem Geschwindigkeitsgesetz 2. Ordnung verläuft, d.h. wenn die Gleichung gilt

$$\frac{\mathrm{d}}{\mathrm{d}t}\bar{c}_{\mathrm{A_R}} = -\frac{\mathrm{d}}{\mathrm{d}t}\bar{c}_{\mathrm{A_O}} = \bar{k}\bar{c}_{\mathrm{A_O}} \cdot \bar{c}_{\mathrm{B_R}}$$

und $\mathrm{B_R}$ durch Elektrolyse mit konstantem Strom erzeugt wird, gelten für jeden Stoff A folgende Differentialgleichungen:

$$\frac{\mathrm{d}}{\mathrm{d}t}\bar{c}_{\mathrm{A_R}} = \bar{k}\left(\frac{it}{v} - \bar{c}_{\mathrm{A_R}}\right)\left(\bar{c}^0 - \bar{c}_{\mathrm{A_R}}\right) \tag{3}$$

$$\frac{\mathrm{d}}{\mathrm{d}t}\bar{c}_{\mathrm{B_R}} = -\bar{k}\bar{c}_{\mathrm{B_R}}\left(\bar{c}^0 - \frac{it}{v} + \bar{c}_{\mathrm{B_R}}\right) + \frac{i}{v} \tag{4}$$

$$\frac{\mathrm{d}}{\mathrm{d}t}\bar{c}_{\mathrm{A_O}} = -\bar{k}\bar{c}_{\mathrm{A_O}}\left(\frac{it}{v} - \bar{c}^0 + \bar{c}_{\mathrm{A_O}}\right) \tag{5}$$

$\bar{c}^0$ ist die Anfangskonzentration von $\mathrm{A_O}$ zu Beginn der Messung,
i der Elektrolysestrom zur Erzeugung von $\mathrm{B_R}$,
$\bar{k}$ die Geschwindigkeitskonstante 2. Ordnung, ausgedrückt im "elektrischen Konzentrationsmaß",
t die Zeit in Sekunden vom Moment der Einschaltung des Generatorstroms an,
v das Volumen der Lösung.

Zur Ermittlung des Konzentrations-Zeit-Verlaufes müssen die Gleichungen integriert werden. Bekannt ist eine Lösung ähnlicher Probleme mit Hilfe von Analogrechnern,[1] die jedoch den Einfluß der Parameter $\bar{k}$ und $\bar{c}^0$ nicht genügend deutlich erkennen lassen würde.

Mit der Randbedingung $\bar{c}^0 = \bar{c}_{\mathrm{A_O}}(t = 0)$ ergeben sich folgende Lösungen der Differentialgleichungen:

$$\bar{c}_{\mathrm{A_O}} = \frac{\exp\left(\bar{k}\bar{c}^0 t - \bar{k}\frac{i}{2v}t^2\right)}{\frac{1}{\bar{c}^0} + \sqrt{\frac{\bar{k}v\pi}{2i}}\exp\left(\frac{\bar{k}\bar{c}^{0^2}v}{2i}\right)\left[\operatorname{erf}\bar{c}^0\sqrt{\frac{\bar{k}v}{2i}} + \operatorname{erf}\frac{\bar{k}i}{2v}\left(t - \frac{\bar{c}^0 v}{i}\right)\right]} \tag{6}$$

$$\bar{c}_{\mathrm{B_R}} = \frac{i}{v}t - \bar{c}^0 + \frac{\exp\left(\bar{k}\bar{c}^0 t - \bar{k}\frac{i}{2v}t^2\right)}{\frac{1}{\bar{c}^0} + \sqrt{\frac{\bar{k}v\pi}{2i}}\exp\left(\frac{\bar{k}\bar{c}^{0^2}v}{2i}\right)\left[\operatorname{erf}\bar{c}^0\sqrt{\frac{\bar{k}v}{2i}} + \operatorname{erf}\frac{\bar{k}i}{2v}\left(t - \frac{\bar{c}^0 v}{i}\right)\right]} \tag{7}$$

$$\bar{c}_{\mathrm{A_R}} = \bar{c}^0 - \frac{\exp\left(\bar{k}\bar{c}^0 t - \bar{k}\frac{i}{2v}t^2\right)}{\frac{1}{\bar{c}^0} + \sqrt{\frac{\bar{k}v\pi}{2i}}\exp\left(\frac{\bar{k}\bar{c}^{0^2}v}{2i}\right)\left[\operatorname{erf}\bar{c}^0\sqrt{\frac{\bar{k}v}{2i}} + \operatorname{erf}\frac{\bar{k}i}{2v}\left(t - \frac{\bar{c}^0 v}{i}\right)\right]} \tag{8}$$

Zur Vereinfachung der im Nenner stehenden Ausdrücke wurde das Gaußsche Fehlerintegral

$$\operatorname{erf}(x) = \frac{2}{\sqrt{\pi}} \int_0^x \exp(-x^2)\,\mathrm{d}x$$

benutzt.

Abbildung 1 zeigt die resultierenden Kurven. Die wichtigste Kurve ist der Konzentrationsverlauf des Titrationsmittels B_R. Den Einfluß der Parameter $\bar{k}$ und $\bar{c}^0$ auf diese Kurve zeigen die Abbildungen 2 und 3. Die Zeit $t = \tau$ würde zur vollständigen Umsetzung von A benötigt, wenn A unendlich schnell reagiert. Für die Konzentrationen zur Zeit τ gilt

$$\bar{c}_{A_0}(\tau) = \bar{c}_{B_R}(\tau) = \bar{c}^0 - \bar{c}_{A_R}(\tau) = \frac{\exp\left(\bar{k}\bar{c}^{0^2} \cdot \frac{v}{2i}\right)}{\frac{1}{\bar{c}^0} + \sqrt{\frac{\bar{k}v\pi}{2i}}\,\exp\left(\frac{\bar{k}\bar{c}^{0^2}v}{2i}\right)\operatorname{erf}\bar{c}^0\sqrt{\frac{\bar{k}v}{2i}}} \qquad (9)$$

Hieraus läßt sich sehr genau $\bar{k}$ bestimmen.

Konzentrations-Zeit-Kurven für zwei titrierbare Stoffe

Die Gesamtkurve für zwei verschieden schnell reagierende Stoffe A_{O_1} und A_{O_2} ergibt sich additiv aus je zwei der Funktionen (6) bis (8), wenn der Unterschied in den Reaktionsgeschwindigkeiten genügend groß ist. Um eine analytische Anwendung

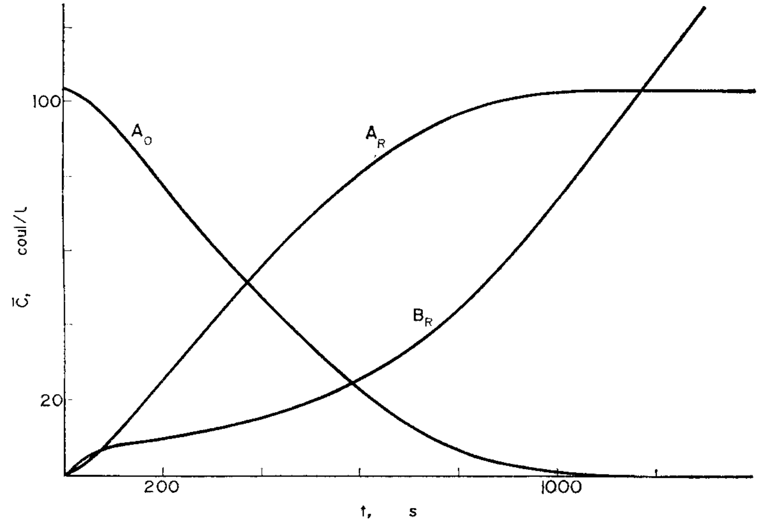

ABB. 1.—Theoretische Konzentrationsänderungen während der coulometrischen Titration einer langsam reagierenden Substanz.
Reaktionsgeschwindigkeitskonstante (elektrisches Maß): 2 . 10^{-4} l/Coul.s.Elektrolysestrom 10,75 mA.Anfangskonzentration der titrierten Substanz (elektrisches Maß) 103,92 Coul/l

B_R Titrationsmittel
A_O titrierte Substanz
A_R Reaktionsprodukt der titrierten Substanz

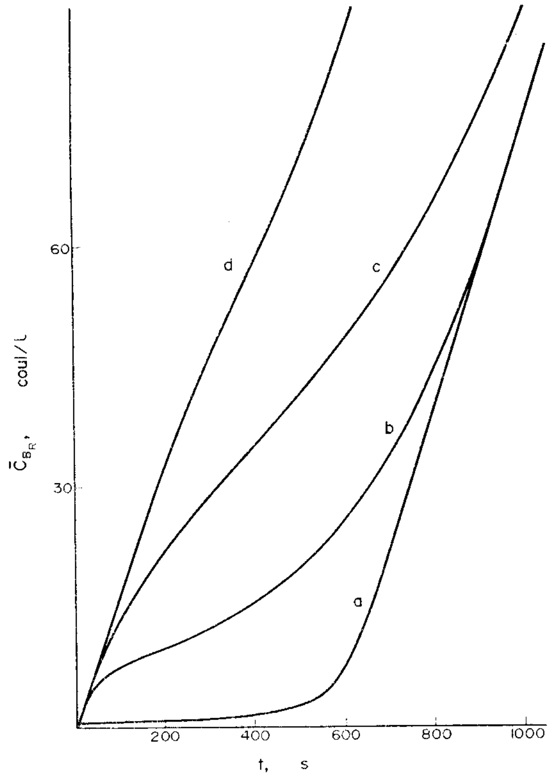

ABB. 2—Theoretischer Konzentrationsverlauf des Titrationsmittels während einer coulometrischen Titration. Einfluß der Reaktionsgeswindigkeitskonstanten. Anfangskonzentration der titrierten Substanz 103,92 Coul/l.Elektrolysestrom 10,75 mA Werte der Geschwindigkeitskonstanten(in l/Coul.s):

(*a*) $3{,}31 \,.\, 10^{-3}$
(*b*) $2 \,.\, 10^{-4}$
(*c*) $5 \,.\, 10^{-5}$
(*d*) $1 \,.\, 10^{-5}$

zu ermöglichen, müssen die Grenzen der Reaktionsgeschwindigkeitskonstanten beider Partner festgelegt werden.

Untere Geschwindigkeitsgrenze der langsameren Reaktion (A_{O_2} mit B_R)

Die Reagenszugabe muß solange fortgesetzt werden, bis die gemessene Kurve in eine Gerade übergeht. Die Länge dieser Geraden muß für eine einwandfreie Extrapolation auf den "Endpunkt" τ ausreichen. Die gesamte Meßzeit soll $\geqslant 2\,\tau$ sein, jedoch den in der Coulometrie üblichen Maximalwert von 6000 Sekunden nicht überschreiten. Zur Zeit $t = 1{,}5\,\tau$ sollen mindestens 99% von A_{O_2} verbraucht sein. Damit ergibt sich:

$$k \geqslant 2\,.\,10^{-4}\,\frac{l}{\text{Coul.s}}$$

$$\text{entsprechend } k \geqslant 20\,\frac{1}{\text{Mol.s}}$$

Untere Geschwindgkeitsgrenze der schnelleren Reaktion (A_{O_1} *mit* B_R)

Der Verlust von A_{O_2} durch Parallelreaktion sei kleiner als 0,1%. Ungünstigstenfalls sind die Anfangskonzentrationen beider titrierter Stoffe gleich. Daraus läßt sich abschätzen, daß die Geschwindigkeit der schnelleren Reaktion etwa um 3 Zehnerpotenzen größer als die der langsameren sein sollte.

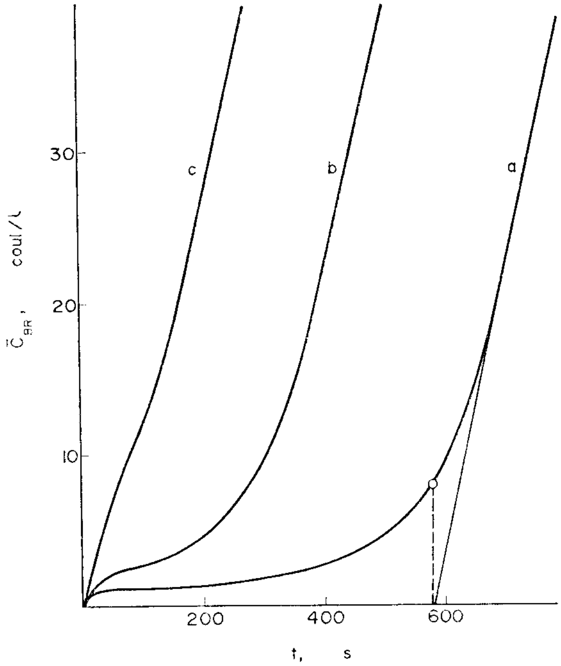

Abb. 3.—Theoretischer Konzentrationsverlauf des Titrationsmittels während einer coulometrischen Titration. Einfluß der Anfangskonzentration des zu bestimmenden Stoffes.
Geschwindigkeitskonstante 3,31 . 10^{-4} Liter/Coul.s.Elektrolysestrom 10,75 mA.
τ Äquivalenzpunkt (Titrationszeit der Prove) Anfangskonzentrationen (in Coul/l):
(*a*) 104 (*b*) 50 (*c*) 10

Obere Geschwindgkeitsgrenze der langsameren Reaktion

Bereits kurz nach Beginn der Titration müssen sich die Kurven von denen für unendlich großes k deutlich unterscheiden. Nachdem eine Zeit von einem Hundertstel τ nach dem Einschalten vergangen ist, sollte die Konzentration des Titrationsmittels mindestens 5 . 10^{-3} Coul.l^{-1} betragen. Diese Forderung ist mit einem Höchstwert der Geschwindigkeitskonstanten von 10^{-2}Coul^{-1}.s^{-1} annähernd erfüllt.

Zusammengefaßt ergeben sich folgende Bedingungen:

$$2\,.\,10^{-4}\frac{l}{\text{Coul.s}} \leqslant k_2 \leqslant 10^{-2}\frac{l}{\text{Coul.s}} \quad \text{(langsamere Reaktion)}$$

$$k_1 \geqslant 10^3\,k_2 \quad \text{(schnellere Reaktion).}$$

Nähere Einzelheiten zur Abschätzung der Konstanten sind der folgenden Arbeit 2 zu entnehmen.

Die Abbildungen 4, 5 und 6 zeigen schematisch, wie sich der gesamte Konzentrationsverlauf einer Titration aus den Einzelkurven zusammensetzen läßt. Aus den durch Addition entstandenen Gesamtkurven sind bei Kenntnis des Ordinatenmaßstabs eindeutig die einzelnen Aquivalenzpunkte τ_1 und τ_2 entnehmbar. Zur Festlegung der Ordinatenmaßstäbe ist je eine Eichmessung notwendig, sofern nicht eine der Kurven selbst mit der Eichgeraden zusammenfällt.

Meßtechnische Verfolgung der zeitlichen Konzentrationsänderungen

Voraussetzungsgemäß ist im vorliegenden Fall mindestens einer der beteiligten Stoffe (das Titrationsmittel) elektrodenaktiv. Daher eignet sich zur Registrierung der

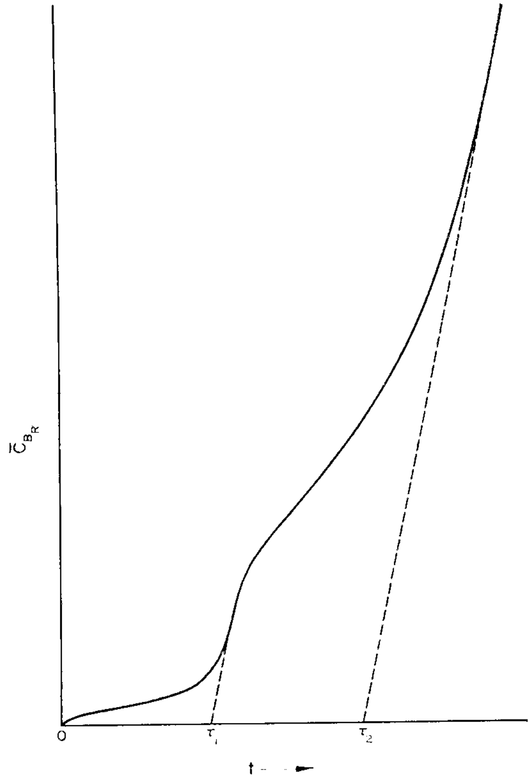

Abb. 4.—Zeitlicher Konzentrationsverlauf des Titrationsmittels bei einer coulometrischen Titration in Anwesenheit zweier verschieden schnell reagierender Probesubstanzen (schematisch)

τ_1 Titrationszeit der schneller reagierenden Probe
$\tau_2 - \tau_1$ Titrationszeit der langsamer reagierenden Probe
gleiche Anfangskonzentrationen der titrierten Substanzen.

Kurven sehr gut der konzentrationsproportionale amperometrische Grenzstrom. Die Amperometrie mit nur einer polarisierten Elektrode ist wegen besserer Proportionaliätt gegenüber der Biamperometrie vorzuziehen. Die Ordinatenmaßstäbe (Anzeigeempfindlichkeiten) werden für verschiedene Stoffe meist unterschiedlich sein. Der Indikatorstrom kann wëhrend der Messung sein Vorzeichen wechseln. Bestimmte Partner können elektrodeninaktiv sein und erscheinen dann nicht in der experimentellen Kurve. Daraus resultiert eine Vielzahl praktisch möglicher Kurvenformen. Alle lassen sich aus den Grundformen der Abbildungen 4, 5 und 6 herleiten. Die Genauigkeit der Bestimmung der beiden Äquivalenzpunkte hängt von der Linearität der amperometrischen Indikationskurve ab, d.h. der Indikationsstrom muß möglichst gut proportional einer der Konzentrationen sein. Weitere Ungenauigkeiten resultieren aus nichtlaminaren Strömungsverhältnissen an den Indikatorelektroden, aus zu starker Dämpfung des Schreibers und sonstigen Fehlern der Registriervorrichtung.

Die Schärfe des Aquivalenzpunktes τ_1 verringert sich mit abnehmender Differenz der beiden Geschwindigkeitskonstanten. Da die Messungen stets von der Genauigkeit beider Äquivalenzpunkte abhängen, ist die erreichbare Genauigkeit prinzipiell

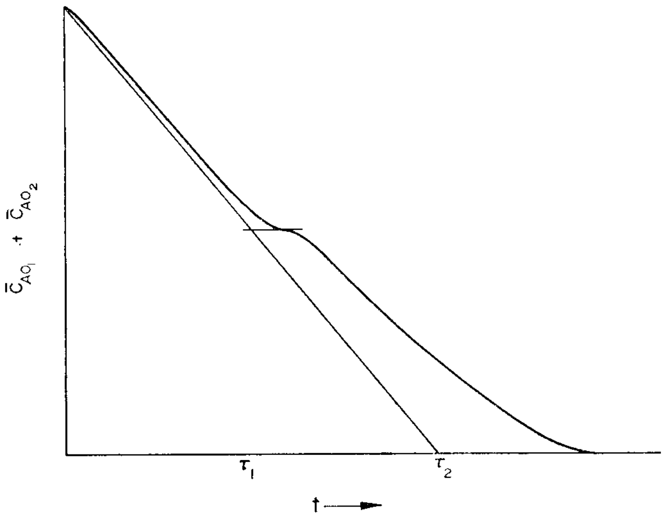

Abb. 5.—Zeitlicher Verlauf der Konzentrationssumme zweier verschieden schnell reagierender Probesubstanzen bei der coulometrischen Titration (schematisch), gleiche Anfangskonzentrationen der titrierten Substanzen.

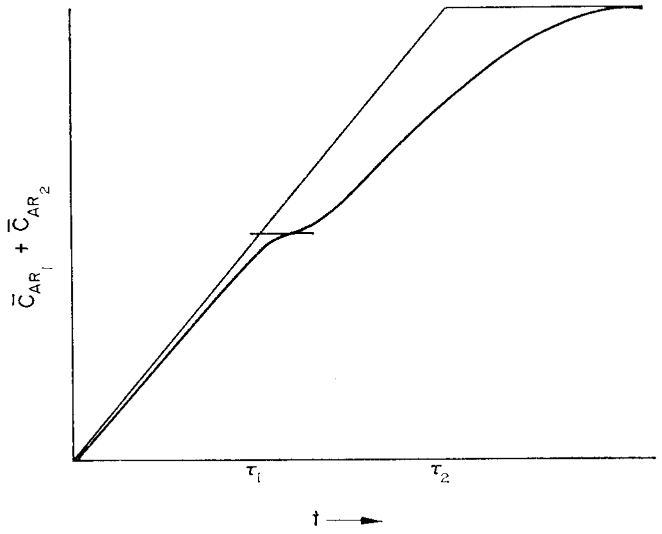

Abb. 6.—Zeitlicher Verlauf der Konzentrationssumme der Reaktionsprodukte zweier verschieden schnell reagierender Probesubstanzen (schematisch), gleiche Anfangskonzentrationen der titrierten Substanzen.

geringer als bei einer einfachen amperometrischen Titration. Diese Einschränkung wird jedoch erst bei ungünstigen Bedingungen spürbar ($\bar{k}_1$ und $\bar{k}_2$ nahe ihren unteren Grenzen).

Temperaturänderungen während der Messungen müssen vermieden werden. Anwendungsbeispiele für die Methode werden im II. Teil beschrieben.

Summary—Differences in the kinetic behaviour of two substances in solution are exploited to allow the determination of both with a common titrant generated coulometrically at constant current. Concentration–time curves for the case of two oxidants in admixture are derived theoretically, and the necessary conditions to be met by the rate constants for the two substances in order to satisfy analytical requirements, and also the effect of amperometric indication on the shape of the experimental curves, are discussed.

Résumé—Les différences dans le comportement cinétique de deux substances en solution sont exploitées de manière à permettre la détermination de ces substances avec un agent de titrage commun, engendré coulométriquement à intensité constante. On déduit théoriquement les courbes concentrationtemps pour le cas de deux oxydants en mélange, et l'on discute des conditions nécessaires que doivent remplir les constantes de vitesse pour les deux substances afin de satisfaire aux exigences analytiques, et aussi de l'influence de l'indication ampérométrique sur l'allure des courbes expérimentales.

LITERATUR

1. G. O'Dom und Q. Fernando, *Anal. Chem.*, 1966, **38**, 844.
2. P. Gründler, *Dissertation*, Leipzig, Juli 1969.

Talanta, 1971, Vol. 18, pp. 147 to 153. Pergamon Press. Printed in Northern Ireland

REAKTIONSSTUFEN-COULOMETRIE—II

ANALYTISCHE UNTERSUCHUNG VON STOFFGEMISCHEN

PETER GRÜNDLER und HEINZ HOLZAPFEL
Sektion Chemie der Karl-Marx-Universität, 701 Leipzig, D.D.R.

(*Eingegangen am* 22. *Januar* 1970. *Angenommen am* 12. *Juni* 1970)

Zusammenfassung—Nach der Methode der Reaktionsstufen-Coulometrie wurden Gemische von Cer(IV) und Chlorat bzw. Hypochlorit und Chlorat analysiert durch Titration mit coulometrisch an einer Quecksilberkathode in saurer, chloridhaltiger Lösung erzeugtem Titan(III). Die Konzentrations-Zeit-Kurven wurden amperometrisch bzw. biamperometrisch verfolgt. Die Reduktionsgeschwindigkeit des Chlorats wurde durch Anwendung des primären Salzeffekts modifiziert. Um Chlorverlust bei der Titration des Hypochlorits zu vermeiden, wird eine geschlossene Elektrolysezelle vorgeschlagen.

IN EINER vorangegangenen Arbeit[1] legten wir die theoretischen Grundlagen der Reaktionsstufen-Coulometrie dar. Diese Methode besteht darin, zwei verschieden schnell reagierende Stoffe mit einem gemeinsamen Titrationsmittel umzusetzen. Letzteres wird coulometrisch mit konstantem Strom erzeugt. Der resultierende Konzentrations-Zeit-Verlauf wird amperometrisch registriert. Sie gestattet die Bestimmung der beiden mit verschiedener Geschwindigkeit reagierenden Stoffe, selbst wenn diese gleiche thermodynamische Eigenschaften zeigen.

Die hier gewählten Stoffpaare [Bestimmung von Cer(IV) neben Chlorat bzw. von Hypochlorit neben Chlorat] haben sehr ähnliche oxydierende Wirkung bei stark unterschiedlichem kinetischen Verhalten. Dies wird durch die bestimmenden Normalpotentiale in saurer Lösung gezeigt:

$$\begin{aligned} ClO_3^-/Cl_2 \quad & \varepsilon_0 = +1{,}47\ V \\ Cl_2/Cl^- \quad & \varepsilon_0 = +1{,}36\ V \\ Ce^{4+}/Ce^{3+} \quad & \varepsilon_0 = +1{,}44\ V \end{aligned}$$

(Hypochlorit liegt unter den Bedingungen unserer Untersuchungen als Cl_2 vor).

Als Reduktionsmittel für alle betrachteten Substanzen hat sich am besten Titan(III) bewährt.

EXPERIMENTELLER TEIL

Chemikalien

Zur Herstellung des Grundelektrolyten wurde Titantetrachlorid "reinst" vorsichtig mit Wasser hydrolysiert und zu Vorratslösungen von *ca.* 3,6*M* gelöst. Ein Milliliter einer solchen Lösung wurde mit 60 ml einer 1*M* Natriumsulfatlösung gemischt und dazu soviel gesättigte Natriumhydrogencarbonatlösung gegeben, daß sich nach 5 Minuten Rühren ein stabiler pH-Wert von 2,3 einstellte.

Lösungen der Probesubstanzen Natriumchlorat, Natriumhypochlorit und Cer(IV) sulfat wurden mit bidestilliertem Wasser in der üblichen Weise bereitet. Der Gehalt dieser Lösungen wurde coulometrisch kontrolliert.[2,3]

Die verwendeten Substanzen waren, falls nicht anders vermerkt, von analytischer Reinheit. Zur Entlüftung wurde gereinigter Stickstoff benutzt, der mittels Zinkamalgam von Sauerstoffspuren befreit worden war.

Elektrische Meßanordnung

Das Schaltschema der elektrischen Anordnung zeigt Abb. 1. Als Konstantstromquelle für den coulometrischen Generatorstrom diente eine elektronische Regelschaltung.[4] Das Potential der

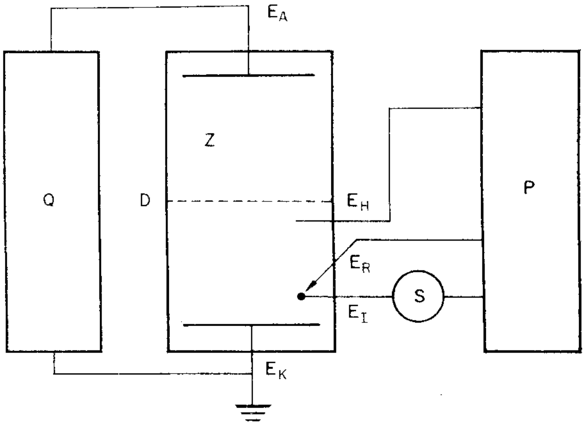

ABB. 1.—Prinzipschaltung der coulometrischen Titration mit amperometrischer Indikation

Z Meßzelle
Q Konstantstromquelle im Generatorkreis
E_A, E_K Elektroden im Generatorkreis
D Diaphragme mit Salzbrücke
E_I amperometrische Indikatorelektrode
E_R Referenzelektrode im Indikatorkreis
E_H Hilfselektrode im Indikatorkreis
S Bandschreiber zur Aufzeichnung der Indikationsströme
P Potentiostat

amperometrischen Indikatorelektrode bzw. die Potentialdifferenz zwischen den Indikatorelektroden (bei biamperometrischer Arbeitsweise) wurde durch einen elektronischen Potentiostaten konstant gehalten. Die Indikatorströme wurden durch einen Bandschreiber registriert. Potentiostat und Scheiber waren Teile des Gerätes "Elektroscan" der Firma Beckman, Fullerton, U.S.A.

Meßzellen

Für die Arbeitsweise mit einer polarisierten Indikatorelektrode wurde eine offene "H-Zelle" mit zwei Schenkeln von je 100 ml verwendet. Titan(III) wurde an einer Schicht Bodenquecksilber kathodisch erzeugt. Gegenelektrode im coulometrischen Generatorkreis war ein Platinblech in 1*M* Natriumsulfatlösung. Zwischen den Elektrolyseräumen befand sich eine Glasfritte mit Salzbrücke aus Gelatine/1*M* Natriumsulfat.

Zum amperometrischen Indikationskreis gehörten eine rotierende Platindrahtelektrode (600 Umdrehungen pro Minute), eine gesättigte Kalomel-Bezugselektrode und eine Hilfselektrode (einige Windungen Platindraht um die Bezugselektrode). Die rotierende Elektrode sorgte außerdem für eine intensive Durchmischung der Lösung im Elektrolyseraum.

Zur Vermeidung von Chlorverlusten bei Analysen in Anwesenheit von Hypochlorit verwendeten wir eine geschlossene Zelle mit biamperometrischer Indikation (Abb. 2). Zur Dosierung wird ein bestimmtes Volumen Probelösung aus der Mikrobürette B eingelassen und eine äquivalente Menge Elektrolytlösung aus der Zelle verdrängt. Nach dem Schließen beider Hähne H beginnt die Titration.

DISKUSSION

Untersuchung der Reaktion von Chlorat mit Titan(III)

Während Cer(IV) und Hypochlorit in sauren, stark chloridhaltigen Lösungen stets unmeßbar schnell mit Titan(III) reagierten, traten bei der Reduktion von Chlorat mit Titan(III) Komplikationen durch Zwischenstoffbildung auf. Die Abbildungen 3, 4 und 5 zeigen einige Titrationen des Chlorats bei verschiedenen Aciditäten in der beschriebenen H-Zelle. Das Potential der Indikatorelektrode wurde so positiv gewählt, wie es die Verhältnisse in der Zelle zuließen.

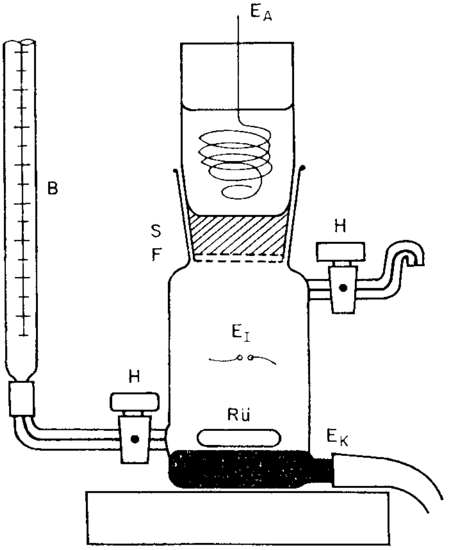

ABB. 2.—Geschlossene Elektrolysezelle zur Coulometrie in Anwesenheit flüchtiger Bestandteile

E_K Generatorkathode (Bodenquecksilber, mit Niveaugefäß verbunden)
E_A Anode des Generatorsystems (Platindraht in $1N$ Natriumsulfat)
F Glasfritte
S Salzbrücke (Gelatine/Natriumsulfat)
B Mikrobürette
E_I Indikatorelektroden (in gegenüberliegende Glaswände eingeschmolzene Platindrähte)
H Hähne mit Kapillarrohr
Rü Magnetrührstäbchen.

In stärker saurer Lösung treten kathodische Indikationsströme auf, die auf oxydierende elektrodenaktive Zwischenstoffe hinweisen. Das kathodische Maximum dieser Ströme liegt für Abb. 3 bei etwa zwei Dritteln der zur vollständigen Reduktion des Chlorats formal notwendigen Zeit, für Abb. 4 bei etwa einem Drittel dieser Zeit. Das würde auf die intermediäre Bildung von Hypochlorit bzw. von Chlorit hindeuten. Folglich verläuft der Anfangsschritt der Umsetzung [bimolekulare Reaktion von Titan(III) mit Chlorat] zu schnell und muß verlangsamt werden. Dies läßt sich durch Verminderung der Säurekonzentration erreichen. Jedoch tritt dann Hydrolyse des im Grundelektrolyten enthaltenen Titantetrachlorids ein. Wir haben deshalb die Ionenstärke des Grundelektrolyten durch Zugabe von Naturiumsulfat stark erhöht. Der eintretende primäre Salzeffekt bewirkt eine starke Verlangsamung des Anfangs-Reaktionsschrittes, ohne daß die Geschwindigkeit der Zwischenstoffreduktion vermindert wird. Die Hydrolyse des Titantetrachlorids wird durch die langsame Einstellung des pH-Wertes in Anwesenheit puffernd wirkender Carbonationen so verlangsamt, daß die Elektrolytlösungen über mindestens einen Tag stabil und klar bleiben.

Der für die Bestimmung gewählte Grundelektrolyt hat die Ionenstärke 3,3. Wie Abb. 5 zeigt, ergibt darin die Reduktion von Chlorat die theoretisch erwartete Kurvenform[1] für den Konzentrationsverlauf des Reduktionsmittels. Beim gewählten Wert des Indikatorelektrodenpotentials ist nur das Titan(III) amperometrisch wirksam.

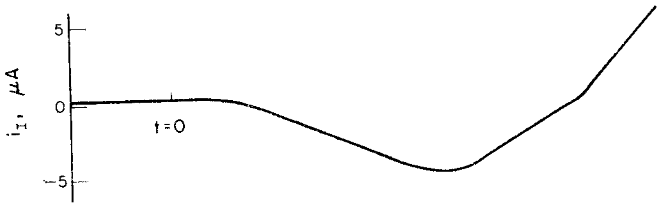

Abb. 3 2,5*M*.

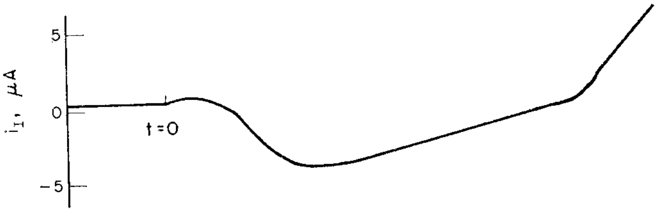

Abb. 4 0,7*M*

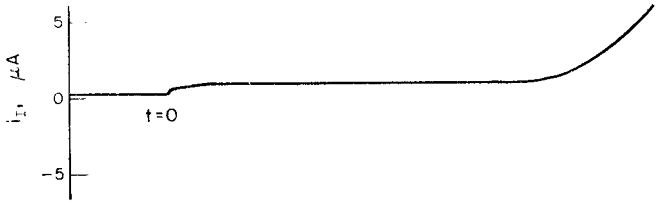

Abb. 5 pH-Wert 2,3.

ABB. 3, 4 und 5.—Coulometrische Titrationskurven von *ca.* 10 µMol Natriumchlorat mit Titan(III) bei verschiedenen Aciditäten. Die Chloridkonzentration betrug stets 0,42*M*, der Elektrolysestrom 10,75 mA und das Potential der Indikatorelektrode +1000 mV gegen SCE. Die Konzentrationen an freier Säure: Abb. 3; 2,5 *M*; Abb. 4; 0,7 *M*; Abb. 5, pH-Wert 2,3.

Der Wert der Geschwindigkeitskonstante berechnet sich nach[1] zu $k = 1{,}92.10^3$ $.\mathrm{Mol}^{-1}.\mathrm{s}^{-1}$.

Analyse von Cer(IV)-Chlorat-Lösungen

Zu 50 ml des Grundelektrolyten werden bis max. 20 ml Probelösung in die Zelle gegeben. Unter Rühren wird die Lösung 5 Minuten mit Stickstoff entlüftet. Das Potential der rotierenden Platinelektrode beträgt +1000 mV gegen SCE. Nachdem die Registrie-vorrichtung für die Indikatorströme in Betrieb gesetzt wurde, wird der Elektrolysestrom (bis 30 mA) eingeschaltet. Eine typische Titrationskurve zeigt die Abb. 6. Infolge des irreversiblen Verhaltens der Cer-Ionen spricht die Indikatorelektrode wiederum nur auf Titan(III) an. Die resultierende Kurve entspricht sehr genau dem in theoretisch berechneten Kurventyp[1] für die Konzentrations-Zeit-Kurve des Titrationsmittels B_R. Die Zeiten τ_1 bzw. τ_2–τ_1 entsprechen dem Gehalt an Cer(IV) bzw. an Chlorat. Gemische von 10 bis 200 µMol Cer(IV) mit 2 bis 75 µMol Chlorat (im Konzentrationsverhältnis 50:1 bis 1:2) wurden mit max. ±0,4% Abweichung analysiert. Dies zeigt, daß die Methode für Systeme mit ähnlichen Eigenschaften wie die untersuchte Mischung sehr gut geeignet ist.

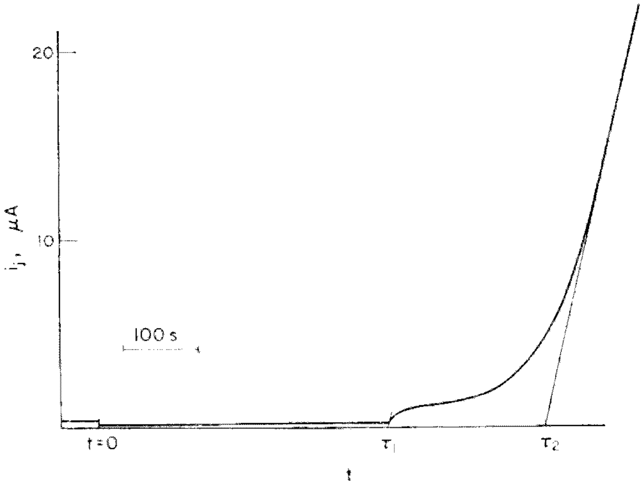

Abb. 6.—Coulometrische Titration von Cer(IV) neben Chlorat mit amperometrischer Indikation in der offenen Elektrolysezelle. Elektrolysestrom 11,07 mA. Potential der Indikatorelektrode +1000 mV gegen SCE.

Analyse von Hypochlorit-Chlorat-Lösungen

Für die Bestimmung von Hypochlorit neben Chlorat in der H-Zelle mit amperometrischer Indikation (Potential der rotierenden Elektrode +1000 mV gegen SCE) zeigt Abb. 7 eine typische Titrationskurve. Der kathodische Anfangsteil entspricht dem Gehalt an Hypochlorit (bzw. Chlor). Vom Zeitpunkt τ_1 an zeigt der Indikationsstrom das sich bildende Titan(III) an. Infolge der sauren Reaktion und des Chloridgehaltes verflüchtigt sich während der Messung aus der offenen H-Zelle Chlor, was zu negativen Fehlern bei der Hypochloritbestimmung führt. Die geschlossene Zelle nach Abb. 2 vermeidet diesen Nachteil. Um die geschlossene Zelle konstruktiv einfach zu halten und die Einführung einer zusätzlichen Bezugselektrode zu vermeiden, haben wir in diesem Falle eine biamperometrische Indikation gewählt. Dadurch verschlechtert sich die Konzentrationsproportionalität der Indikationsströme. Die Reproduzierbarkeit der Kurven wird ebenfalls schlechter.

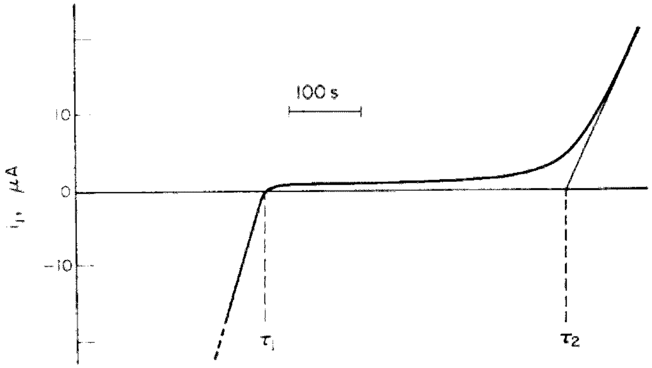

Abb. 7.—Coulometrische Titration von Hypochlorit neben Chlorat mit amperometrischer Indikation in der offenen Elektrolysezelle. Elektrolysestrom 10,75 mA. Potential der Indikatorelektrode +1000 mV gegen SCE.

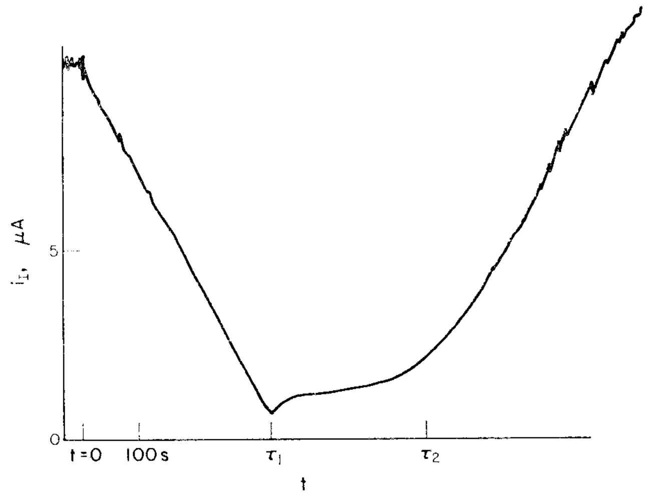

ABB. 8.—Coulometrische Titration von Hypochlorit neben Chlorat mit biamperometrischer Indikation in der geschlossen Elektrolysetelle nach Abb. 2. Elektrolysestrom 10,75 mA. Potentialdifferenz der Indikatorelektroden 1000 mV.

Es ergeben sich Titrationskurven wie in der Abb. 8 (Potentialdifferenz der ndikatorelektroden 1000 mV). In der Zelle können ohne Elektrolytwechsel mehrere roben nacheinander analysiert werden (bis zu einem Probevolumen von max. 10 ml). ie nachfolgende Tabelle gibt die Ergebnisse einiger Analysen wieder.

TABELLE I.—ANALYSENERGEBNISSE

Hypochlorit			Chlorat			Strom, *mA*
Einwaage, *μMol*	Ergebnis, *μMol*	Fehler, %	Einwaage, *μMol*	Ergebnis, *μMol*	Fehler %	
170,9	171,1	+0,1	59,97	59,5	−0,8	$28{,}7_6$
62,31	62,6	+0,5	19,99	20,0	+0,1	$18{,}9_9$
29,45	29,9	+1,5	11,84	11,7	−0,8	$11{,}0_7$
18,07	17,9	−1,2	7,102	7,14	+0,5	$6{,}87_5$
11,91	11,8	−1,2	4,735	4,77	+0,7	$4{,}66_6$
7,551	7,49	+0,9	2,505	2,48	−1,0	$2{,}47_6$
3,80	3,84	+1,0	1,253	1,26	+0,5	$1{,}43_2$

Mit gleichem Erfolg wurden hypochlorit-und chlorathaltige Natriumchloridösungen, wie sie im Anodenraum der technischen Chloralkali-Elektrolyse anfallen, nalysiert. Die geschlossene Elektrolysezelle kann unmittelbar an Behälter mit erartigen Laugen angeschlossen werden und ermöglicht deren analytische Kontrolle urch Stichproben. Die Ergebnisse belegen die Brauchbarkeit des Verfahrens für ndustrielle Zwecke.

Summary—Mixtures of cerium(IV) and chlorate, and of hypochlorite and chlorate have been analysed by titration with titanium(III) generated coulometrically at a mercury cathode in acidic chloride solution. The concentration-time curves were recorded with amperometric or biamperometric indication respectively. The rate of reduction of chlorate was modified by the addition of a large amount of strong electrolyte. Loss of chlorine during the titration of hypochlorite was avoided by using a closed electrolysis cell.

Résumé—On a analysé des mélanges de cérium(IV) et de chlorate, et d'hypochlorite et de chlorate, par titrage au titane(III) engendré coulométriquement sur une cathode de mercure en solution acide de chlorure. On a enregistré les courbes concentration–temps avec indication ampérométrique et biampérométrique respectivement. On a modifié la vitesse de réduction du chlorate par l'addition d'un forte quantité d'électrolyte fort. On a évité la perte de chlore pendant le titrage de l'hypochlorite en utilisant une cellule d'électrolyse fermée.

LITERATUR

1. P. Gründler und H. Holzapfel, *Talanta*, 1971, **18**, 139.
2. *Idem, ibid.*, 1971, **18**, 246.
3. L. Meites, *Anal. Chem.*, 1952, **24**, 1057.
4. P. Gründler, *Dissertation*, Leipzig, Juli 1969.

Talanta, 1971, Vol. 18, pp. 155 to 164. Pergamon Press. Printed in Northern Ireland

MOLECULAR EMISSION CHARACTERISTICS OF VARIOUS FLUORIDES IN A LOW-TEMPERATURE-HYDROGEN DIFFUSION FLAME

R. M. DAGNALL, B. FLEET and T. H. RISBY
Chemistry Department, Imperial College of Science and Technology,
London, S.W.7., U.K.

D. R. DEANS
Imperial Chemical Industries Limited, Heavy Organic Chemicals
Division, Billingham, Teesside, U.K.

(*Received* 11 *March* 1970. *Accepted* 18 *June* 1970)

Summary—A capillary burner supporting a nitrogen/hydrogen diffusion flame has been evaluated as a possible means of detection for several volatile fluorides after their gas-chromatographic separation. The fluorides of As, B, C, Ge, I, Mo, P, Re, S, Sb, Se, Si, Te and W were formed by the reaction of the element with chlorine trifluoride, and the intense molecular emission given by each was recorded. An attempt was made to identify the emitting species.

THE GAS-CHROMATOGRAPHIC separation and determination of elements *via* reaction or complexation with halogen molecules or ligands has aroused considerable interest recently. Of special concern has been the separation of metal fluorides which, because of their corrosive character, cause special problems not only in their preparation and separation, but also in detection. Flame emission spectroscopy not only provides selectivity but also solves the problem of detection of corrosive materials. Juvet and Durbin[1,2] have proposed the use of a turbulent oxy-hydrogen flame burning on a total consumption burner for the selective detection, *via* molecular emission, of chromium, iron and rhodium hexafluoroacetylacetonates and titanium, arsenic and zirconium chlorides. Zado and Juvet,[3] in a similar study, used a filter and a monochromator photometric system to view the flame non-selectively and selectively to determine molybdenum and tungsten fluorides, tin chloride and aluminium, chromium and rhodium fluoroacetylacetonates. However, no details were presented of the spectra observed except the optimum wavelength of measurement for each element. Furthermore, it is probable that the range of elements which can be detected by using this type of flame is somewhat limited because the high temperature would tend to produce mainly atomic species.

A nitrogen/hydrogen diffusion flame supported on a burner into which aqueous solutions can be nebulized has been used in our laboratories for molecular emission studies of sulphur,[4] phosphorus,[5] tin,[6] and the halogens (except fluorine).[7] It was found that this type of flame provided an efficient reaction cell for the production of many excited (chemiluminescent) species. This communication describes a new type of capillary burner supporting a nitrogen/hydrogen diffusion flame which may be used for the selective and sensitive detection of relatively volatile fluorides, *viz.* those of antimony, arsenic, boron, carbon, germanium, iodine, molybdenum, phosphorus, rhenium, selenium, silicon, sulphur, tellurium and tungsten after a gas-chromatographic separation. An attempt is made to identify the molecular emitting species.

The fluorides may be prepared for gas-chromatographic purposes by the method described by Juvet and Fisher,[8] who reacted the element or its oxide, sulphide, carbide or other salt with fluorine on an electrically heated nickel filament in a specially designed reactor-injection vessel; the fluorides were flushed subsequently onto a PTFE column (packed with 15% w/w Kel-F oil No. 10 on Chromosorb T).

EXPERIMENTAL

Apparatus

The apparatus was designed to provide a continuous flow of gaseous fluoride which was then fed into the capillary burner (Fig. 1). The chlorine trifluoride was diluted with nitrogen in order to moderate the reaction, and flow-rate was controlled by two stainless-steel needle valves (Autoclave Engineers, Erie, Pennsylvania, U.S.A.) in series. The silica reaction tube used to prepare the fluorides could be heated to *ca.* 80° by an external fan heater. The fluorides were passed into the flame *via* a 1·27-mm stainless-steel capillary situated at the centre of a circular (10-mm diameter) emission burner-head. The head was connected *via* a screw thread to a stainless-steel cylindrical stem with two gas inlets at the base.

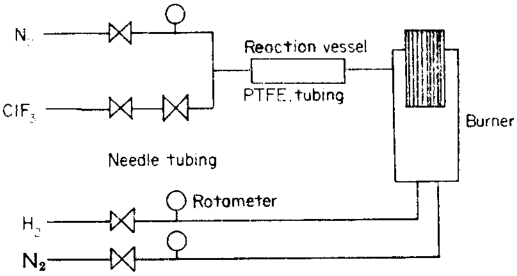

FIG. 1

The burner was similar in design to those previously used in our laboratories for atomic spectroscopic purposes,[9] and was made from 0·69-mm diameter hypodermic stainless-steel tubing cut into 36 20-mm lengths which were smeared with high-temperature resistant epoxy resin (Araldite type AY105 with hardener HY953F, Ciba Ltd.) and packed with the 1·27-mm sample inlet capillary at the centre. The epoxy resin was allowed to fill the interstitial gaps so that the gas flowed only inside the capillaries. The tube was left projecting about 6 mm above the level of the burner body to prevent overheating of the burner head. The tops of the individual capillaries were ground level once the resin hardened (Fig. 2). The gas flow-rates to the burner head and the reaction vessels were controlled and measured with rotameters.

The Beckman D.U. spectrophotometer used was modified by replacing the photocells with an 11-stage photomultiplier (E.M.I. 9601B), and the source and cuvette holder with the burner assembly. A wavelength drive motor was fitted to facilitate the plotting of spectra. The photomultiplier was powered by an E.H.T. stabilized power supply and the signal produced was displayed on to a 0–1 mV chart recorder. To reduce the background radiation, the flame was enclosed by a brass shield painted matt black.

Method

The E.H.T. supply was set to supply 1150 V and the dark current and background radiation were backed-off on the chart-recorder. About 0·5 g of the element to be studied was placed inside the silica reaction tube, and the nitrogen diluent gas was adjusted to a flow-rate of 100 ml/min. It is impossible to measure accurately the flow-rate of the chlorine trifluoride because of its high reactivity. In consequence it was adjusted to the minimum which was sufficient to give spontaneous and controlled reactions. The volatile fluorides thus produced passed directly into the low-temperature hydrogen diffusion flame (nitrogen and hydrogen flow-rates of 4·7 and 2·6 l./min. respectively) and a spectrum was recorded from 280 to 700 nm. The elements studied included As, B, C, Ge, I, Mo, P, Re, S, Sb, Se, Si, Te, U and W. Uranium was the only element investigated which did not give rise to either a line or band spectrum.

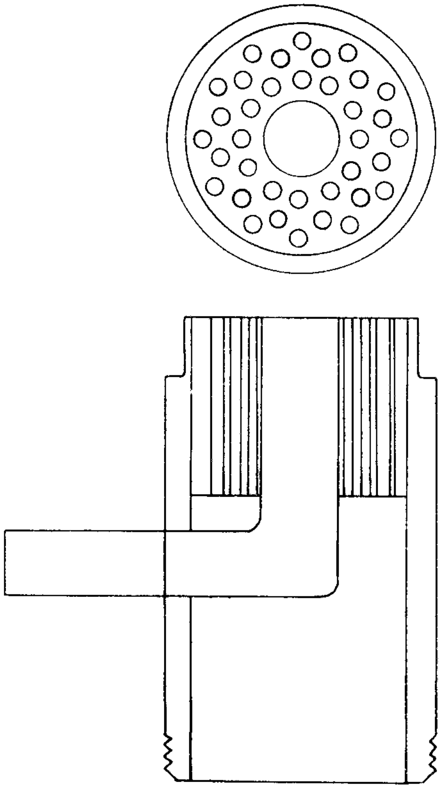

FIG. 2

RESULTS AND CONCLUSIONS

Spectra and species

Flame background. The only observed emission was a weak OH band head at *ca.* 301 nm. In the presence of chlorine trifluoride the OH background increased slightly. No other lines or bands were observed.

Antimony. Antimony was found to emit a broad continuum over the range 440–700 nm with a maximum at *ca.* 580 nm (Fig. 3). The only continuum reported,[10,11,12] obtained by using either arcs or a discharge tube, was found to occur over the range 450–700 nm and was attributed to the SbO species. A comparison with these spectra suggests that the continuum given in the low temperature flame is also due to the SbO species.

Arsenic. Arsenic gave a broad continuum with pronounced maxima over the range 360–600 nm (Fig. 4). The species responsible for the observed emission is not known.

Boron. Boron was found to give a banded emission (Fig. 5) which resembles the spectrum reported earlier[13] and attributed as perhaps due to the BO_2 species. It appears to be conclusive that the emission in the hydrogen diffusion flame is also due to the same species as in the oxy-hydrogen flame.

Carbon. Carbon emitted a broad continuum over the region 420–700 nm with a maximum at 560 nm. Emission from carbon in a discharge tube is well documented,[14] and a comparison of the spectra shows the spectrum to be due to the CO molecule.

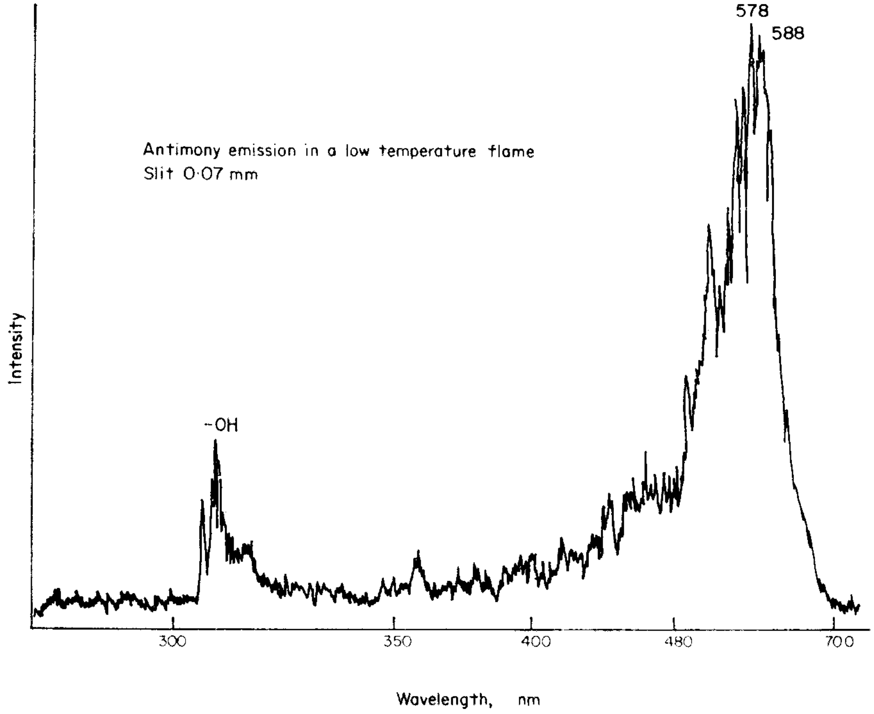
Antimony emission in a low temperature flame
Slit 0·07 mm
Intensity
-OH
578
588
300
350
400
480
700
Wavelength, nm

FIG. 3

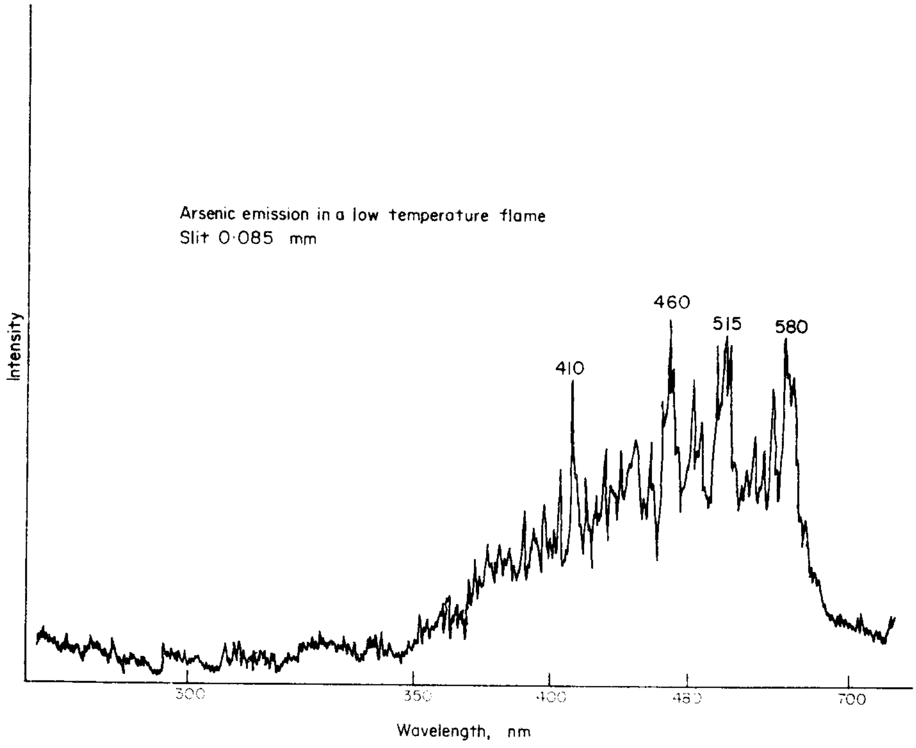
Arsenic emission in a low temperature flame
Slit 0·085 mm
Intensity
410
460
515
580
300
350
400
480
700
Wavelength, nm

FIG. 4

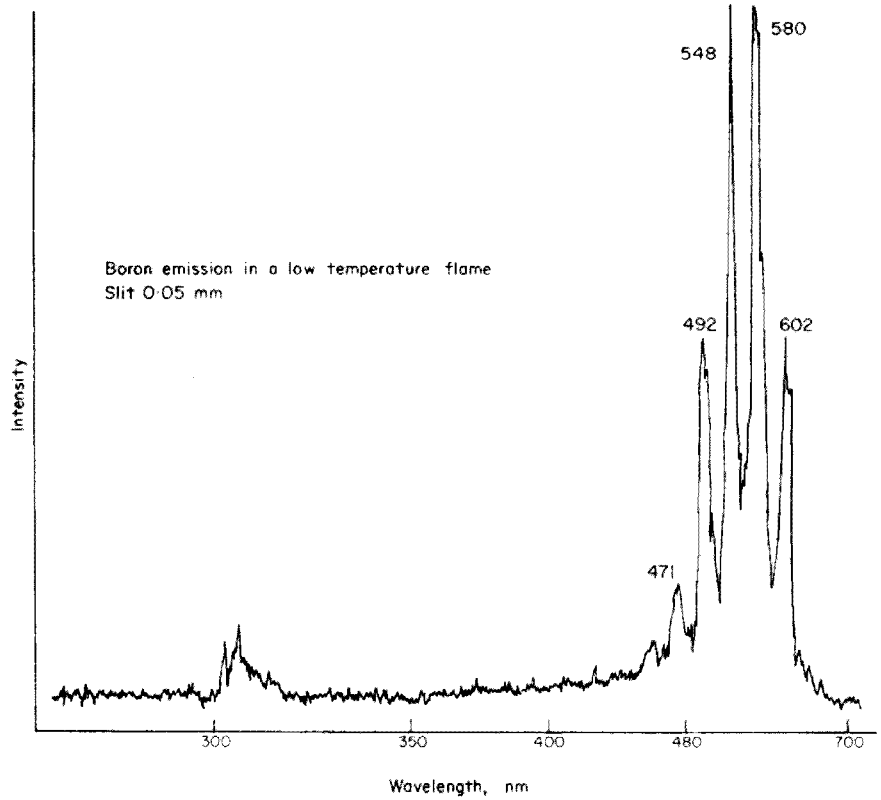

FIG. 5

Germanium. Germanium showed a continuum over the region 350–700 nm with a maximum at 458 nm. A continuum (270–480 nm) obtained from GeF_4 in a discharge tube was reported earlier,[15] and attributed to GeF, but did not correspond particularly well with that observed in this study, though a band head at 459 nm was mentioned. The continuum due to the GeO species has been examined only over the region 250–300 nm.[16]

Iodine. Iodine emitted a broad continuum over the region 490–700 nm with a maximum at 616 nm. This resembles the continuum (due to the IF species) given in a flame produced by the reaction between iodine and fluorine,[17] and also the continuum given by the IO species in an oxy-hydrogen flame.[18] It is probable that the spectrum emitted in the diffusion flame is a result of the presence of both these species.

Molybdenum. The broad continuum given over the region 490–700 nm with maxima at 580 and 622 nm (Fig. 6) is apparently due to excited MoO molecules. It closely resembles the spectrum given by the MoO species formed in an arc continuum over the region 480–660 nm with maxima at 522 and 630 nm,[19] and in a separated nitrous oxide–acetylene flame (band heads at 599·1, 601·0, 611·0, 612·2, 613·4, 614·7, 623·0 and 624·6 nm).[20]

Phosphorus. Phosphorus was found to emit a broad continuum over the region 420–700 nm with a maximum at 528 nm. This corresponds well with the continuum due to the H—P—O species,[5] in a similar hydrogen diffusion flame.

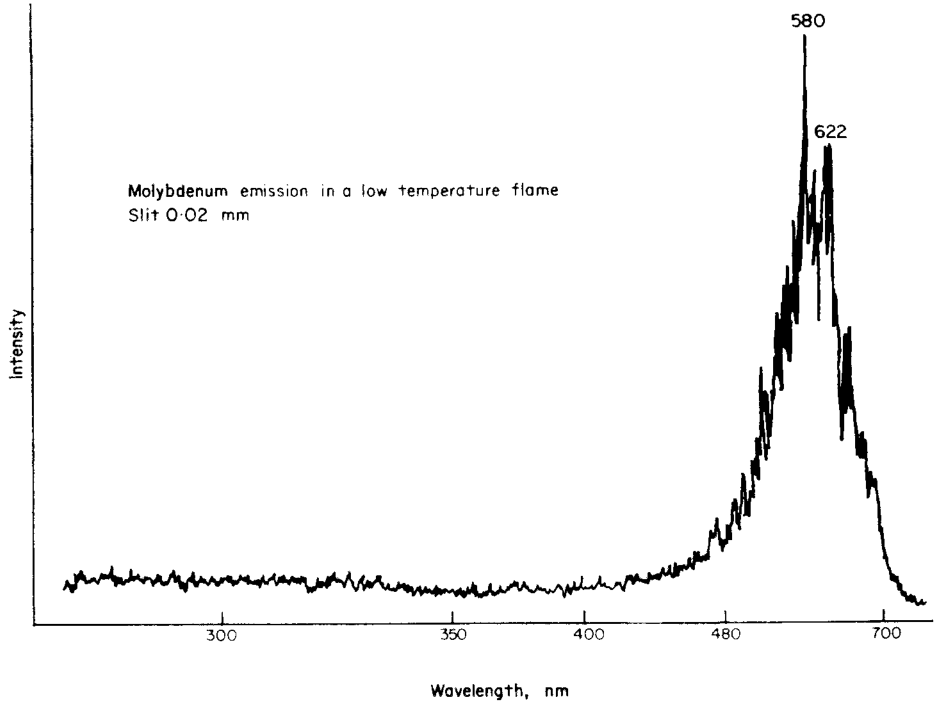

Fig. 6

Rhenium. Rhenium was found to emit a broad continuum over the region 400–700 (Fig. 7) with a maximum at 525 nm. No such molecular emission spectrum appears to have been reported previously for rhenium.

Selenium. Selenium gave a banded emission (Fig. 8) with eight principal band heads over the range 360–600 nm. This spectrum closely resembles that obtained from the SeO species in a hydrogen discharge tube,[21] and that obtained from the Se_2 molecule.[22,23]

Silicon. Silicon emitted a banded emission (Fig. 9) with six principal band heads over the range 400–700 nm. At least part of the spectrum can be attributed to the SiF species which has been obtained previously in discharge tubes.[24,25,26]

Sulphur. Sulphur was found to give a banded emission with numerous band heads over the range 340–480 nm, and these can be attributed to the S_2 molecule.[4]

Tellurium. Tellurium emitted a complex banded system over the region 360–700 nm (Fig. 10) with a maximum at *ca.* 525 nm. The only reported continuum appears to be due to the Te_2 species (occurring in a discharge tube)[27] over the region 490–640 nm and to the TeO species (also occurring in a discharge tube[23]) over the region 330–620 nm. It is not known which is the predominant species in the low-temperature hydrogen diffusion flame.

Tungsten. Tungsten was found to emit a broad continuum over the region 440–700 nm with maxima at 590 and 622 nm (Fig. 11). A similar continuum is reported over the same region with maxima at *ca.* 587, 590, 622, 626 and 630 nm for the WO species in an arc discharge.[28,29]

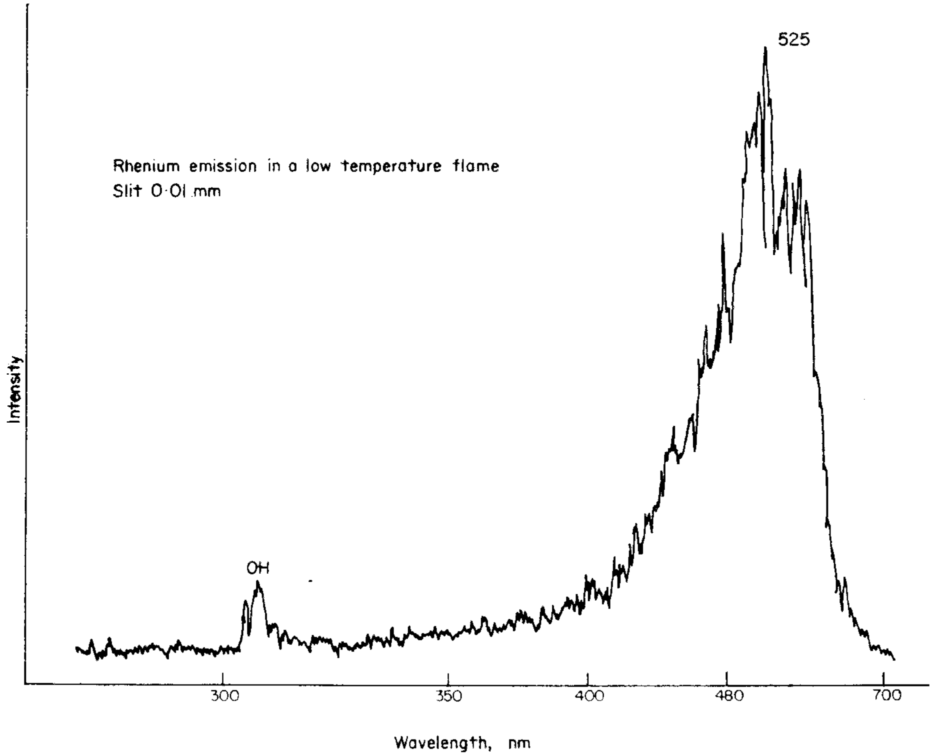
525
Rhenium emission in a low temperature flame
Slit 0·01 mm
OH
Intensity
300
350
400
480
700
Wavelength, nm

FIG. 7

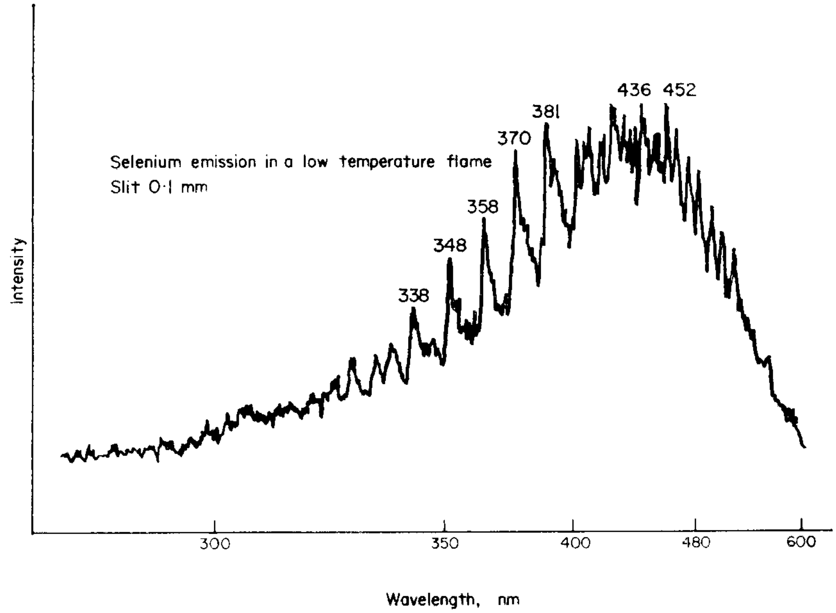
436 452
381
370
358
348
338
Selenium emission in a low temperature flame
Slit 0·1 mm
Intensity
300
350
400
480
600
Wavelength, nm

FIG. 8

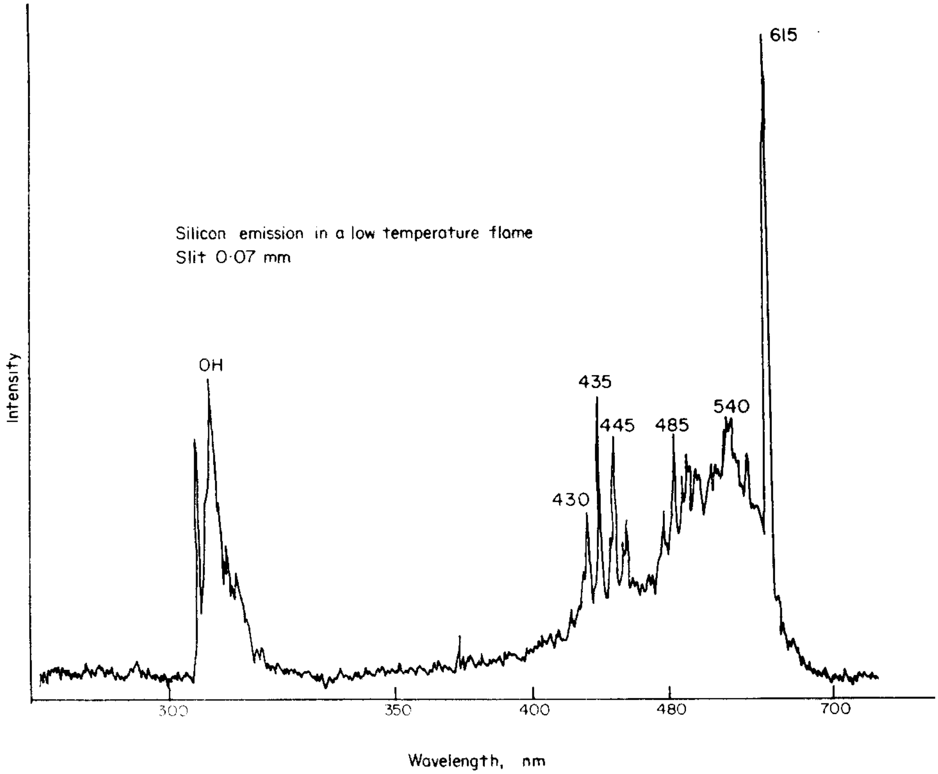
Silicon emission in a low temperature flame
Slit 0·07 mm
Intensity
OH
430
435
445
485
540
615
300
350
400
480
700
Wavelength, nm

FIG. 9

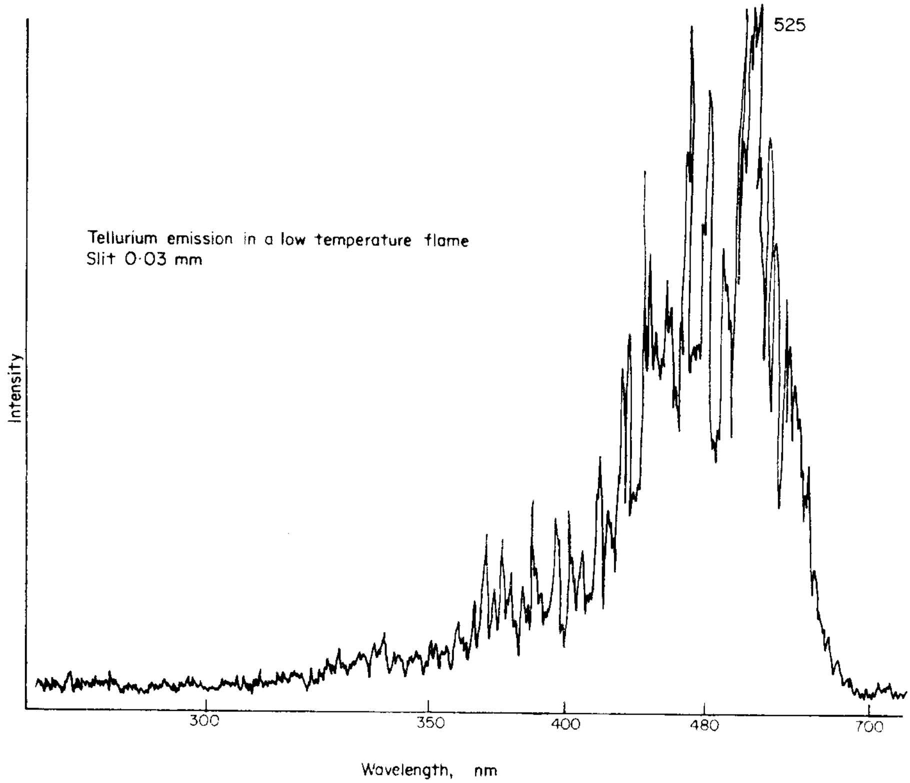
Tellurium emission in a low temperature flame
Slit 0·03 mm
Intensity
525
300
350
400
480
700
Wavelength, nm

FIG. 10

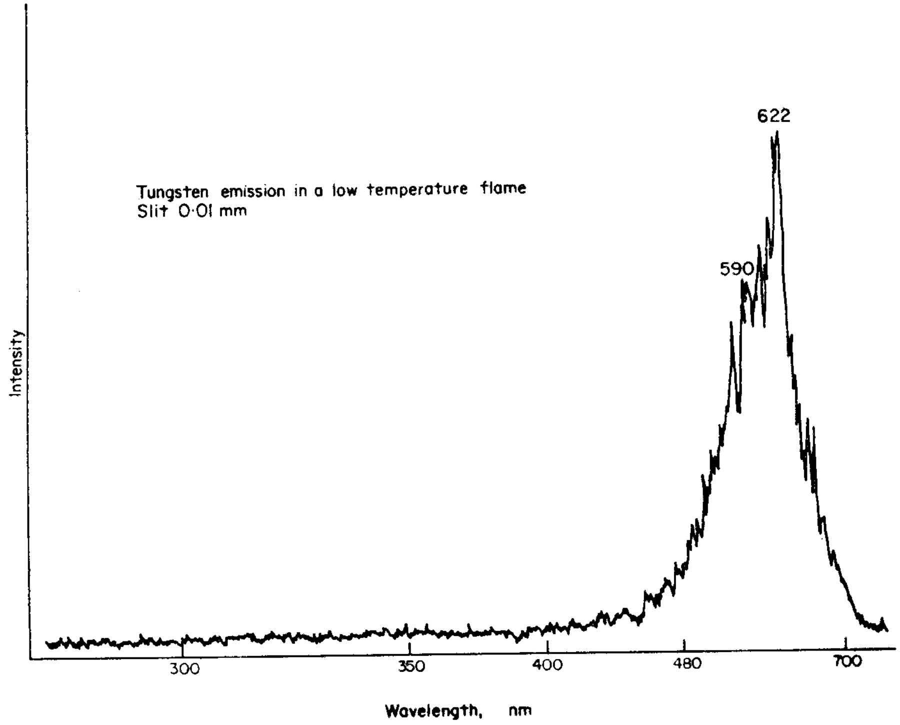

FIG. 11

Applications

Each of the fluorides examined (except that of uranium) gives rise to a specific molecular emission in the hydrogen diffusion flame. The emission for all elements except carbon is very intense and may be used qualitatively provided the fluorides are first separated on a gas-chromatographic column.[8] The very low background and noise given by the flame is advantageous and could allow the use of wide band-pass filters to achieve maximum sensitivity.

The predominant emitting species have been identified in all instances except for Ge and Re. For the elements As, Se and Te it is probable that more than one species is responsible for the emission observed, *e.g.*, the oxide and the diatomic fluoride. It is considered unlikely that any of the emissions observed can be attributed to particulate matter such as incandescent element or oxide particles.

The following wavelengths (in nm) should provide optimum results for both qualitative and quantitative purposes: Sb 580, As 460 (or 580), B 580 (or 548), C 560, Ga 458, I 616, Mo 580 (or 622), P 528, Re 525, S 374, 384 and 394, Se 381, 394, 436 and 452, Si 616, Te 525, W 622 (or 590).

Acknowledgements—We wish to thank Imperial Chemical Industries Limited, Heavy Organic Chemical Division, for the loan of the gas chromatograph and other equipment. We would also like to thank Southend-on-Sea Corporation for providing financial assistance to T. H. R.

Zusammenfassung—Ein Kapillarbrenner, der eine Stickstoff-Wasserstoff-Diffusionsflamme in Gang hält, kann möglicherweise als Nachweisinstrument für verschiedene flüchtige Fluoride nach ihrer gaschromatographischen Trennung dienen. Die Fluoride von As, B, C, Ge, J, Mo, P, Re, S, Sb, Se, Si, Te und W bildeten sich aus den Elementen und Chlortrifluorid; ihre intensiven molekularen Emissionen wurden registriert. Es wurde versucht, die emittierenden Spezies zu identifizieren.

Résumé—On a évalué un brûleur capillaire portant une flamme de diffusion azote-hydrogène en tant que moyen possible de détection de plusieurs fluorures volatils après leur séparation par chromatographie en phase vapeur. Les fluorures de As, B, C, Ge, I, Mo, P, Re, S, Sb, Se, Si, Te et W ont été formés par la réaction de l'élément avec le trifluorure de chlore, et l'on a enregistré l'émission moléculaire intense donnée par chacun d'eux. Un essai a été fait pour identifier l'espèce émettrice.

REFERENCES

1. R. S. Juvet and R. P. Durbin, *J. Gas Chromatog.*, 1963, **1**, 12, 14.
2. *Idem*, *Anal. Chem.*, 1966, **38**, 565.
3. F. M. Zado and R. S. Juvet, *ibid.*, 1966, **38**, 569.
4. R. M. Dagnall, K. C. Thompson and T. S. West, *Analyst*, 1967, **92**, 506.
5. *Idem*, *ibid.*, 1968, **93**, 72.
6. *Idem*, *ibid.*, 1968, **93**, 518.
7. *Idem*, *ibid.*, 1969, **94**, 643.
8. R. S. Juvet and R. L. Fisher, *Anal. Chem.*, 1966, **38**, 1860.
9. K. M. Aldous, R. F. Browner, R. M. Dagnall and T. S. West, *ibid.*, 1970, **42**, 939.
10. S. V. J. Lakshman, *Z. Physik*, 1960, **158**, 367.
11. *Idem*, *ibid.*, 1960, **158**, 386.
12. A. K. Sen Gupta, *Indian J. Phys.*, 1939, **13**, 145; 1944, **17**, 216.
13. W. E. Kaskan and R. C. Millikan, *J. Chem. Phys.*, 1960, **32**, 1273.
14. R. C. Johnson and R. K. Asundi, *Proc. Roy. Soc.*, 1929, **123**, 560.
15. E. B. Andrews and R. F. Barrow, *Proc. Phys. Soc.*, 1950, **A63**, 185.
16. W. Jevons, L. A. Bashford and H. V. A. Briscoe, *ibid.*, 1937, **49**, 543.
17. R. A. Durie, *Proc. Roy. Soc.*, 1951, **207**, 388.
18. E. H. Coleman, A. G. Gaydon and W. M. Vaidya, *Nature*, 1948, **162**, 108.
19. G. Piccardi, *Accad. Lincei. Atti.*, 1934, **17**, 654.
20. G. F. Kirkbright, A. Semb and T. S. West, *Talanta*, 1968, **15**, 441.
21. Choong Shin-Piaw, *Ann. Phys. Paris*, 1938. **10**, 173.
22. T. E. Nevin, *Phil. Mag.*, 1935, **20**, 347.
23. M. Miyanisi, *Inst. Phys. Chem. Res. Tokyo Res. Pap.*, 1940, 955.
24. R. C. Johnson and H. G. Jenkins, *Proc. Roy. Soc.*, 1927, **116**, 327.
25. R. K. Asundi and R. Samuel, *Proc. Indian Acad. Sci.*, 1936, **3**, 346.
26. E. H. Eyster, *Phys. Rev.*, 1937, **51**, 1078.
27. N. Durga Prasad and P. Tiruvenganna Rao, *Indian J. Phys.*, 1954, **28**, 549.
28. V. Vittalachar and S. G. Krishnamurty, *Current Sci. India*, 1954, **23**, 357.
29. A. Gatterer and S. G. Krishnamurty, *Nature*, 1952, **169**, 543.

Talanta, 1971, Vol. 18, pp. 165 to 173. Pergamon Press. Printed in Northern Ireland

MASSENSPEKTROMETRISCHE UNTERSUCHUNGEN ZUR ELEMENTARANALYSE ORGANISCHER VERBINDUNGEN—I

EINLASSSYSTEM ZUR ANALYSE VON GASEGMISCHEN IN GROSSEN TEMPERATUR- UND DRUCKBEREICHEN*

WALTER WALISCH® und OTTOKAR JAENICKE
Institut für Organische Chemie, Universität des Saarlandes, 66 Saarbrücken, B.R.D.

(*Eingegangen am* 12. *Juni*, 1970. *Angenommen am* 20. *Juli* 1970)

Zusammenfassung—Es wird gezeigt, daß ein einstufiger viskoser Einlaß eine genaue Proportionalität zwischen den Partialdrucken der betrachteten Komponenten in der bei Normaldruck vorliegenden Probe und den entsprechenden Ionenströmen garantiert, solange die Viskosität der Mischung sich nicht verändert. Dies ist nahezu immer dann der Fall, wenn eine der Komponenten in großem Überschuß als Trägergas vorliegt. Es wurde eine Gleichung hergeleitet, die das Verhalten dieses "quantitativen" Einlaßsystems beschreibt. Eine experimentelle Überprüfung bestätigt die sich aus der Einlaßgleichung ergebenden Abhängigkeiten. Die Kontrollmessungen zeigen darüberhinaus, wie vielseitig dieses schnelle und einfache Einlaßsystem, das in der Regel aus einer Quarzkapillare besteht, eingesetzt werden kann.

DIE QUANTITATIVE Bestimmung der in einer organischen Verbindung enthaltenen Elemente ist nach wie vor ein unentbehrliches Hilfsmittel bei der Aufklärung neuer Verbindungen. Bei dieser großen Bedeutung der Elementaranalyse und der steil ansteigenden Analysenzahl erscheint eine Weiterentwicklung der bekannten Verfahren dringend geboten und die Suche nach neuen Methoden gerechtfertigt.

Eine prinzipiell neue Methode ist beispielsweise die genaue Bestimmung der Masse des Moleküls mit einem doppelfokussierenden Massenspektrometer, die, wie Beynon[1] gezeigt hat, in vielen Fällen eine eindeutige Schlußfolgerung auf die Molekularformel zuläßt. Allerdings erfordert diese Art der Bestimmung der prozentualen Zusammensetzung schon bei einem Molekulargewicht von 200 eine Auflösung des Massenspektrometers von etwa 10^5. Der hierzu erforderliche Aufwand sowie die bekannten Schwierigkeiten in der Feststellung des Molekülpeaks lassen es ungewiß erscheinen, ob diese Art der Elementaranalyse Bedeutung erlangen wird.

Vorerst sind die Verbesserungen (Verkleinerung der Probemenge, weitgehende Automatisierung, Schnelligkeit und die Möglichkeit der Bestimmung von Kohlenstoff, Wasserstoff und Stickstoff mit einer Einwaage), die beispielsweise durch die von uns entwickelten Ultramikroverfahren[2-6] erzielt wurden, sicher von größerer Bedeutung für die Praxis. Eine weitere Verkleinerung der Einwaage, eine nochmalige Verkürzung der Analysendauer sowie die gleichzeitige Bestimmung von allen in der Verbindung enthaltenen Elementen (Total-Elementaranalyse) erscheinen uns jedoch mit den beschriebenen Meßverfahren[2-6] kaum möglich. Will man auf die bekannten Vorteile, welche ein Aufschluß der Probe durch Verbrennung gewährleistet, nicht verzichten, so muß die angestrebte Erweiterung und Verbesserung der Elementaranalyse

---

* Teil der Dissertation von O. Jaenicke, Saarbrücken, 1969.

in der Anwendung anderer Meßprinzipien bei der Bestimmung der für jedes Element charakteristischen Verbrennungsprodukte liegen.

Ein solches Meßprinzip stellt beispielsweise die Massenspektrometrie dar, die es unter entsprechenden Bedingungen erlauben müßte, kleinste Mengen eines Vielkomponenten-Gasgemisches ohne vorausgehende Trennung schnell und genau zu analysieren. Darüberhinaus wären so auch die Isotopengehalte der in organischen Verbindungen vorkommenden Elemente zu bestimmen. Allerdings fehlen der Massenspektrometrie bei der Verwendung zur Gasanalyse zur Zeit noch geeignete Einlaßsysteme, die eine schnelle und proportionale Überführung der Gase in die Ionenquelle garantieren, und es ist zu befürchten, daß die Langzeitkonstanz aller für die Empfindlichkeit bedeutsamen Parameter (Ionenquelle, Versorgungs- und Anzeigeelektronik) noch ungenügend ist.

Ziel dieser Arbeit ist es,

- —ein dynamisches Einlaßsystem zu entwickeln, bei dem die Komponentenpartialdrucke in der Ionenquelle streng proportional den entsprechenden Partialdrucken in der bei Normaldruck vorliegenden Probe sind,
- —unter Anwendung dieses Einlaßsystems Verbrennungsvorgänge unter "elementaranalytischen Verbrennungsbedingungen" zu untersuchen,
- —Meßbedingungen für analytisch verwertbares, strukturspezifisches Verbrennungsverhalten zu finden,
- —Kinetik und Mechanismen von Verbrennungsreaktionen aufzuklären,
- —die Verwendung von Klein-Massenspektrometern bei der Vielfach Elementaranalyse zu ermöglichen.

THEORETISCHE GRUNDLAGEN

Soll die quantitative Zusammensetzung zeitlich veränderlicher Gasmischungen, die bei Atmosphärendruck vorliegen, mittels eines Massenspektrometers momentan und genau angezeigt werden, so kann die sonst übliche statische Druckreduktion nicht eingesetzt werden. Vielmehr muß fortlaufend mittels einer geeigneten dynamischen Druckreduktion ein repräsentativer Anteil der Gasmischung in die Ionenquelle geleitet werden.

Bei analoger Problemstellung[7] arbeitet man häufig mit der zweistufigen Kombination* von viskosem- mit molekularem Einlaß,[8] da man offensichtlich die jeweiligen einstufigen Systeme[9] für ungeeignet hält. Dabei bedingen zweistufige Einlaßsysteme einen wesentlich höheren Aufwand, der zusätzliche Störgrößen mit sich bringt; der Arbeitsbereich ist durch eine starke Abhängigkeit der Proportionalitätsfaktoren von der Viskosität und dem Molekulargewicht sehr begrenzt, und der Probenbedarf ist für viele Anwendungsmöglichkeiten zu hoch.

Ein mit adiabatischer Gasströmung arbeitendes einstufiges System[10] vermeidet zwar einige der oben genannten Nachteile, doch hängen hier die Proportionalitätsfaktoren vom mittleren Molekulargewicht und vom Verhältnis der Molwärmen C_p/C_v ab.

Eine von Greene und Milne[11] vorgeschlagene Einlaßapparatur scheint dagegen allen Genauigkeitsanforderungen zu genügen. Der apparative Aufwand ist jedoch sehr groß (allein zwei Vorvakuumpumpen und zwei Hochvakuumpumpen) und die Empfindlichkeit trotz des großen Probenverbrauchs wegen des niedrigen Ausnutzungsgrades sehr gering.

---

* Einlaßsystem CS 3 der Firma VARIAN-MAT, Bremen.

Bei der Gasanalyse von Isotopengemischen hat sich ein einstufiger viskoser Einlaß gut bewährt. In diesem Sonderfall ist die Viskosität praktisch unabhängig von der Zusammensetzung, so daß verhältnismäßig einfache Gesetzmäßigkeiten zu erwarten sind, die allerdings bei Kistemaker[12] nicht voll zum Tragen kommen können, da die Einlaßkapillare über ein zu großes Totvolumen mit dem Probenvorrat verbunden ist.

Da sich die Viskosität eines Gasgemisches mit der Zusammensetzung kaum ändert, solange eine Komponente in großem Überschuß vorhanden ist (Trägergas) müßte eigentlich ein verbesserter viskoser Einlaß unseren Anforderungen genügen, denn die zu bestimmenden Verbrennungsprodukte liegen in einem Trägergas vor. Neben der Einfachheit sollte dieser Einlaßtyp noch folgende Vorteile gegenüber den sonst üblichen Systemen besitzen:

—kurze Ansprechzeit,
—kontinuerlichie Probenahme möglich,
—keine Fraktionierung im Vorratsgefäß durch die Probenahme,
—anwendbar in großen Temperatur- und Druckbereichen,
—verhältnismäßig unempfindlich gegen Verschmutzung und leicht zu reinigen,
—mit geringen Kosten für die verschiedensten Aufgabenstellungen selbst herstellbar.

Die Eigenschaften und Grenzen dieses Einlaßsystems lassen sich mittels der auch von Kistemaker[12] verwendeten Ausgangsgleichung (1) herleiten, welche die Beziehung zwischen dem Partial-Gasmengenstrom q^i [Torr. l/sec] und dem entsprechenden Partialdruck $p_4{}^i$ (vergleiche Abb. 1) sowie dem Summendruck P_4 [Torr] auf der Hochdruckseite einer Einlaßkapillare EK angibt. Gleichung (1) folgt aus dem Hagen-Poiseuilleschen Gesetz bei laminarer Strömung in ein Vakuum.

$$q_{4-5}^i = P_4 \cdot p_4{}^i/\eta \cdot K_{4-5} \tag{1}$$

Hierbei bedeuten K_{4-5} die Kapillarenkonstante* für viskose Strömung und η [Poise] die Viskosität der Gasmischung. Durch die sich an EK anschließende Vakuumleitung und die Ionenquelle 5 strömt das Gasmisch molekular in den Massenspektrometerraum 6, und der Partial-Gasmengenstrom hängt gemäß Gleichung (2) vom jeweiligen Molekulargewicht M^i, der Temperatur T [K] und der Leitungskonstanten† w_{5-6} ab.[13]

$$q_{5-6}^i = (p_5{}^i - p_6{}^i) \cdot (M^i/T)^{-1/2}/w_{5-6} \tag{2}$$

Bei Temperaturgleichheit muß, nach Einstellung des Gleichgewichts, $q_{5-6}^i = q_{4-5}^i$ sein, und durch Kombination von (1) und (2) erhält man in (3) den Druck $p_5{}^i$ der betrachteten Komponente i in der Ionenquelle.

$$p_5{}^i = p_6{}^i + (w_{5-6}/K_{4-5})(M^i/T)^{1/2} \cdot P_4 \cdot p_4{}^i/\eta \tag{3}$$

Faßt man alle Leitungskonstanten zwischen Massenspektrometerraum 6 und Diffusionspumpe 7 unter w_{6-7} zusammen, und benutzt man den der Leitungskonstanten vergleichbaren Ausdruck der Pumpenkonstanten‡ $d = (T)^{1/2}/D$, so ergibt sich der

---

* Im Falle zylindrischer, gerader Rohre gilt bekanntlich: $K = 2L/0{,}52 \cdot r^4 [1^{-1}]$ wenn Länge L und Radius r in [cm] eingesetzt werden.

† Bei zylindrischen, geraden Rohren kann der Betrag von w_{5-6} nach $w_{5-6} = L/30{,}5 \cdot r^3$ berechnet werden. Aus der Leitungskonstanten ergibt sich für die Gasart i der Strömungswiderstand bei der Temperatur T zu $W_{5-6} = w_{5-6}(M^i/T)^{1/2}$.

‡ Üblicherweise wird die Sauggeschwindigkeit einer Diffusionspumpe $s^i = D(M^i)^{-1/2}$ [1/sec] mit D als Pumpenkonstanten angegeben.

Druck in 6 zu:

$$p_6^i = q_{4-5}^i(M^i/T)^{1/2}(w_{6-7} + d) \tag{4}$$

Durch Kombination der Gleichungen (1), (3) und (4) erhält man mit $w = (w_{5-6} + w_{6-7} + d)$ die gesuchte Beziehung:

$$p_5^i = (w/K_{4-5})(M^i/T)^{1/2} \cdot P_4 \cdot p_4^i/\eta \tag{5}$$

Bei konstantem Summendruck und gleichbleibender Viskosität ist demnach im Strömungsgleichgewicht der Partialdruck in der Ionenquelle dem jeweiligen Partialdruck vor der Einlaßkapillare proportional, solange die Temperaturgleichheit des gesamten Systems gewährleistet ist. In der Praxis muß jedoch mit erheblichen Unterschieden zwischen der Temperatur T_K der Einlaßkapillare und der Temperatur T_w der Strömungswiderstände im Massenspektrometer- und Pumpenbereich gerechnet werden. Mit $q_{T_w} = q_{T_K} \cdot T_w/T_K$ ergibt sich bei Durchführung des bisherigen Rechenganges die Endgleichung:

$$p_5^i = (w/K_{4-5})(M^i \cdot T_w)^{1/2} \cdot P_4 \cdot p_4^i/\eta \cdot T_K \tag{6}$$

Unter günstigen Bedingungen[1] ist der Ionenstrom I^i in einem weiten Druckbereich dem entsprechenden Partialdruck in der Quelle proportional.* Bei Verwendung der üblichen Elektrometerverstärker (Arbeitswiderstand R) ergibt sich, unter Zusammenfassung der verschiedenen Apparatekonstanten in $C^i = E_5^i \cdot R \cdot w/K_{4-5}$, in der Einlaßgleichung (7) die gesuchte Beziehung zwischen der Ausgangsspannung U^i und den wesentlichen Parametern.

$$U^i = C^i(M^i \cdot T_w)^{1/2} \cdot P_4 \cdot p_4^i/\eta \cdot T_K \tag{7}$$

Es müßte also in einem weiten Bereich Proportionalität zwischen der leicht und sehr genau meßbaren Ausgangsspannung U^i und dem Eingangspartialdruck p_4^i bestehen, wenn es gelingt, die verschiedenen Faktoren konstant zu halten. Besonders günstig sind die Bedingungen bei einer weitgehend geschlossenen Ionenquelle, da dort $w_{5-6} \gg (w_{6-7} + d)$ ist, sodaß die unvermeidbaren Schwankungen der Saugleistung des Pumpsystems (Kühlfallen, Baffles usw.) keine nachteiligen Folgen haben.

EXPERIMENTELLE ÜBERPRÜFUNG DER EINLAßGLEICHUNG

Zur Absicherung der theoretischen Überlegungen erschien eine experimentelle Kontrolle der aus Gleichung (7) folgenden Abhängigkeiten zwischen der Ausgangsspannung und den wichtigsten Variablen—Summendruck P_4, Partialdruck p_4^i und Temperatur der Einlaßkapillare T_K—angebracht und zwar unter Bedingungen, die denen der späteren Verwendung möglichst nahe kommen sollten.

Die hierzu konzipierte Kontrolleinrichtung ist in Abb. 1 dargestellt. Das Gasgemisch wird dynamisch in der Mischkammer 4 dadurch erzeugt, daß gleichzeitig die konstanten Gasmengenströme Q_{1-4}, Q_{2-4} und Q_{3-4} verschiedener reiner Gase durch die entsprechenden Dosierkapillaren DK_{1-4} und DK_{2-4} und DK_{3-4} in 4 einströmen. Von dort gelangt das Gemisch an der Öffnung der Einlaßkapillare EK vorbei durch das diese umgebende Schutzrohr SR (ϕ_i *ca.* 3 mm) bei A ins Freie, sodaß der Summendruck P_4 in der Mischkammer und damit am Eingang von EK immer gleich dem

---

* Der Proportionalitätsfaktor, durch dessen Maximalwert üblicherweise die interne Empfindlichkeit E_5^i[Amp/Torr] des Massenspektrometers gekennzeichnet wird, hängt allerdings sehr stark von den Ionenquellenparametern (Elektronenstrom, Fokussierung, Spaltweiten usw.) ab.

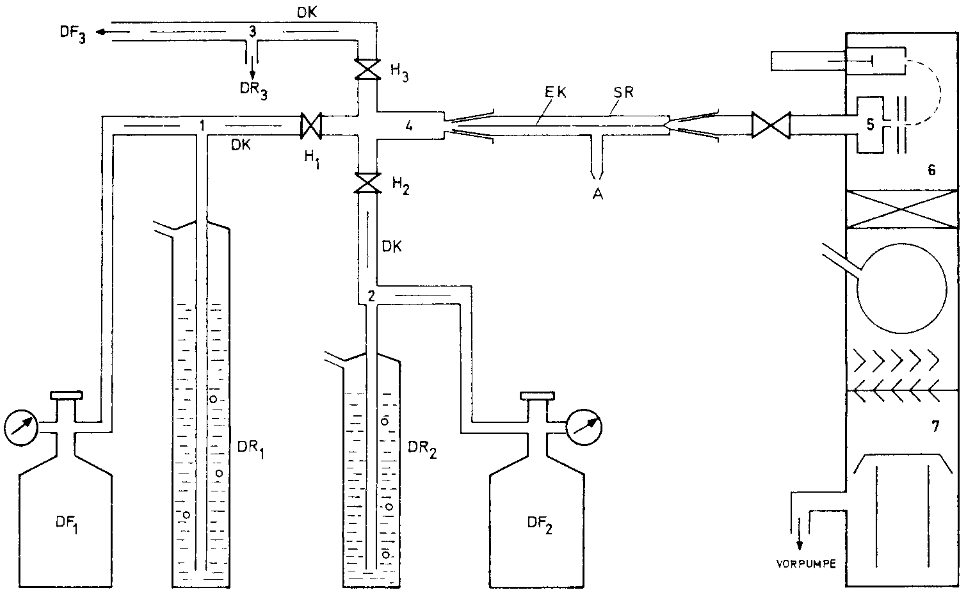

ABB. 1.—Schema der Kontrolleinrichtung (Siehe Text).

konstanten Atmosphärendruck P_A ist, und gleichzeitig ein Eindringen von Gasen aus der Atmosphäre wirksam verhindert wird.

Die Konstanz der verschiedenen Gasmengenströme (Q_{1-4}, Q_{2-4} und Q_{3-4}) wird durch konstante Überdrucke* (P_1, P_2 und P_3) an den entsprechenden Dosierkapillaren erreicht.[2] Die sich in 4 einstellenden Partialdrucke ergeben sich aus den durch Einzelmessungen bestimmten Teilgasströmen und der Summe Q_4 dieser Teilströme gemäß Gleichung (8).

$$p_4{}^i = P_4 \cdot Q_{i-4}/Q_4 \tag{8}$$

Zur Überprüfung des Einflusses von P_4 bleiben H_2 und H_3 geschlossen und ein Gasgemisch bekannter Zusammenstzung ist in DF_1 enthalten. Von hier strömt es durch die Mischkammer, an der Öffnung der Einlaßkapillare vorbei, über eine an A angeschlossene zusätzliche Wassersäule der Höhe ΔP ins Freie. Damit wird $P_4 = P_A + \Delta P$. Wenn der Molenbruch der untersuchten Komponente x^i beträgt, dann ist $p_4{}^i = P_4 \,.\, x^i$, d.h., unter diesen Bedingungen müßte gemäß Gleichung (7) die Ausgangsspannung U^i dem Quadrat von P_4 proportional sein.

Die Einlaßkapillare ist aus Quarz gezogen und wird, zur Untersuchung der T_K-Abhängigkeit, in einen elektrisch beheizten Rohrofen, der in diesem Fall als Mischkammer dient, eingebracht. Auch hier wird die Untersuchung mit einem in DF_1 enthaltenen Gemisch durchgeführt. Dabei wird der durch Temperaturänderung bedingten Viskositätsänderung dadurch Rechnung getragen, daß die nach (7) zu erwartende Konstanz von $(U^i \eta T_K)$ überprüft wird. Die benötigten Viskositäten wurden durch Interpolation der von Trautz und Mitarb.[14] mitgeteilten Werte gewonnen.

---

* P_1, P_2 und P_3 sind durch Veränderung der Höhe der Wassersäulen in den entsprechenden Druckausgleichsrohren DR sehr genau einstellbar.

Die in den Tabellen I–IV angeführten Ergebnisse einiger typischer Meßreihen beweisen, daß Gleichung (7) die Eigenschaften der Einlaßkapillare in den wesentlichen Punkten richtig wiedergibt. Dies konnte durch zahlreiche weitere Meßreihen bestätigt werden, bei denen unter anderem für Sauerstoff und Helium im Träger Stickstoff; Sauerstoff im Träger Helium sowie Helium, Kohlendioxid, Kohlenmonoxid und Methan im Träger Sauerstoff die Proportionalität zwischen Eingangspartialdruck $p_4{}^i$ und Ausgangsspannung U^i überprüft wurde.

TABELLE I.—PARTIALDRUCKEMPFINDLICHKEIT MIT EINER FREMDGASKOMPONENTE; $P_4 = P_A = 730$ Torr

(*a*) Stickstoff in Helium			(*b*) Kohlendioxid in Helium			(*c*)* Methan in Stickstoff		
p_{N_2}, *Torr*	U_{28}, *mV*	$\frac{U_{28}}{p_{N_2}}$, $\frac{mV}{Torr}$	p_{CO_2}, *Torr*	U_{44}, *mV*	$\frac{U_{44}}{p_{CO_2}}$, $\frac{mV}{Torr}$	p_{CH_4}, *Torr*	U_{16}, *mV*	$\frac{U_{16}}{p_{CH_4}}$, $\frac{mV}{Torr}$
4,80	177	36,87	3,93	107	27,22	10,8	330	30,5
8,01	295	36,84	5,87	164	27,93	22,0	655	29,8
11,20	413	36,87	7,84	220	28,06	32,5	975	30,0
14,42	533	36,98	9,81	273	27,82	43,2	1300	30,1
17,61	650	36,91	11,81	325	27,51	53,6	1625	30,3
20,82	769	36,93	13,79	376	27,26	64,3	1935	30,1
22,40	827	36,92	14,79	400	27,04			
24,02	884	36,80	15,79	427	27,04			

* Diese Meßreihe entstammt der Dissertation von G. Humme, Saarbrücken, 1970. Sie wurde mit dem Massenspektrometer CH-5 der Firma VARIAN-MAT, Bremen, aufgenommen.

TABELLE II.—PARTIALDRUCKEMPFINDLICHKEIT MIT ZWEI FREMDGASKOMPONENTEN; STICKSTOFF IN (HELIUM-KOHLENDIOXID) $P_4 = 728$ Torr

p_{N_2} *Torr*	U_{14} *mV*	U_{14}/p_{N_2} *mV/Torr*	p_{CO_2} *Torr*	U_{44} *mV*	U_{44}/p_{CO_2} *mV/Torr*
6,27	209	33,33	14,66	3453	235,5
9,41	315	33,48	14,60	3429	234,9
12,54	422	33,65	14,53	3416	235,1
15,70	530	33,76	14,47	3411	235,7
17,26	585	33,89	14,44	3408	236,0
18,83	642	34,09	14,41	3402	236,1
21,96	739	33,65	14,34	3392	236,5
23,55	792	33,63	14,31	3384	236,5

TABELLE III.—SUMMENDRUCKABHÄNGIGKEIT; STICKSTOFF IN HELIUM; x_{N_2} = konst. = 0,022

P_4, *Torr*	U_{28}, *mV*	$U_{28}/(P_4)^2$, *mV/Torr*^{2}
755,7	1335	0,00234
763,0	1365	0,00234
770,4	1392	0,00235
777,7	1419	0,00235
785,0	1444	0,00234
792,4	1480	0,00236
799,7	1517	0,00237

TABELLE IV.—TEMPERATURABHÄNGIGKEIT; STICKSTOFF IN SAUERSTOFF; x_{N_2} = konst. = 0,011

T_K, K	U_{28}, mV	η_{O_2}, $\mu Poise$	$U_{28}\cdot\eta\cdot T_K$, $mV\cdot K\cdot Poise$
723	1258	383	348
759	1168	395	350
835	1000	421	351
910	865	444	349
969	782	462	350
1023	720	478	352
1060	683	488	353
1091	657	497	356

In allen untersuchten Fällen ist allerdings die eingangs gemachte Voraussetzung erfüllt, daß die Viskosität des Trägergases durch die Fremdgaszusätze kaum[15] verändert wird. Wie Heath[16] gezeigt hat, ist die Änderung der Viskosität mit der Zusammensetzung in der Nähe der reinen Komponenten oft erheblich kleiner, als aufgrund der Viskositäten der reinen Komponenten zu erwarten wäre. So ist beispielsweise die Viskosität von Helium mit einem Stickstoffgehalt von 20% um weniger als 1% von der des reinen Heliums verschieden. Lediglich Wasserstoff ändert die Viskosität als Folge geringer Fremdgaszusätze verhältnismäßig stark, sodaß die Verwendung von Wasserstoff als Träger nur bei Berücksichtigung der Nichtlinearität möglich ist.

Die in Tabelle I erkennbare ausgezeichenete Proportionalität* zwischen dem äußeren Partialdruck $p_4{}^i$ und der Ausgangsspannung des Massenspektrometers U^i beweist, daß mit dieser einstufigen, viskosen Druckreduzierung durch eine Kapillare ein für sehr viele Aufgabenstellungen geeignetes Einlaßsystem zur Verfügung steht. Die Konstanz der "externen Partialdruckempfindlichkeit" $E_i = U^i/p_4{}^i$ ist insbesondere in Tabelle I.*a*), die mit extremer Sorgfalt vermessen wurde, so gut, daß alle vernünftigen Genauigkeitsanforderungen erfüllbar sein werden. Die in den anderen Tabellen erkennbaren größeren Schwankungen in E_i sind teilweise darauf zurückzuführen, daß bei den entsprechenden Versuchen die Messung von Q_1 und Q_2 nicht mit der gleichen nur sehr umständlich zu realisierenden Genauigkeit erfolgte, wie bei Tabelle I.*a*).

Die Kohlendioxidempfindlichkeit E_{CO_2} ist in Tabelle II nahezu zehnmal größer als in Tabelle I. Dies ist auf eine Änderung der internen Massenspektrometerempfindlichkeit $E_5{}^i$ durch Optimierung der Fokussierung zurückzuführen. Es wurde manchmal aber auch festgestellt, daß $E_5{}^i$ sich ohne äußere Ursache änderte. Insbesondere nach Wiedereinschalten der Ionenquelle war es nahezu unmöglich, den gleichen Wert von $E_5{}^i$ zu reproduzieren. Im übrigen zeigt Tabelle II, daß die unterschiedlichen Stickstoffgehalte die Kohlendioxidempfindlichkeit nicht beeinflussen. Bei optimaler Einstellung des Massenspektrometers ist $E^{44}_{CO_2}$ mit 235 mV/Torr so hoch, daß CO_2-Partialdrucke von 0,01 Torr in einem Trägergas bei 1000 Torr noch einfach nachweisbar sind. Bei entsprechend niedrigem Untergrund und der Verwendung eines Sekundärelektronenvervielfachers anstelle des Faraday-Fängers, kann die Nachweisgrenze sicher noch wesentlich weiter herabgesetzt werden.

Die in den Tabellen III und IV zum Ausdruck kommenden Summendruck- und

---

* Mit Ausnahme der Tabelle I.*c*) wurden alle hier wiedergegebenen Resultate mit dem Massenspektrometer THN 205 E der Firma Thomson-Houston, Paris (Auflösung bei 10% Tal etwa 70), gefunden. Wir danken der Herstellerfirma für die leihweise Überlassung des Gerätes.

Temperaturabhängigkeiten bestätigen ebenfalls die Gültigkeit der Gleichung (7). Damit ist einerseits die Möglichkeit gegeben, kleine Schwankungen in P_A und T_K rechnerisch zu berücksichtigen, und andererseits ist hiermit nachgewiesen, daß die Kapillare auch bei höheren Drucken und bis zu sehr hohen Meßtemperaturen einsetzbar ist.

SCHLUẞBETRACHTUNG*

Die beschriebene Einlaßkapillare erfüllt alle von uns an ein dynamisches Einlaßsystem gestellten Anforderungen. Die durch die Kapillare selbst bedingte Einstellzeit bei sprunghafter Änderung von $p_4{}^i$ ist etwa 0,1 sec und damit vernachlässigbar gegenüber anderen Zeitkonstanten des Meßsystems (Zeitkonstante des Elektrometerverstärkers, Einstellzeit des Schreibers, Einstellung des $p_6{}^i$-Gleichgewichts im Massenspektrometerraum bei Komponenten die zu einem merklichen Teil an der Massenspektrometeroberfläche adsorbiert werden usw.). Damit ist auch die Möglichkeit gegeben, schnell ablaufende Veränderungen der Zusammensetzung von Gasgemischen messend zu beobachten und zwar auch unter extremen Bedingungen hinsichtlich Druck und Temperatur. So können, wie wir in einer der folgenden Arbeiten noch ausführlich zeigen werden, beispielsweise die Vorgänge bei der Verbrennung organischer Verbindungen unter verschiedenen bei der Elementaranalyse üblichen Bedingungen in jeder Phase des Geschehens qualitativ und quantitativ erfaßt werden.

Der Verbrauch an Probegas ist mit etwa 0,001 ml/sec so gering, daß das untersuchte System und der zu beobachtende Vorgang durch die Entnahme nur geringfügig beeinflußt werden. Die Kapillare kann als feine Meßsonde ausgebildet und fast überall so eingebracht werden, daß ihre Anwesenheit nicht stört. Insbesondere kann mittels einer Einlaßkapillare des geschilderten Typs auch die Kopplung zwischen Gaschromatograph und Massenspektrometer in einfachster Weise bewerkstelligt werden. Selbstverständlich arbeitet das System auch in diesem Fall "quantitativ" und ist mindestens in dieser Hinsicht den gebräuchlichen Typen überlegen.

Neben der generellen Möglichkeit, diesen Einlaß zur Prozeßkontrolle und -regelung mittels geeigneter Massenspektrometer überall dort einzusetzen, wo der Prozeß durch die ständige Überprüfung der Zusammensetzung gasförmiger Proben überwacht werden kann, gestattet diese Einlaßkapillare in einfachster Weise die routinemäßige Analyse von komprimierten Gasen. Hierzu wird die betreffende Druckgasflasche unmittelbar über ein Metallkapillarrohr mit dem Schliff der Einlaßkapillare verbunden. Die Metallkapillare ist so zu dimensionieren, daß bei dem vorhandenen Flaschendruck einige ml/sec an EK vorbei bei A ins Freie strömen. Die Eichung erfolgt in diesem und anderen Fällen am günstigsten dadurch, daß von Zeit zu Zeit ein in einer Druckflasche befindliches Eichgasgemisch, das alle infrage kommenden Komponenten enthält, in analoger Weise an EK angeschlossen bzw. über ein entsprechendes "Umpolventil" auf die Einlaßkapillare gegeben wird. Auf diese Weise werden alle Einflußgrößen mit erfaßt, und die gemessenen Werte haben ein Höchstmaß an Sicherheit.

Summary—It has been shown that a single-stage, viscous inlet system ensures under certain conditions accurate proportionality between the partial pressures of the components in a sample at normal pressure and the corresponding ion currents. The main condition is that the

---

* Wir danken dem "Fonds der chemischen Industrie" für die Förderung dieser Arbeit.

viscosity of the mixture does not change with the composition; this is nearly always the case when one of the components is present in large excess as carrier gas. An equation has been derived which describes the behaviour of this "quantitative" inlet system. Experimental testing has confirmed the validity of this inlet equation and demonstrates, moreover, the wide range of application of this simple and rapid inlet system, consisting usually of a quartz capillary.

Résumé—On a montré qu'un système d'introduction visqueux, à un seul stage, assure dans certaines conditions une proportionnalité précise entre les pressions partielles des composants dans un échantillon à pression normale et les courants d'ion correspondants. La condition principale est que la viscosité du mélange ne change pas avec la composition; ceci est presque toujours le cas lorsque l'un des composants est présent en large excès comme gaz porteur. On a établi une équation qui décrit le comportement de ce système d'introduction "quantitatif." L'épreuve expérimentale a confirmé la validité de cette équation d'introduction et démontre, en outre, le large domaine d'application de ce système d'introduction simple et rapide, consistant habituellement en un capillaire en quartz.

LITERATUR

1. J. H. Beynon, *Mass Spectrometry*, Elsevier, Amsterdam, 1960.
2. W. Walisch, *Chem. Ber.*, 1961, **94**, 2314.
3. W. Walisch und K. Schäfer, *Mikrochim. Acta*, 1968, 765.
4. W. Walisch und W. Marks, *ibid.*, 1967, 1051.
5. W. Walisch und O. Jaenicke, *ibid.*, 1967, 1147.
6. W. Walisch und G. Humme, *ibid.*, 1968, 748.
7. K. Muysers, Vortrag auf der Tagung *The Mass Spectrometer Applied to Lung Physiology* der European Soc. for Clinical Respiratory Physiology, London, Mai 1967.
8. M. Knudsen, *Ann. Phys.*, 1909, **28**, 489.
9. R. E. Honig, *J. Appl. Phys.*, 1945, **16**, 646.
10. M. Barber, J. Farren und J. W. Linnett, *Proc. Roy. Soc.* (*London*) 1963, **A274**, 293.
11. F. T. Greene und T. A. Milne, *Advan. Mass Spectrometry*, 1966, **3**, 841.
12. J. Kistemaker, *Physica*, 1952, **18**, 163.
13. K. Diels und R. Jaeckel, *Leybold Vakuum-Taschenbuch*, Springer-Verlag, Berlin, 1962.
14. M. Trautz, A. Melster und R. Zink, *Ann. Phys.*, 1930, **7**, 409; 427.
15. J. O. Hirschfelder, R. B. Bird und E. L. Spotz, *Chem. Rev.*, 1949, **44**, 205.
16. H. R. Heath, *Proc. Phys. Soc.*, (*London*), 1953, **B66**, 362.

Talanta, 1971, Vol. 18, pp. 175 to 182. Pergamon Press. Printed in Northern Ireland

MASSENSPEKTROMETRISCHE UNTERSUCHUNGEN ZUR ELEMENTARANALYSE ORGANISCHER VERBINDUNGEN—II

BESTIMMUNG VON VERBRENNUNGSPRODUKTEN IM TRÄGERGASSTROM DURCH PEAKINTEGRATION

OTTOKAR JAENICKE und WALTER WALISCH®
Institut für Organische Chemie, Universität des Saarlandes, 66 Saarbrücken, B.R.D.

(*Eingegangen am* 12. *Juni* 1970. *Angenommen am* 20. *Juli*, 1970)

Zusammenfassung—Die organische Probe wird in einem leeren Düsenrohr im Trägergas Sauerstoff verbrannt. Die Verbrennungsprodukte strömen mit konstanter Geschwindigkeit an der Einlaßkapillare vorbei, welche die Verbindung zum Massenspektrometer herstellt. Die Ausgangsspannung des auf die Masse eines Verbrennungsproduktes eingestellten Massenspektrometers wird einem Integrator zugeführt. Das so gemessene zeitliche Peakintegral ist der Menge des Verbrennungsproduktes proportional. Überführt die Verbrennung das betrachtete Element in ein einheitliches Endprodukt, so kann aus dem Peakintegral und der vorgelegten Einwaage der Gehalt der organischen Verbindung an dem betreffenden Element berechnet werden. Bei Verwendung eines Massenspektrometers mit mehreren Faraday-Fängern können gleichzeitig mehrere Elemente bestimmt werden. Die angeführten Kontrollergebnisse lassen erkennen, daß das Verfahren zwar grundsätzlich zur Elementaranalyse geeignet ist, daß aber die Konstanz der internen Partialdruckempfindlichkeit noch einige Wünsche bezüglich der erreichbaren Genauigkeit offen läßt.

DER im I. Teil dieser Arbeit beschriebene einstufige, viskose Einlaß ermöglicht in einfacher Weise eine massenspektrometrische Analyse von Gasgemischen, bei denen eine Komponente als Trägergas in großem Überschuß vorliegt. Damit sollte auch die Bestimmung der gasförmigen Endprodukte, welche bei der Verbrennung organischer Verbindungen entstehen, mittels eines geeigneten Massenspektrometers durchführbar sein.

In der klassischen Elementaranalyse ist man bestrebt, Verbrennungsbedingungen vorzugeben, die das zu bestimmende Element quantitativ in ein einziges Endprodukt überführen. Nur so ist es möglich, unspezifische Bestimmungsverfahren (Gravimetrie, Wärmeleitfähigkeitsmessung, Volumetrie) zur Messung einzusetzen und eine zeitraubende Nachbehandlung in flüssiger Phase, wie sie bei Halogen[1] und Schwefel[2] noch erforderlich ist, zu vermeiden. Die teilweise beim Auftreten mehrerer Endprodukte geübte Praxis, nur eines dieser Produkte zu bestimmen und im übrigen auf dessen gleichbleibenden Anteil zu vertrauen, bedarf immer noch einer theoretischen und experimentellen Bestätigung.

Die bei den klassischen Bestimmungsmethoden notwendige Herbeiführung der Einheitlichkeit verwischt allerdings eine möglicherweise vorhandene strukturspezifische Verhaltensweise vollständig und verzichtet damit auf eine zusätzliche Information von hohem Aussagewert. Die massenspektrometrische Bestimmung erlaubt dagegen die Messung aller Reaktionsprodukte eines Elementes und damit den Einsatz schonender Verbrennungsbedingungen.

Ein weiterer Vorteil der massenspektrometrischen Elementaranalyse besteht in

---

* Teil der Dissertation von O. Jaenicke, Saarbrücken, 1969.

der Möglichkeit der gleichzeitigen Bestimmung mehrerer Elemente. Während immer noch bei vielen Methoden nur ein Element pro Analyse bestimmt wird, und erst relativ spät die Bestimmung von C, H und N mit einer Einwaage gelang,[3] ist ein massenspektrometrisches Meßverfahren grundsätzlich für eine Vielfach-Elementaranalyse (u.U. sogar Total-Elementaranalyse) geeignet.

Diese beiden interessanten Möglichkeiten—strukturspezifische- und totale Elementaranalyse—sind allerdings schlecht miteinander vereinbar, da im ersten Falle einfache und schonende Verbrennungsbedingungen benötigt werden, während bei der Totalanalyse zusätzlich zur Primärverbrennung noch vereinheitlichende Nachbehandlungen erforderlich sein können. Wir werden uns deshalb vorerst darauf beschränken, diese beiden Grenzfälle nebeneinander zu behandeln, ohne schon jetzt eine Kombination anzustreben.

Die Einheitlichkeit der gasförmigen Endprodukte kann für die Elemente Kohlenstoff, Wasserstoff und Stickstoff verhältnismäßig einfach[3] und fast ausnahmslos[4] durch dynamische Verbrennung[5] in einem entsprechend gefüllten Rohr erreicht werden. Auch im "leeren Rohr" kann, wie wir in einer der folgenden Arbeiten ausführlich zeigen werden, die vollständige Verbrennung von C zu CO_2 und H zu H_2O bei den meisten Stoffklassen realisiert werden. Dieser Probenaufschluß im Trägergasstrom und leeren Rohr ist für eine nachfolgende massenspektrometrische Messung besonders geeignet, da hierbei die Gefahr unbeabsichtigter Reaktionen an Rohrfüllungen am geringsten ist.

Die Messung selbst kann statisch und dynamisch erfolgen. Im ersten Fall werden die Verbrennungsabgase in ein Reservoir geleitet und dort gesammelt. Nach dem vermuteten Ende der Verbrennung wird der Trägergasstrom abgeschaltet, ein normierter Druck eingestellt und die Homogenität des Gasgemisches abgewartet bzw. herbeigeführt. Mit dem Massenspektrometer, das über die Einlaßkapillare mit dem Reservoir verbunden ist, kann das Fortschreiten der Durchmischung (bei entsprechender Ausführung des Reservoirs auch der Verlauf der Verbrennung) dadurch beobachtet werden, daß das Massenspektrometer auf einem für die Verbrennung repräsentativen Massenpeak eingestellt bleibt. Nach Erreichen des Endwertes wird der interessierende Massenbereich durchfahren und man erhält so in einfacher Weise aus der Lage der Peaks eine *qualitative*- und aus der Peakhöhe eine *quantitative* Analyse der Verbrennungsprodukte. Die prinzipielle Unterlegenheit statischer Verfahren[5] wird hierbei dadurch kompensiert, daß auf diese Weise eine Vielfachanalyse auch mit einem einfachen und kleinen Massenspektrometer möglich ist. Unsere diesbezüglichen Untersuchungen sind noch nicht abgeschlossen und wir werden später ausführlich über eine derartige Anordnung berichten. Vorerst haben wir—in Analogie zu unserer CHN- und O-Apparatur[3–6]—einem dynamischen Verfahren mit integraler Mengenmessung den Vorzug gegeben.

PRINZIP DES VERFAHRENS

Die in Abb. 1 schematisch wiedergegebene Anordnung enthält mehrere Bauelemente unseres CHN-O-Automaten.[3–6,*] Das in der Druckflasche DF befindliche Trägergas tritt durch die Kapillare DK und das Absorptionsrohr AR bei TG in das Düsenverbrennungsrohr[2] VR ein und strömt von dort zum größeren Teil durch das Düsenrohr und die Austrittskapillare AK ins Freie. Der kleinere Teil des Trägergases

[*] Hersteller: Technicon International Division S.A., 81 Route de l'aire, Genf, Schweiz.

gelangt an der Einfüllöffnung EF und dem Einschieberohr ER vorbei über das Druckausgleichsrohr DR nach außen. Wie früher$^{3-6}$ gezeigt wurde, wird auf diese Weise:

—beim Einfüllvorgang eine wirksame Umkehrspülung aus EF heraus bewirkt, die das Eindringen von Gasen aus der Atmosphäre weitgehend verhindert,

—eventuell doch in EF gelangte oder durch die nie ganz dichten Gummistopfenverschlüsse von EF und HF dauernd eindringende "Atmosphäre" sofort wieder ins Freie geblasen,

—ein konstanter Überdruck (und damit auch ein konstanter Druck) innerhalb der Anordnung garantiert,

—die für ein dynamisches Verfahren erforderliche Konstanz des Gasmengenstromes erreicht.

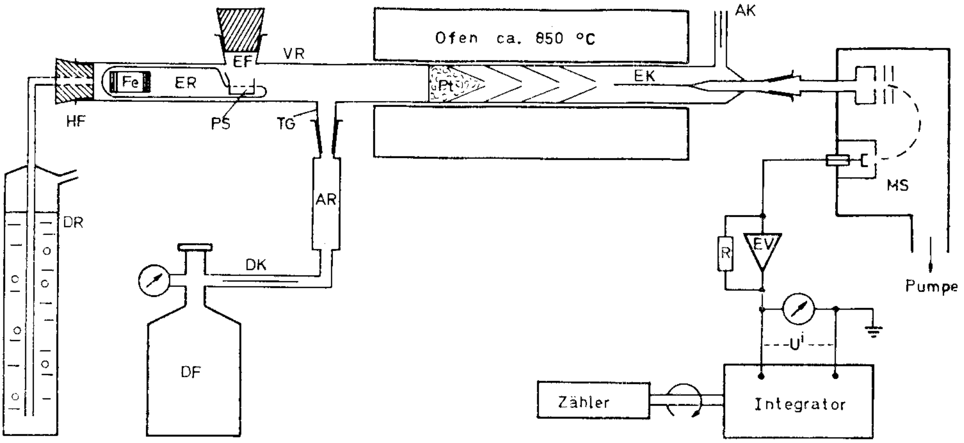

Abb. 1.—Schema der Meßanordnung (Siehe Text).

Die in dem Platinschiffchen PS eingewogene Substanz wird mittels des von außen magnetisch betätigten Einschieberohres ER, in dessen hinterem Ende der Permanentmagnetstab Fe eingeschmolzen ist, in den heißen Teil des Verbrennungsrohres unmittelbar vor die Platinwolle Pt geschoben. Die explosionsartig entstehenden primären Verbrennungsprodukte werden vom Trägergas über die Platinwolle und durch das Düsenrohr geleitet, wo die Verbrennung bis zu den Endprodukten CO_2 und H_2O vervollständigt wird, strömen an der Einlaßkapillare EK vorbei, welche die Verbindung zum Massenspektrometer MS herstellt und verlassen zuletzt das Verbrennungsrohr durch die Austrittskapillare AK.

Das Massenspektrometer ist auf das Plateau des jeweils interessierenden Massenpeaks (beispielsweise auf Masse 44 für CO_2) fest eingestellt. Ohne Verbrennung gelangt nur Trägergas durch EK ins Massenspektrometer und die Ausgangsspannung U_0^i wird durch die betreffende Verunreinigung des Trägergases und dem aus dem Massenspektrometer stammenden Untergrund bestimmt. Dieser "Blindwert" wird durch Veränderung des Nullpunktes des Elektrometerverstärkers EV kompensiert, sodaß $U_0^i = 0$. Damit wird das vom Integrator^7 gemessene und vom Zähler digital angezeigte Integral dieser Ausgangsspannung unverändert auf dem zu Beginn einer Integration vorliegenden Wert w_0^i stehen bleiben und zwar auch über lange Zeiträume, wenn die "chemische-" und elektronische Nullstabilität entsprechend gut sind.

Als Folge einer zur Zeit Null durch Einschieben einer Probe ausgelösten Verbrennung wird eine "Verbrennungsbande" an EK vorbeiwandern, die etwa das Aussehen einer Glockenkurve besitzt.[8] Wenn der Wert von U^i nach der Zeit t wieder den Ausgangswert $U_0{}^i = 0$ erreicht hat, gilt mit $w_0{}^i = 0$

$$w_t{}^i - w_0{}^i = \int_0^t U^i \, \mathrm{d}t = W^i \tag{1}$$

Wegen der im I. Teil nachgewiesenen Proportionalität zwischen U^i und p^i sowie der durch die Anordnung garantierten Konstanz des Gasmengenstromes ist W^i der in der Fremdgasbande enthaltenen Menge der betrachteten Komponente proportional.

Wird beispielsweise das Massenspektrometer auf das Plateau des CO_2-Peaks eingestellt, so ist $W^{44}_{CO_2} = \int_0^t U^{44}_{CO_2} \cdot \mathrm{d}t$ der eingesetzten Kohlenstoffmenge proportional, wenn die Verbrennung vollständig ist und ausschließlich zu CO_2 führt. Bei Kenntnis der vorgelegten Probenmenge g und des durch Verbrennung einer Eichsubstanz bestimmten Proportionalitätsfaktors $f^{44}_{CO_2}$ läßt sich der Kohlenstoffgehalt %C der eingesetzten Verbindung nach Gleichung (2) in einfacher Weise berechnen.

$$\%\mathrm{C} = f^{44}_{CO_2} \cdot W^{44}_{CO_2} / g \tag{2}$$

In analoger Weise kann der Wasserstoffgehalt bestimmt werden, wenn das Massenspektrometer auf das Plateau des Wasserpeaks bei M = 18 eingestellt wird. Eine Stickstoffbestimmung ist dagegen nicht ohne weiteres möglich, da mit dieser einfachen Verbrennungsanordnung kein einheitliches Verbrennungsprodukt erhalten wird.

KONTROLLERGEBNISSE

Die Überprüfung der Methode der Peakintegration erfolgt einmal dadurch, daß Gaskonzentrationsbanden bekannter Menge dynamisch erzeugt und durch das Verbrennungsrohr an EK vorbeigeleitet werden.

Hierzu wird das Trägergas ausnahmsweise bei EF eingeleitet, während bei TG Fremdgas-Rechteckimpulse konstanter Intensität $p_0{}^i$ und unterschiedlicher Dauer α zugegeben werden. Auf diese Weise bleibt der gesamte Gasmengenstrom aus AK konstant, und die in einem Fremdgasimpuls enthaltene Fremdgasmenge ist proportional der jeweiligen Impulsdauer α.

Wie an anderer Stelle[8] gezeigt ist, wird als Folge der Diffusion im leeren Rohr aus einer Rechteckbande sehr schnell eine Glockenkurve mit gleichem Fremdgasgehalt. Demnach strömen, als Folge der Zugabe von Rechteckimpulsen verschiedener Dauer, Glockenkurven unterschiedlicher Höhe und Halbwertsbreite an der Einlaßkapillare vorbei, und die verschiedensten Verbrennungsbanden können ohne großen Aufwand bei ausreichender Ähnlichkeit der Meßbedingungen und genauer Kenntnis der in einer Fremdgasbande enthaltenen Menge simuliert werden*. Wenn

---

* Erst bei unzulässig großer Impulsdauer wird das Impulsplateau auf der Strecke zwischen TG und EK nicht vollständig abgebaut. Zur Vermeidung dieser nicht repräsentativen abgeflachten Banden wird $p_0{}^i$ so hoch gewählt, daß der interessierende Mengenbereich mit zulässigen α-Werten erfaßt wird.

$U_0{}^i = 0$ und der Gasmengenstrom konstant ist, muß das für einen Impuls gefundene Integral W proportional der Impulsdauer α sein.

In den Tabellen I und II sind die Ergebnisse derartiger Kontrolluntersuchungen zusammengestellt. In beiden Trägergasen ist die Konstanz von W/α befriedigend. Da keine systematischen Abweichungen erkennbar sind, ist einerseits noch einmal bewiesen, daß die Ausgangsspannung U^i des Massenspektrometers dem Partialdruck der betrachteten Komponente streng proportional ist, und andererseits ist die Brauchbarkeit des integralen Meßverfahrens und des von uns entwickelten Motorzählers,[3,7] der in diesem Falle ohne Linearisierungsglied eingesetzt wird, unter Beweis gestellt.

Zur weiteren Kontrolle wurden entsprechend dem eingangs beschriebenen Verfahren Eichsubstanzen verbrannt, und die Beziehung zwischen der Einwaage g und dem Peakintegral W überprüft. Das zufriedenstellende Ergebnis ist in Abb. 2 dargestellt. Bei der Verbrennung von Benzoesäure mit Sauerstoff als Trägergas findet man Proportionalität zwischen $W_{CO_2}^{44}$ bzw. $W_{H_2O}^{18}$ und der jeweiligen Einwaage (Abb. 2, A und B).

TABELLE I.—PEAKINTEGRATION IM TRÄGERGAS HELIUM

α,	(*a*)		(*b*)		(*c*)	
sec	$W_{N_2}^{28}$	W/α	$W_{O_2}^{32}$	W/α	$W_{CO_2}^{44}$	W/α
10	425	42,5	340	34,0	268	26,8
20	844	42,2	710	35,5	539	27,0
30	1262	42,1	1075	35,8	821	27,4
40	1700	42,2	1412	35,3	1102	27,6
50	2126	42,5	1767	35,3	1366	27,3
60	2543	42,4	2134	35,6	1652	27,5

TABELLE II.—PEAKINTEGRATION IM TRÄGERGAS SAUERSTOFF

α,	(*a*)		(*b*)		(*c*)	
sec	$W_{CO_2}^{44}$	W/α	$W_{N_2}^{28}$	W/α	$W_{N_2}^{14}$	W/α
10	457	45,7	267	26,7	345	34,5
20	890	44,5	523	26,2	685	34,3
30	1351	45,0	789	26,3	1047	34,9
40	1813	45,3	1050	26,2	1393	34,8
50	2280	45,6	1312	26,2	1747	34,9
60	2721	45,4	1583	26,4	2087	34,8

(Bei Meßreihe (*c*) war dem Trägergas *ca.* 1% CO_2 zugesetzt.)

TABELLE III.—BESTIMMUNG DES C-GEHALTES ORGANISCHER VERBINDUNGEN

Verbindung	Summenformel	Probe, *mg*	$\%C_{gef.}$	$\%C_{theor.}$
Benzoesäure	$C_7H_6O_2$	0,2797	68,6	68,84
Anthracen	$C_{14}H_{10}$	0,4955	94,8	94,34
Vanillin	$C_8H_8O_3$	0,5557	63,3	63,15
Dinitrophenylhydrazin	$C_6H_6O_4N_4$	0,3245	35,2	36,37
Chlor-Benzoesäure	$C_7H_5O_2Cl$	0,4600	53,5	53,69
Cyclohexanonsemicarbazon	$C_7H_{13}ON_3$	0,1376	53,0	54,17
Melamin	$C_3H_6N_6$	0,3348	29,1	28,57
Harnstoff	CH_4ON_2	0,3783	20,7	20,00

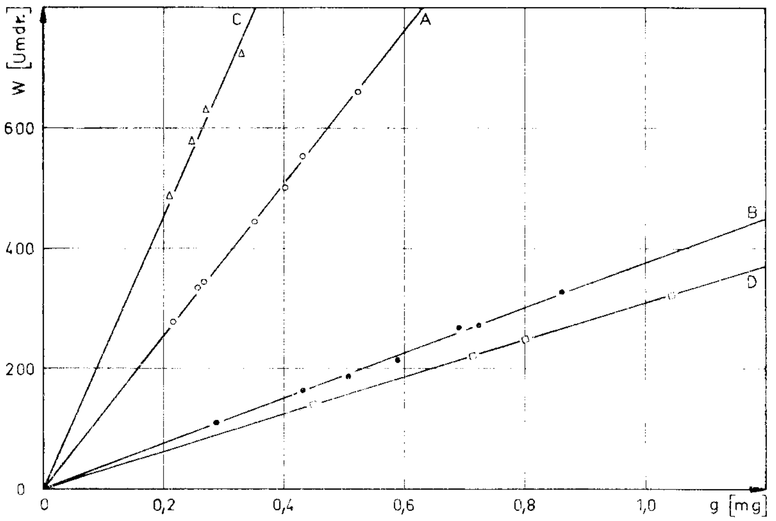

ABB. 2.—Einwaageabhängigkeit des Peaktintegrals.
A. $W^{44}_{CO_2}$ bei der Verbrennung von Benzoesäure
B. $W^{18}_{H_2O}$ bei der Verbrennung von Benzoesäure
C. W^{30}_{NO} bei der Pyrolyse von Blei(II)-nitrat
D. $W^{28}_{N_2}$ bei der Pyrolyse von Azobenzol

Die Geraden C und D der Abb. 2 beweisen, daß das integrale Meßverfahren unter günstigen Umständen auch zur Messung von Pyrolyseprodukten herangezogen werden kann. Im Falle C wurde Blei(II)-nitrat unter den oben geschilderten Verbrennungsbedingungen (allerdings ohne Pt-wolle) im Sauerstoffstrom zersetzt. Der vorhandene Stickstoff erscheint quantitativ als Stickstoffmonoxid und W^{30}_{NO} ist der Einwaage proportional. Die Verbrennung organischer Verbindungen führt dagegen zu einem unterschiedlichen Anteil an Stickstoffmonoxid. Während beispielsweise[9] Dinitrobenzol einen hohen Anteil an NO ergibt, entsteht bei Azobenzol praktisch kein Monoxid. Umgekehrt zeigt Kurve D, daß bei der Pyrolyse von Azobenzol im Trägergas Helium (sonstige Bedingungen wie bei C) ausschließlich Stickstoff entsteht.

Die Verwendbarkeit des Verfahrens zur Elementaranalyse wird definitiv durch Tabelle III belegt. Hier sind die bei verschiedenen Verbindungen gefundenen Kohlenstoffwerte mit den theoretischen Werten der vorgelegten Proben verglichen. Die Auswertung nach Gleichung (2) erfolgte dabei mit einem auf Benzoesäure basierenden Faktor. Obwohl die Kohlenstoffwerte zwischen 20 und 95% liegen und trotz des sicher sehr unterschiedlichen Verbrennungsverhaltens der gewählten Stoffklassen, liegen die gefundenen Werte innerhalb der derzeitigen Fehlergrenzen des Verfahrens.

SCHLUßBETRACHTUNGEN

Die Ergebnisse unserer orientierenden Untersuchungen erweisen einerseits die prinzipielle Eignung des beschriebenen Verfahrens; andererseits werden aber auch die Schwächen deutlich sichtbar. So kann mit dem von uns benutzten einfachen Massenspektrometer (Modell THN 205 E der Firma Thomson-Houston, Paris) jeweils nur ein Element pro Experiment bestimmt werden. Die praktische Verwertbarkeit der Methode setzt aber die gleichzeitige Bestimmung mehrerer Elementevoraus. Hierzu bietet sich das 180°-Gerät GD 150–4 der Firma VARIAN-MAT, Bremen, an, welches vier Faraday-Fänger besitzt, die auf vier gewünschte Massen fest eingestellt werden können. Würde an die dazugehörigen Elektrometerverstärker je ein Integrator angeschlossen, so könnten vier verschiedene Elemente mit einer Einwaage bestimmt werden, wenn die in der Einleitung präzisierten Bedingungen hinsichtlich der Einheitlichkeit der Verbrennungsprodukte gleichzeitig für vier Elemente realisierbar sein sollten.

Dieser verhältnismäßig hohe Aufwand erscheint uns erst dann gerechtfertigt, wenn gleichzeitig auch die Genauigkeit und die Langzeitkonstanz der einzelnen Proportionalitätsfaktoren besser werden, als es zur Zeit der Fall ist. Die Streuung der Meßwerte ist einfach noch zu groß. Der Fehler kann aber nicht in der dynamischen Methode und der integralen Messung liegen, denn das analoge Verfahren[3–6] ergibt wesentlich kleinere Fehlergrenzen. Es bleibt also nur die Inkonstanz der die interne Partialdruckempfindlichkeit bestimmenden Ionenquellenparameter (Elektronenstrom, Fokussierung, Spaltweiten usw.) die auch andere massenspektrometrische Analyseverfahren erheblich beeinträchtigt.

Unsere Untersuchungen über eine Verbesserung der Langzeitkonstanz der Ionenquellenempfindlichkeit werden zur Zeit mit einem anderen Gerätetyp (VARIAN-MAT, CH 5) fortgesetzt. Hier wirkt sich die Verwendung einer Rhenium-Kathode in der Quelle insbesondere auf die Kohlendioxidmessung, die bei einer Wolframkathode durch Memoryeffekte erheblich gestört ist, sehr vorteilhaft aus. Die Möglichkeit einer einstellbaren, konstanten Quellentemperatur ist ebenfalls zu begrüssen.* Schwierigkeiten bereitet dagegen auch hier die Reproduzierbarkeit der Fokussierungsbedingungen, da schon geringfügige Unterschiede in den Fokussierungspotentialen zu großen Veränderungen in der internen Partialdruckempfindlichkeit führen. Dabei sind diese Veränderungen bei verschiedenen Massen oft sogar noch gegenläufig, sodaß eine Optimierung bei einer Masse nicht ausreicht.

Selbstverständlich läßt sich das dynamische Verfahren mit Peakintegration auch mit einem Einfachfänger-Massenspektrometer zur gleichzeitigen Bestimmung mehrerer Massen verwenden, wenn analog zum CHN-Automaten[3–6] eine zeitliche Aufeinanderfolge der verschiedenen Verbrennungsprodukte erzwungen wird, und ein Massenprogrammwähler die jeweils vorliegende Masse einschaltet. Da die Messung einer Komponente sehr kurz gehalten werden kann, ist sicher auch auf diese Weise ein erheblicher Zeitgewinn zu realisieren.

Die Entscheidung, ob dem hier beschrittenen Weg mit Mehrfachfänger bzw. zeitlicher Aufspaltung oder dem in der Einleitung kurz skizzierten statischen Meßverfahren der Vorzug zu geben ist, kann erst getroffen werden, wenn unsere zur Zeit laufenden vergleichenden Untersuchungen abgeschlossen sind. Unabhängig vom Ergebnis dieses Vergleiches kann schon jetzt mit Sicherheit ausgesagt werden, daß die zur Zeit angebotenen Massenspektrometertypen den in diesem Falle gebotenen Anforderungen hinsichtlich Langzeitkonstanz und Reproduzierbarkeit nur leidlich gerecht werden, und es bleibt zu hoffen, daß die Herstellerfirmen diese Marktlücke bald ausfüllen werden. Die zudem sehr ungünstige Relation zwischen Aufwand und Genauigkeit läßt vorerst eine Verwendung von Massenspektrometern bei der

---

* Leider schwingt der Temperaturregelkreis, und die periodischen Änderungen der Heizleistung der "Hilfsheizer" führen zu störenden Schwankungen im Untergrundspektrum.

Elementaranalyse allenfalls dort sinnvoll erscheinen, wo die klassischen Verfahren versagen, wie beispielsweise bei der Analyse von angereicherten Isotopengemischen.

Wir danken dem Fonds der chemischen Industrie für die Förderung dieser Arbeit.

Summary—The organic sample is ignited in the oxygen carrier gas in an empty "jet" tube. The products of combustion flow at constant speed past the inlet capillary which is linked to the mass spectrometer. The output voltage from the mass spectrometer, set at the mass of one combustion product, is fed to an integrator. The integral measured is proportional to the amount of the combustion product. If combustion of the element under consideration yields a single product, the amount of this element in the organic compound can be calculated from the peak integral and the weight of sample. Several elements can be determined simultaneously by using a mass spectrometer with several collectors. The control data quoted show that the procedure is fundamentally suitable for elementary analysis but that the reproducibility is not quite good enough.

Résumé—L'échantillon organique est brûlé dans le gaz vecteur oxygène dans un tube "jet" vide. Les produits de combustion s'écoulent à vitesse constante au-delà du capillaire d'entrée qui est lié au spectromètre de masse. Le voltage de sortie du spectromètre de masse, ajusté à la masse d'un produit de combustion, est transmis à un intégrateur. L'intégrale mesurée est proportionnelle à la quantité du produit de combustion. Si la combustion de l'élément considéré donne un seul produit, la quantité de cet élément dans le composé organique peut être calculée à partir de l'intégrale du pic et du poids d'échantillon. On peut déterminer plusieurs éléments simultanément en utilisant un spectromètre de masse avec plusieurs collecteurs. Les données de contrôle réunies montrent que la technique convient fondamentalement à l'analyse élémentaire mais que la reproductibilité n'est pas encore suffisamment bonne.

LITERATUR

1. W. Walisch und O. Jaenicke, *Mikrochim. Acta*, 1967, 1147.
2. W. Walisch und G. Humme, *ibid.*, 1968, 748.
3. W. Walisch, *Chem. Ber.*, 1961, **94**, 2314.
4. W. Walisch und K. Schäfer, *Mikrochim. Acta*, 1968, 765.
5. L. Foissac, *Chim. Anal. Paris*, 1966, **48**, 354.
6. W. Walisch und W. Marks, *Mikrochim. Acta*, 1967, 1051.
7. W. Walisch, *Dtsch. Bundespatent Nr.* 1051386.
8. G. Humme, *Dissertation*, Saarbrucken 1970.
9. O. Jaenicke, *Dissertation*, Saarbrücken 1969.

Talanta, 1971, Vol. 18, pp. 183 to 211. Pergamon Press. Printed in Northern Ireland

SPECTROPHOTOMETRIC DETERMINATION OF THE PROTOLYTIC DISSOCIATION CONSTANTS OF THE NEW CHROMOGENIC REAGENT "PALLADIAZO"—I*

INVESTIGATIONS WITH SODIUM HYDROXIDE, PERCHLORIC ACID AND DIFFERENT AQUEOUS BUFFER SOLUTIONS

J. A. PÉREZ-BUSTAMANTE and F. BURRIEL-MARTÍ
Consejo Superior de Investigaciones Científicas, Departamento de Química
Analítica, Universidad de Madrid, Facultad de Ciencias,
Ciudad Universitaria, Madrid (3), Spain

(*Received* 24 *March* 1970. *Accepted* 19 *May* 1970)

Summary—The "palladiazo" reagent has been subjected to a detailed spectrophotometric investigation in concentrated perchloric acid, different aqueous buffers and concentrated sodium hydroxide solutions. K_1–K_{10} and ε_1–ε_{10} values corresponding to the instability constants of the protolytic equilibria involved and to the molar absorptivities at 540 and 630 nm of the different proton complex species of the system have been calculated by a number of analytical and graphical spectrophotometric methods. Special attention has been paid to the study of the complicated phenomena implied by the interaction of the reagent with perchloric acid, which has been shown to give rise to alteration of the initial isomeric composition of the reagent and to the formation of addition and/or oxidation products derived from side-reactions undergone by the reagent with the medium. All the instability constants and molar absorptivities, which have been determined by several methods, are tabulated for comparison.

THE REAGENT 1,8-dihydroxynaphthalene-3,6-disulphonic-2,7-bis(azobenzene-*p*-arsonic) acid, which is a symmetric structural isomer of the well known reagent arsenazo III first synthesized by Savvin[1] was prepared and submitted to a preliminary investigation by us.[2] The reagent exhibits to a lesser extent the characteristic reactivity of most compounds containing *o*-hydroxyazo functional groups,[3] but is nevertheless so selective and sensitive under a number of experimental conditions towards palladium(II)[2,4–6] that we have given it the trivial name of "palladiazo". We and others have found that the assumption[7] that the lack of salt-forming groups in the benzene rings *ortho* to the azo groups in compounds derived from the general bisazochromotropic acid structure gives rise to reagents of limited analytical value is not true.[8–13]

On the other hand substitution *para* to the azo groups has been shown to increase the selectivity properties of this type of reagent.[14] It is interesting that even the Russian authors who for 10 years have exclusively investigated many *o*- and *o*,*o'*-substituted derivatives of the bis(azophenylarsonic) chromotropic acid structure have turned their attention recently towards the investigation of *p*,*p'*-substituted compounds,[15–18] especially those that react with the alkaline earth metals to form very stable ML_2 complex species with "sandwich" structures and very good spectrophotometric properties.

---

* Communication presented at the International Symposium on Analytical Chemistry, Birmingham, July, 1969.

The most remarkable reaction of palladiazo with palladium(II) which serves to differentiate it from any other arsenazo-type reagent which reacts with palladium(II), has been shown to take place in the absence of chloride ions at pH 2·4 ± 0·1. An ML_3-type complex species is formed during the initial reaction period (0·5–7 min), and in a few hr gives rise to a stable ML_2 compound.[6,19] The molar absorptivity of the ML_3 compound shows it to give one of the most sensitive reactions known between palladium(II) and *o*-hydroxyazo compounds of this type ($\varepsilon_{ML_3}^{660} = 5{\cdot}3 \times 10^3$ l. mole^{-1}. mm^{-1}).* Only a few of the recently synthesized reagents of this type, containing salt-forming groups in the benzene rings in positions *o*- and *o,o'* to the azo groups, are more sensitive.[20,21] Other interesting reactions of palladiazo with a few elements are being investigated in our Department.

As depicted by its structural formula

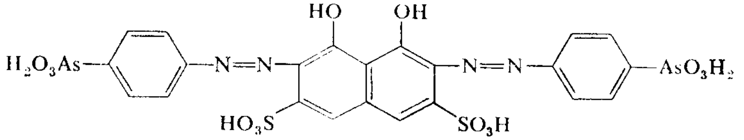

the palladiazo reagent in the acid form exhibits 8 groups of greatly varying acidic strength which can undergo stepwise protolysis as the acidity of the medium decreases.

By independent potentiometric titration and ion-exchange experiments,[2,4] it has been shown that 4 of these groups are titrated together at a first well-defined equivalence point (protolysis of the two —SO_3H_1 groups), while two additional groups are titrated at a second, considerably less well-defined equivalence, point. The main differences in the potentiometric titration of the two structural isomers palladiazo and arsenazo III (which has 4 acid groups neutralized at the first equivalence point and a fifth acid group at a second, less clearly-defined, equivalence point) have been clearly stated in earlier communications.[2,22]

It is reasonable to expect that the two phenolic groups will behave similarly to those of chromotropic acid, which has been investigated by Heller and Schwarzenbach.[23] There is a very great difference in the acidity exhibited by the two groups, because of the formation of a very strong hydrogen bond between the two phenolic groups. In addition to the 8 protons considered, the —N=N— groups of the palladiazo molecule may be protonated in strong acid media.

As a result, palladiazo must be considered as an acid potentially capable of releasing 10 protons within the wide acidity interval between concentrated perchloric or sulphuric acid solutions and concentrated alkali solutions. This fact makes it mandatory to carry out a very detailed experimental study under widely varying conditions when facing the particular problem imposed by the determination of the values corresponding to the molar absorptivities and dissociation constants of all the species and equilibria involved in the palladiazo–H^+–OH^- system.

The purpose of this study was to carry out this type of investigation exclusively by spectrophotometric methods. This approach can be complicated by the existence of acidity intervals where the spectral changes exhibited by the reagent solutions are too small for numerical evaluation, as a result of the poor chromogenic effects brought about by the dissociation of several groups. Consequently, large discrepancies exist

---

* Our latest findings with specially pure palladiazo preparations have resulted in molar absorptivities for this complex of ~7 × 10^3 l.mole^{-1}.mm^{-1} (to be published).

between the numerical results obtained by different authors, or even by the same author using different experimental methods. Such differences can amount to several orders of magnitude in the instability constants. A most illustrative correlation of these facts can be found in a recently published paper.[24] Very important errors might also derive from the large number of successive protolytic equilibrium steps shown by this type of reagent. Since most of the methods are based on successive treatment of the different equilibria, with systematic use of the numerical values obtained for the preceding equilibrium steps, the cumulative relative errors can become very great for the last steps, especially when ill-defined intermediate steps are encountered. Important uncertainties might derive even from the theoretical assumptions upon which the whole numerical treatment is based (*e.g.*, establishment of the number of equilibrium steps; protonation of one or two azo groups; proper interpretation of the isosbestic points and pH intervals; side-reactions and kinetic phenomena, *etc*). These problems can be illustrated by the determination of the dissociation constants of arsenazo III, by the same author and by similar spectrophotometric methods.[25,26] Not only were the numerical differences between pK's too great but the overall interpretation of the true number of protolytical equilibrium steps differed significantly.

EXPERIMENTAL

Reagents

Palladiazo. Samples were synthesized and purified by the authors as described elsewhere.[2,4] The analysis of the reagent used in the present investigation was: As 18·2 ± 0·5%, N 7·1 ± 0·2%; theory 19·30% and 7·22% respectively.[27,28] The overall purity of the reagent was found to be 97·2% by potentiometric titration and 98·1% from the ion-exchange determination of the average number of acid groups dissociated in aqueous solution.[2,4] The yields were 35–45%.

The use of sulphamic acid for the synthesis appears to be disadvantageous[2,4] since the products obtained undergo extensive or even total thermal degradation on drying of the reagent at 90–110°, thereby rendering the reagent quite useless for analytical purposes.

The infrared spectrum of the reagent has been reported.[29] The product used left no insoluble residue on dissolution in water and the aqueous solutions were stable for years. These solutions have absorption maxima at 230, 310, 395, 540 and 630 nm. Of special interest are the peaks at 540 and 630 nm, which exhibit molar absorptivities (at pH 4·0) of $3{\cdot}54 \times 10^3$ and $1{\cdot}90 \times 10^3$ $\text{l.mole}^{-1}.\text{mm}^{-1}$ respectively.[4] The ratio between the molar absorptivities of these two peaks has been shown to vary from sample to sample, probably because of the changing isomeric composition exhibited by the different reagent preparations,[4,30] and the ratio may vary within the same solution over a long period because of alteration of the initial isomeric composition of the anhydrous preparation. Paper chromatography with ethanol–water (1 : 4) disclosed the presence of a bluish-pink major component and a light red minor component, with R_f values 0·81 and 0·84 respectively.[4]

Control of pH. Perchloric acid (Merck, U.C.B.), sodium hydroxide (Merck) and a number of buffering reagents of the best available quality were used.

Apparatus

Spectrophotometers. A manual single-beam Beckman DU and double-beam Beckman DK-2A and Perkin–Elmer UV 137 spectrophotometers furnished with a set of 10-mm matched glass or silica cells. The accuracy of the wavelength settings and the absorbance values was checked with standard solutions of copper sulphate pentahydrate and sodium chromate.[31]

pH meters. Metrohm Model E-338 and Pye pH-meters with combined or separate calomel and glass electrodes. Several pH determinations were made in strongly alkaline media under a nitrogen atmosphere in a specially designed magnetically-stirred closed cell, through which a stream of scrubbed nitrogen was bubbled.[32]

All experiments were carried out at room temperature (20 ± 2°).

RESULTS AND DISCUSSION

Study of the protolytic equilibria in aqueous media(pH 1–13)

The absorbance (at 540 and 630 nm) of a number of samples containing a constant overall palladiazo concentration ($c_L = 2{\cdot}5 \times 10^{-5}$ M) was measured as a function of pH. The classical Robinson–Stokes[33] and the strongly complexing buffer solutions described by Buděšínský *et al.*[34] were used to establish the desired pH values. The results obtained are reproduced in Fig. 1, which was interpreted by means of a detailed parallel investigation of the isosbestic points exhibited by the system within the pH interval 1–13, as summarized in Fig. 2.

From the appearance of the isosbestic points we can safely conclude that throughout the pH interval 1–13 the stepwise protolytic equilibria involve the coexistence of only two protonated reagent species over well-defined pH intervals.[35–38]

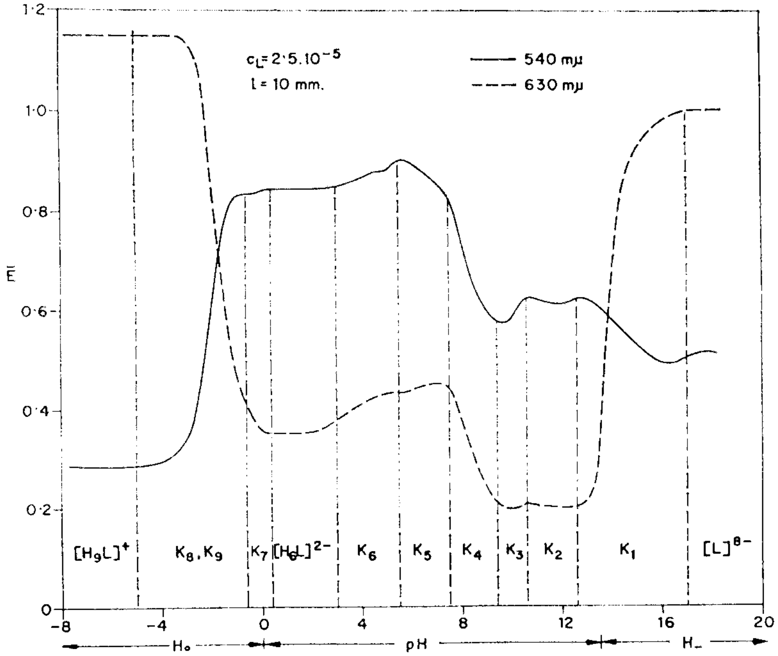

FIG. 1.—Graphical representation of the experimental $\bar{E} = f(\text{pH}, H_0, H\text{-}, \lambda)$ palladiazo functions as determined at 540 and 630 nm.

Table I summarizes the main protolytic and spectral features exhibited by the palladiazo reagent. For conciseness the order in which the acid groups undergo deprotonation is included together with the most probable mechanism and the structural characteristics of the different species. However, some important aspects will be dealt with here because our views differ from those of other workers.

The absorption maxima shown by the reagent at 540 and 630 nm in media of moderate acidity or alkalinity ($0 < \text{pH} < 8·5$, Fig. 2) derive, in our opinion, from the predominance of the more acidic *trans-trans* tautomeric azo-structures as a result of the considerable stabilizing effect brought about by the intramolecular hydrogen-bond established between the *peri* phenolic groups and the azo-groups.[39–42] This qualitatively logical interpretation has recently found more conclusive quantitative confirmation from the application of the MO–LCAO method by Savvin *et al.*[17,43–48] to a great number of bisazo chromotropic acid derivatives. The disappearance of the 630-nm absorption band at pH > 8·5 (Fig. 2) could be ascribed to the cleavage of the two intramolecular hydrogen-bonds as a result of the formation of the phenolic

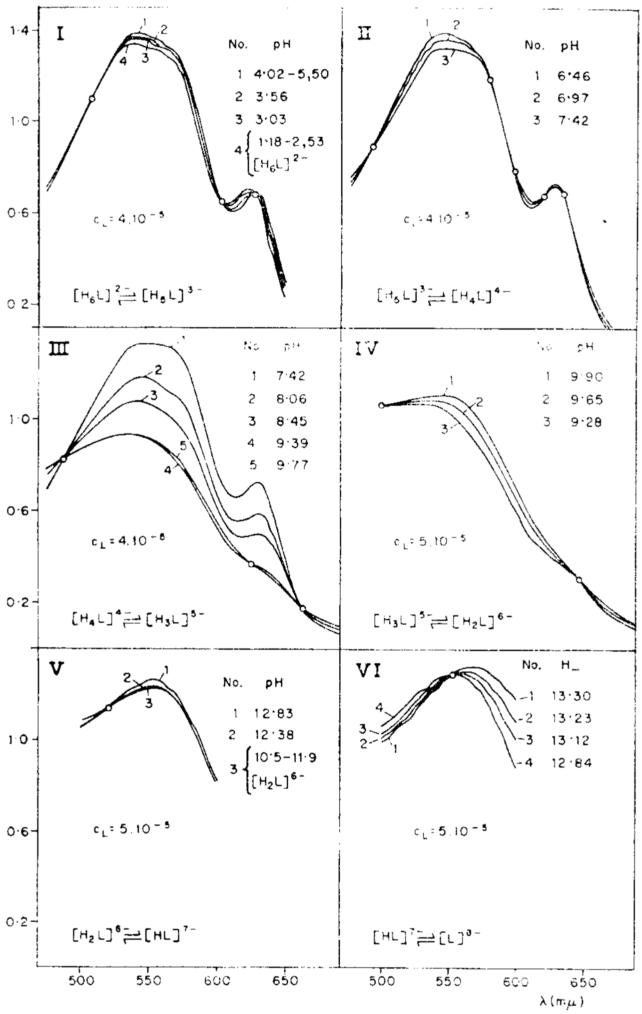

FIG. 2.—Isosbestic points exhibited by the palladiazo reagent within the pH scale.

chelate between the two *peri* phenolic groups of the chromotropic acid structure. If this were so, it would imply that the cleavage of the intramolecular hydrogen-bonds occurs before the last proton of the two —AsO_3H_2 groups has been split off. This interpretation disagrees with most currently-accepted views,[48,49] which assume the following deprotonation sequence with increasing pH: —SO_3H (two groups; two protons); —AsO_3H_2 (two groups; four protons); —OH (two groups; two protons). However, the marked spectral changes shown by the reagent after the titration of the first four protons (Fig. 2; II and III) seem to show clearly that the strength of the intramolecular hydrogen-bonds is greatly decreased immediately after the removal of the two protons in the first dissociation step of the —AsO_3H_2 groups, as depicted by the strong hypochromic effects shown by the 540- and 630-nm absorption bands. On the other hand the results obtained from the potentiometric titration of palladiazo[2] indicate, in agreement with the interpretation of the isosbestic points (Fig. 2), that 4

TABLE I.—SUMMARY OF THE MAIN PROTOLYTIC REACTIONS AND ABSORBANCE FEATURES OF PALLADIAZO AND ITS DISSOCIATION PRODUCTS

Acidity interval, Δ pH	Isosbestic points, *nm*	λ_{max}, *nm*	λ_{max}, *nm*	Step, *n*	Species in equilibrium	Constants of the system	Deprotonating group(s)	Remarks
<1	425; 465; 585	540	630	7	$H_7L^- \rightleftharpoons H_6L^{2-}$	$K_6, K_7, \varepsilon_6, \varepsilon_7$	2nd —SO_3H	(1)
1–2·5	425; 465; 585	540[a]	630[a]	—	$[H_6L]^{2-}$	ε_6	—	(2), (3)
2·5–4	520; 605; 630	540[b]	630[c]	6	$H_6L^{2-} \rightleftharpoons H_5L^{3-}$	$K_5, K_6, \varepsilon_5, \varepsilon_6$	1st —AsO_3H_2	(3)
4·5–5	520; 605; 630	540[a]	630[a]	—	$[H_5L]^{3-}$	ε_5	—	(2), (3)
5·5–7·5	495; 580; 620; 635	540[d]	630[a]	5	$H_5L^{3-} \rightleftharpoons H_4L^{4-}$	$K_4, K_5, \varepsilon_4, \varepsilon_5$	2nd —AsO_3H_2	(3), (4)
7·5–9	490; 665	540[e]	630[e]	4	$H_4L^{4-} \rightleftharpoons H_3L^{5-}$	$K_4, K_3, \varepsilon_4, \varepsilon_3$	1st —OH	(5)
9–10	500; 645	540[b,g]	—[f]	3	$H_3L^{5-} \rightleftharpoons H_2L^{6-}$	$K_3, K_2, \varepsilon_3, \varepsilon_2$	1st —AsO_3H^-	(6), (7)
10–12	500; 645	550[a,g]	—	—	$[H_2L]^{6-}$	ε_2	—	(2), (6)
12–13	525	555[b]	—	2	$H_2L^{6-} \rightleftharpoons HL^{7-}$	$K_2, K_1, \varepsilon_2, \varepsilon_1$	2nd —AsO_3H^-	(6)
13–16	555	555[c]	(635)[g,h,i,j]	1	$HL^{7-} \rightleftharpoons L^{8-}$	$K_1, \varepsilon_1, \varepsilon_0$	2nd —OH	(8), (9)
>16	—	—[j]	635[i]	—	$[L]^{8-}$	ε_0	—	(8), (9)

[a] No appreciable spectral changes are observed.

[b] Slight hyperchromic effect with increasing pH.

[c] Coincidence of isosbestic point with wavelength of maximum absorption.

[d] Moderate hypochromic effect with increasing pH.

[e] Strong hypochromic effect with increasing pH.

[f] The disappearance of the 630-nm absorption band is attributed to the weakening of the tautomeric *peri* phenolic and –N=N– bonds accompanied by the increasing establishment of tautomeric equilibria between the phenolic groups (–O - - - H - - - O– hydrogen-bonded chelate).

[g] Slight bathochromic shift with increasing pH.

[h] For alkalinities higher than pH 14 the isosbestic point and absorption maximum located at 555 nm disappear, and simultaneously the 630 nm absorption band appears.

[i] Strong hyperchromic effect with increasing alkalinity.

[j] Upon the disappearance of the absorption maximum at 555 nm a strong hypochromic effect sets in on the 425–550 nm spectral region with increasing alkalinity.

(1) The characteristics of the acidity interval 1 > pH; $H_0 \leq -7$ will be described in detail at the end of this paper.

(2) Flat portion of the $\bar{E}$ *vs.* pH function as derived from the existence of a unique $[H_nL]$ species.

(3) The more acidic (azo) tautomeric form of the reagent is supposed to predominate.

(4) Potentiometric titration of the reagent points to the neutralization of four acid groups (1st equivalence point).

(5) The very important spectral changes are assumed to derive from the deprotonation of the 1st phenolic group whereby a *peri*-OH tautomeric equilibrium sets in (H-bond phenolic chelate) accompanied by a progressive weakening of the azoquinonehydrazone tautomeric equilibrium established between the *peri* phenolic and –N=N– bridging groups.

(6) Establishment to a major extent of the tautomeric equilibrium between the H-bond and phenolate groups building the strong phenolic chelate.

(7) Potentiometric titration points to the titration of six acid groups (2nd, less-pronounced, equivalence point).

(8) Establishment of mesomerism resonance mechanism between the anionic phenolates and bridging azo-groups accompanied by the progressive disappearance of the tautomeric equilibrium between the H-bridged chelated phenolates.

(9) Described in detail later in the paper.

TABLE II.—RESULTS OBTAINED FOR THE INSTABILITY CONSTANTS (K_1–K_6) AND MOLAR ABSORPTIVITIES (ε_1–ε_6) OF PALLADIAZO

Parameter calculated	λ_1 *nm*	Method used for the calculations			
		Formulae (5) and (6)		Formulae (7)–(10)	
		K_n*	ε_n,* *l.mole⁻¹.mm⁻¹*	K_n	ε_n, *l.mole⁻¹.mm⁻¹*
K_1, ε_1	540	$1\cdot13 \times 10^{-14}$	$2\cdot51 \times 10^3$	$1\cdot77 \times 10^{-4}$	$2\cdot73 \times 10^3$
					$2\cdot10 \times 10^3$
					$2\cdot44 \times 10^3$
	630	$3\cdot24 \times 10^{-14}$	800	$1\cdot34 \times 10^{-14}$	636
					638
					783
K_2, ε_2	540	$3\cdot57 \times 10^{-12}$	$2\cdot46 \times 10^3$		
	630	$1\cdot47 \times 10^{-12}$	811	$8\cdot65 \times 10^{-12}$	847
K_3, ε_3	540	$1\cdot08 \times 10^{-10}$	$2\cdot25 \times 10^3$	$2\cdot99 \times 10^{-11}$	$2\cdot21 \times 10^3$
		$2\cdot19 \times 10^{-10}$	$2\cdot25 \times 10^3$		$2\cdot18 \times 10^3$
					$2\cdot30 \times 10^3$
	630	$7\cdot77 \times 10^{-11}$	813		
		$5\cdot89 \times 10^{-10}$	851		
K_4, ε_4	540	$6\cdot95 \times 10^{-9}$	$3\cdot37 \times 10^3$	$9\cdot30 \times 10^{-9}$	$3\cdot61 \times 10^3$
		$7\cdot97 \times 10^{-9}$	$2\cdot91 \times 10^3$		$3\cdot36 \times 10^3$
					$3\cdot13 \times 10^3$
	630	$7\cdot28 \times 10^{-9}$	$1\cdot83 \times 10^3$	$1\cdot20 \times 10^{-8}$	$2\cdot14 \times 10^3$
		$7\cdot50 \times 10^{-9}$	$1\cdot49 \times 10^3$		$1\cdot62 \times 10^3$
					$1\cdot81 \times 10^3$
K_5, ε_5	540	$1\cdot41 \times 10^{-6}$	$3\cdot53 \times 10^3$		
		$1\cdot88 \times 10^{-6}$	$3\cdot54 \times 10^3$		
		$1\cdot55 \times 10^{-6}$	$3\cdot62 \times 10^3$		
	630	$1\cdot06 \times 10^{-6}$	$1\cdot72 \times 10^3$	$1\cdot59 \times 10^{-6}$	$1\cdot64 \times 10^3$
		$5\cdot75 \times 10^{-7}$	$1\cdot72 \times 10^3$		$1\cdot70 \times 10^3$
		$3\cdot59 \times 10^{-7}$	$1\cdot73 \times 10^3$		$1\cdot77 \times 10^3$
K_6, ε_6	540	$5\cdot16 \times 10^{-4}$	$3\cdot39 \times 10^3$	$3\cdot11 \times 10^{-4}$	$3\cdot35 \times 10^3$
		$3\cdot45 \times 10^{-4}$	$3\cdot43 \times 10^3$		
	630	$5\cdot65 \times 10^{-4}$	$1\cdot51 \times 10^3$	$2\cdot19 \times 10^{-4}$	$1\cdot49 \times 10^3$
		$2\cdot99 \times 10^{-4}$	$1\cdot57 \times 10^3$		

* Calculated from the limiting ε_{n-1} values obtained directly from the experimental $\bar{E} = f(\text{pH}, \lambda, c_L)$ function (Fig. 1) in strongly alkaline media ($\varepsilon_0^{540} = 2\cdot06 \times 10^3$; $\varepsilon_0^{630} = 4\cdot00 \times 10^3$ l.mole⁻¹.mm⁻¹).

acid groups are titrated together at the first equivalence point and 2 additional groups at the second less well-defined, equivalence point.

However, as more experimental material is obtained and basic knowledge increases,[50] many of the original hypotheses have been revised more and more frequently. Thus Savvin,[51] contrary to earlier statements,[48,49] speculates that the fifth proton expelled from arsenazo III derivatives might be split off the first phenolic group or alternatively that the proton from this group might be the seventh to be lost (pH ~ 10) after the total deprotonation of the two arsonic groups.

Our hypothesis that the first phenolic proton is dissociated just after the first deprotonation stage of the two arsonic groups seems to be supported by the appearance of a rather clear second equivalence point corresponding to the neutralization of 5 protons in the potentiometric titration of arsenazo III.[22] This has also been found by

TABLE III.—MAIN AGING CHARACTERISTICS EXHIBITED BY THE PALLADIAZO SOLUTIONS AS INFERRED FROM THE SPECTROPHOTOMETRIC INVESTIGATION OF THE PALLADIAZO–PERCHLORIC ACID–WATER SYSTEM

c_L, $10^{-5}M$	Acidity interval	Colour of the solutions		Most significant spectral changes undergone by the solutions (maximum absorption wavelengths in *nm*)		Remarks
		Freshly prepared	Aged (6 months)	Freshly prepared	Aged (6 months)	
1·25	$-0{\cdot}1 \leq H_0 \leq -1$	pale pink	pale pink	230; 310; 395; 540; 625	no changes; 230*	(1)
1·25	$-1{\cdot}3 \leq H_0 \leq -1{\cdot}5$	brilliant pink	lilac	230; 310; 395; 540; 625	230*; 310; 395*; *530*†; (575)	(2)
1·25	$-1{\cdot}5 \leq H_0 \leq -2{\cdot}3$	purple; bluish	weak orange	230; 310; 575; 630	230; 310; 420*; *505*; *525*; 630†	(2)
1·25	$-2{\cdot}5 \leq H_0 \leq -3{\cdot}8$	bluish-green; greenish	weak yellow	310; 665	230; *415*; *495*; (525); 665†	(2), (3), (4)
1·25	$-4{\cdot}5 \leq H_0 \leq -5{\cdot}8$	emerald green	emerald green	230; 430; 665	230; *380*; 430*; 665†	(3), (5)
1·25	$-5{\cdot}8 \leq H_0 \leq -6{\cdot}8$	emerald green	yellowish-green	230; 425; 665	230*; *270*; 425*; 665†; (620)	(3), (5)
1·25	$H_0 > -6{\cdot}8$	emerald green	strong yellow	230; 425; 665	230*; 270*; *425**; 650†	(3), (4)
1·625	$H_0 \leq -2{\cdot}8$			230; 310	230; 310	(6)
1·625	$-3{\cdot}3 \leq H_0 \leq -5{\cdot}3$			230	230	
1·625	$H_0 > -6$			230		(7)

(1) No appreciable progress of side-reactions is assumed to occur.
(2) Enrichment of the original solutions in the rose-coloured stereoisomeric species is assumed to occur.
(3) Formation of perchloric acid addition and/or oxidation products is assumed to occur to a considerable extent.
(4) Extensive destruction of the reagent azo chromogenic groups takes place.
(5) The protonated conjugate acid forms built by the reagent azo groups remain unchanged to a considerable extent.
(6) Acidities lower than $H_0 < -2{\cdot}8$ were not investigated, because of occurrence of pronounced precipitation and colloidal phenomena.
(7) The aged solutions failed to exhibit the 230 and 270 nm absorption maxima shown systematically by all the $1{\cdot}25 \times 10^{-5}M$ palladiazo solutions.
* The indicated wavelengths exhibited varying hyperchromic effects with increasing acidity.
† The indicated wavelengths exhibited varying hypochromic effects with increasing acidity.

TABLE IV.—PRELIMINARY INVESTIGATION OF THE ISOSBESTIC POINTS OF THE PALLADIAZO–PERCHLORIC ACID–WATER SYSTEM

c_L, *M*	Time, *hr*	Acidity interval, ΔH_0	Isosbestic points, *nm*
$2{\cdot}5 \times 10^{-5}$	6–7	$-1 \le H_0 \le -1{\cdot}7$	467·5; 575
		$-2{\cdot}4 \le H_0 \le -3{\cdot}5$	467·5; 592·5
	30	$-4{\cdot}1 \le H_0 \le -7{\cdot}45$	457·5; 540; 660
	54	$-1{\cdot}0 \le H_0 \le -3{\cdot}75$	470
$2{\cdot}0 \times 10^{-5}$	2–3	$-1{\cdot}7 \le H_0 \le -2{\cdot}9$	—
	4–5	$-0{\cdot}1 \le H_0 \le -1{\cdot}9$	472·5
$1{\cdot}25 \times 10^{-5}$	4–5	$-2{\cdot}3 \le H_0 \le -3{\cdot}1$	597·5
		$-0{\cdot}7 \le H_0 \le -1{\cdot}8$	580
	9–10	$-2{\cdot}3 \le H_0 \le -3{\cdot}1$	597·5
		$-3{\cdot}6 \le H_0 \le -7{\cdot}7$	665
		$-0{\cdot}7 \le H_0 \le -1{\cdot}4$	467·5; 580
	48	$-2{\cdot}3 \le H_0 \le -3{\cdot}1$	470; 600
		$-3{\cdot}1 \le H_0 \le -7{\cdot}7$	642·5

Savvin with arsenazo III,[49] arsenazo M[51] and other reagents of this type.[51,52] Contrary to palladiazo, in the case of the reagents arsenazo III, arsenazo M and some other compounds investigated which exhibit arsonic groups *o*- or *o*,*o*′- to the azo-groups, the strong electrophilic nature of these substituents might give rise to an increase of the acidity of the phenolic groups, resulting in the appearance of a second equivalence point corresponding to neutralization of a phenolic proton before the second dissociation stage of the arsonic groups sets in. As a matter of fact, the p*K* values for this group in palladiazo and arsenazo III are 8·2 ± 0·1 (see Table VII) and [24]5·3–7·1 respectively (pK_4 according to our notation).

It is interesting to note that the dissociation constants for the last two deprotonations of chromotropic acid are 5·4 ± 0·1,[53–55] and 15·6 ± 0·3,[23] as compared with the values 8·15 ± 0·1 and 14·0 ± 0·2 which have been obtained for its bis(azo-phenyl 4.4′-arsono) derivative, palladiazo (see Table VII).

These interesting implications and logical reaction possibilities have apparently not been fully realized by most authors working in this field.

Another very interesting question is the origin of the 625–640 nm secondary absorption band, exhibited by most bisazochromotropic acid derivatives, to which practically no attention has hitherto been paid. Only very recently has it been hinted[51] that this absorption band could be due to the presence of some reacting cationic impurity. However, after careful repetition of syntheses of arsenazo M to check this point, Savvin *et al.*[51] concluded that the appearance of this band derives from a special tautomeric quinone–hydrazone form of the reagent. Although we assume that the spectral variations shown by this band within the pH interval 1–8 are related to the extent of displacement of the azo–quinonehydrazone tautomeric equilibria (*vide supra*) it must be said that the ratio between the molar absorptivities of palladiazo at 540 and 630 nm varies from preparation to preparation over very wide and unpredictable limits ($\varepsilon_{540}/\varepsilon_{630} = 1{\cdot}8$–$2{\cdot}5$) when measured under identical conditions. A literature survey of the spectral characteristics exhibited by *o*,*o*′-, *p*,*p*′-, *m*,*m*′- and combinations of these phenyl-substituted bisazochromotropic acid derivatives indicates clearly that most of the reagents of this type which have been investigated in

TABLE V.—SYSTEMATIC INVESTIGATION OF THE ISOSBESTIC POINTS EXHIBITED BY THE PALLADIAZO–PERCHLORIC ACID–WATER SYSTEM AS A FUNCTION OF TIME ($c_L = 1{\cdot}25 \times 10^{-5}M$; $l = 10$ mm)

Time, *hr*	Acidity range	Isosbestic points, *nm*	Remarks
24	$-0{\cdot}1 \leq H_0 \leq -1{\cdot}8$ $-2{\cdot}5 \leq H_0 \leq -3{\cdot}8$ $-4{\cdot}4 \leq H_0 \leq -7{\cdot}3$	400; 450; 582·5 465; 600 450; 555	For $H_0 \geq -3$ no changes in the main absorption band (540 nm) take place; the secondary absorption maximum (630 nm) exhibits a progressive bathochromic shift up to 665 nm within the acidity interval $-1{\cdot}5 \leq H_0 \leq -4{\cdot}5$
48	$-0{\cdot}8 \leq H_0 \leq -1{\cdot}25$ $-1{\cdot}6 \leq H_0 \leq -2{\cdot}0$ $-2{\cdot}5 \leq H_0 \leq -3{\cdot}8$ $-4{\cdot}4 \leq H_0 \leq -7{\cdot}3$	587·5 467·5; 592·5 467·5; 605, 640 445; 555	A pronounced hypochromic effect is observed for most samples within the 630–660 nm interval at acidity $H_0 > -2$. At lower acidity values the corresponding 540 nm absorption band does not vary appreciably.
96	$-0{\cdot}9 \leq H_0 \leq -1{\cdot}7$ $-2{\cdot}0 \leq H_0 \leq -2{\cdot}5$ $-2{\cdot}8 \leq H_0 \leq -3{\cdot}4$ $-4{\cdot}5 \leq H_0 \leq -6{\cdot}3$	387·5; 405 462·5; 587·5 387·5; 405; 465; 597·5 387·7; 405; 480; 605; 642·5 555	Most congruent isosbestic picture. Taken as the "kinetic optimum" time. The corresponding absorption spectra are reproduced in Fig. 7.
192	$-0{\cdot}1 \leq H_0 \leq -1{\cdot}4$ $-4{\cdot}5 \leq H_0 \leq -6{\cdot}3$	595 545	Very strong kinetic variations (bathochromic shifts of the isosbestic points and maximum absorption wavelengths; disappearance of isosbestic points; hypochromic and strong general spectral variations observed, *etc*). Important interaction of palladiazo with perchloric acid
480	$-0{\cdot}1 \leq H_0 \leq -1{\cdot}6$	605	
960	$-0{\cdot}3 \leq H_0 \leq -1{\cdot}4$	647·5	Very important general discoloration. Extensive progress of side-reactions.

TABLE VI.—TENTATIVE INTERPRETATION OF THE STEPWISE EQUILIBRIA IN THE PALLADIAZO–PERCHLORIC ACID–WATER SYSTEM AS INFERRED FROM THE EXPERIMENTAL DATA IN TABLE V AND FIGS. 1, 2 AND 7

Acidity interval	Isosbestic points,* *nm*	Equilibria likely to occur	Remarks
$pH \leq 2{\cdot}5$	425; 462·5; 587·5	free $[H_6L]^{2-}$ species	Absence of specific isosbestic points
$2{\cdot}5 \geq pH, H_0 \leq -0{\cdot}7$	*425*; 462·5; 587·5	$H_6L^{2-} \underset{-H^+}{\overset{+H^+}{\rightleftharpoons}} H_7L^-$	Protonation of the 1st—SO_3^- group
$-0{\cdot}7 \leq H_0 \leq -1{\cdot}8$	*387·5*; *405*; 462·5; *587·5*	$H_7L^- \underset{-H^+}{\overset{+H^+}{\rightleftharpoons}} H_8L^0$	Protonation of the 2nd—SO_3^- group. Minimum solubility of the $[H_8L]$ species at $H_0 = -1{\cdot}6 \pm 0{\cdot}1$
$-1 \leq H_0 \leq -2{\cdot}5$	387·5; 405; 462·5; (*597*)	free $[H_7L]^-$, $[H_8L]$ and $[H_9L]^+$ species in equilibrium	Range where precipitation and colloidal phenomena are more pronounced. Purple, bluish and greenish transition tints.
$-2{\cdot}5 \leq H_0 \leq -3{\cdot}4$	387·5; 405; *480*; (*605*); *642·5*	$H_8L^0 \underset{-H^+}{\overset{+H^+}{\rightleftharpoons}} H_9L^+$	Protonation of the 1st-N=N- group
$-3{\cdot}5 \leq H_0 \leq -4{\cdot}5$	387·5; 405	free $[H_9L]^+$ species	Absence of specific isosbestic points
$-4{\cdot}5 \leq H_0 \leq -6{\cdot}3$	*555*	$H_9L^+ \underset{-H^+}{\overset{+H^+}{\rightleftharpoons}} H_{10}L^{2+}$	Protonation of the 2nd-N=N- group
$H_0 > -6{\cdot}3$	605(?); 642·5(?)	free $[H_{10}L]^{2+}$ species	Doubtful interpretation of the isosbestic points

* The isosbestic points in italics refer to "specific" points which might be directly related with more probability to the establishment of successive stepwise equilibria. Numbers in parentheses refer to isosbestic points which are probably of kinetic origin.

TABLE VII.—INSTABILITY CONSTANTS AND MOLAR ABSORPTIVITIES OF THE REAGENT "PALLADIAZO"

n	K_n	ε_n^{540} l.mole^{-1}.mm^{-1}	ε_n^{630} l.mole^{-1}.mm^{-1}	pK_n
0	—	$(1·97 \pm 0·16) \times 10^{3}$(I)	$(3·80 \pm 0·18) \times 10^{3}$(I)	—
0	—	$2·06 \times 10^{3}$(III)	$3·92 \times 10^{3}$(II)	—
0	—	—	$4·00 \times 10^{3}$(III)	—
1	$(1·87 \pm 0·94) \times 10^{-14}$(I)	$(2·45 \pm 0·18) \times 10^{3}$(I)	$(7·40 \pm 1·24) \times 10^{3}$(I)	$13·76 \pm 0·21$(I)
1	$2·34 \times 10^{-14}$(II)	—	—	14·2(IV); $14·08 \pm 0·13$(V)
2	$(4·56 \pm 4·38) \times 10^{-12}$(I)	$(2·68 \pm 0·14) \times 10^{3}$(I)	$(8·29 \pm 0·18) \times 10^{2}$(I)	$11·89 \pm 0·85$(I)
2	—	—	—	11·55(IV, V)
3	$(8·72 \pm 4·77) \times 10^{-11}$(I)	$(2·24 \pm 0·01) \times 10^{3}$(I)	$(8·32 \pm 0·19) \times 10^{2}$(I)	$10·14 \pm 0·27$(I)
3	—	—	—	10·35(IV); 10·25(V)
4	$(8·50 \pm 1·30) \times 10^{-9}$(I)	$(3·28 \pm 0·12) \times 10^{3}$(I)	$(1·78 \pm 0·09) \times 10^{3}$(I)	$8·08 \pm 0·07$(I)
4	—	—	—	8·15(IV); 8·25(V)
5	$(1·20 \pm 0·22) \times 10^{-6}$(I)	$(3·51 \pm 0·06) \times 10^{3}$(I)	$(1·70 \pm 0·01) \times 10^{3}$(I)	$5·93 \pm 0·08$(I)
5	—	—	—	5·90(IV); $6·51 \pm 0·44$(V)
6	$(3·76 \pm 0·66) \times 10^{-4}$(I)	$(3·39 \pm 0·02) \times 10^{3}$(I)	$(1·52 \pm 0·07) \times 10^{3}$(I)	$3·43 \pm 0·08$(I)
6	—	—	—	3·90(IV); $3·88 \pm 0·43$(V)
7	$\sim$1(IV)	$(3·35 \pm 0·10) \times 10^{3}$(I)	$(1·50 \pm 0·10) \times 10^{3}$(I)	$\sim$0(IV)
8	$(2·85 \pm 0·25) \times 10^{1}$(VI)	$(3·31 \pm 0·11) \times 10^{3}$(VI)	—	$-1·46 \pm 0·04$(VI)
9	$(9·70 \pm 0·21) \times 10^{1}$(VI)	$(1·15 \pm 0·05) \times 10^{3}$(III)	$3·50 \times 10^{3}$(III)	$-1·99 \pm 0·1$(VI); $-1·95$(IV)
9	$(1·74 \pm 0·04) \times 10^{2}$(IV, VII)	—	$(3·75 \pm 0·10) \times 10^{3}$(III)	$-2·4 \pm 0·1$(IV); (VII)
10	$\sim 2·5 \times 10^{7}$(IV, VII)	$\sim 1·0 \times 10^{3}$(IV, VII)	$\sim 3·7 \times 10^{3}$(IV, VII)	$-7·4$(IV, (VII)

(I) Average values calculated by statistical treatment of the data obtained from equations (5)–(10).
(II) Calculated graphically from equation (16).
(III) Calculated directly from the available experimental data.
(IV) Calculated graphically from equation (13).
(V) Calculated graphically from equation (11).
(VI) Calculated graphically from equation (22).
(VII) Calculated graphically from the investigation of protonation of palladiazo in sulphuric acid.[77]

detail also exhibit these two absorption bands within the pH region 1–8. Therefore, we think it logical to assume that their $\varepsilon_{\lambda_{max}}/\varepsilon_{\lambda'_{max}}$ ratios might also vary from preparation to preparation. One of the few exceptions seems to be arsenazo III, which, under special experimental conditions, we have shown to possess a number of unexpected strong spectral bands located at 540–575, 600 and 650 nm, giving rise to the appearance of stable isomeric arsenazo III "blue solutions".[4,5,30,56] This will be dealt with more fully in subsequent communications. At present we believe the phenomenon is in part due to varying stereoisomeric composition caused by uncontrolled factors in the synthesis and in the dissolution of the solid preparations under different experimental conditions. There is a possibility that isomeric mixtures occur containing varying ratios of *cis-cis*, *cis-trans* and *trans-trans* stereoisomers, the existence of which has been postulated by Brode *et al.*[39,57] for the molecules of compounds containing two azo groups. In the special case of the palladiazo–Pd(II) system we have concluded[30] that the reaction characteristics of the different isomeric reagent species with a given cation, and the protonation features in concentrated sulphuric or perchloric acid media, vary rather sharply from preparation to preparation so that the results to be expected are not apparently related to the initial $\varepsilon_{540}/\varepsilon_{630}$ absorbance ratios established for the reagents in weakly acidic media. These heretofore unmentioned facts imply the need for careful reconsideration of a number of the criteria currently used in the identification and establishment of purity of this type of reagent,[52,58] as we have pointed out briefly elsewhere.[5]

Evaluation of the instability constants and molar absorptivities of palladiazo within the pH *range* 1–13 *in differently buffered aqueous media*

The values of the protolytic instability constants K_2–K_7 of palladiazo have been calculated from the molar absorptivity values ε_{540} and ε_{630} obtained for different pH values, as assessed by analytical and graphical methods.

Starting from the assumption that within the pH interval 1–13 stepwise equilibria of the general type

$$H_nL \rightleftharpoons H_{n-1}L + H \qquad (1)$$

are established (charges are omitted throughout for the sake of simplicity), the apparent (non-thermodynamic) dissociation constants are defined by the general expression

$$K_n = [H]\,[H_{n-1}L]/[H_nL] \qquad (2)$$

referring to any equilibrium step n (where L means the anionic species of the fully deprotonated palladiazo molecule). The overall (analytical) concentration of the reagent for this equilibrium step is given by

$$c_L = [H_nL] + [H_{n-1}L]. \qquad (3)$$

The value of the absorbance of such a mixture (see Fig. 1) conforms to the general additivity condition

$$\bar{E} = \varepsilon_n \,.\, l \,.\, [H_nL] + \varepsilon_{n-1} \,.\, l \,.\, [H_{n-1}L] \qquad (4)$$

where l is the path-length.

On solving the system of equations (2)–(4) for each pair of absorbance values ($\bar{E}$, $\bar{E}'$) measured at the same wavelength and at pH values (pH, pH′) within the acidity limits corresponding to two successive isosbestic points (see Fig. 2), the following expression is obtained

$$K_n = \frac{(\bar{E} - \varepsilon_n \,.\, l \,.\, c_{\mathrm{L}})\,[\mathrm{H}]}{(c_{\mathrm{L}} \,.\, \varepsilon_{n-1} \,.\, l - \bar{E})} = \frac{(\bar{E}' - \varepsilon_n \,.\, l \,.\, c_{\mathrm{L}})\,[\mathrm{H}']}{(c_{\mathrm{L}} \,.\, \varepsilon_{n-1} \,.\, l - \bar{E}')} \tag{5}$$

from which the value ε_n can easily be obtained as

$$\varepsilon_n = \frac{[\mathrm{H}]\,(\bar{E}' - \varepsilon_{n-1} \,.\, c_{\mathrm{L}} \,.\, l)\mathrm{E} - [\mathrm{H}']\,(\bar{E} - \varepsilon_{n-1} \,.\, c_{\mathrm{L}} \,.\, l)\bar{E}'}{c_{\mathrm{L}} \,.\, l\{[\mathrm{H}]\,(\bar{E}' - c_{\mathrm{L}} \,.\, l \,.\, \varepsilon_{n-1}) - [\mathrm{H}']\,(\bar{E} - c_{\mathrm{L}} \,.\, l \,.\, \varepsilon_{n-1})\}} \,. \tag{6}$$

The limiting value of ε_{n-1}, which is the basis for progressive calculation of the molar absorptivities of all the different proton complex species of the reagent, and hence for calculation of the successive instability constants, has been determined directly from the absorbance of concentrated sodium hydroxide solutions of the reagent. Under such conditions of high alkalinity (16–17*M* hydroxide) we can safely assume that only the fully deprotonated $[\mathrm{L}]^{8-}$ species of the reagent is present (molar absorptivity ε_0). If we put the value ε_0 into equation (6) we can calculate the value ε_1 within the next isosbestic interval, and this in turn becomes the ε_{n-1} value used to calculate ε_2 within the next isosbestic interval, and so on up to the limiting value $n = 6$. The results obtained for the ε_n and K_n values calculated by this method have been summarized in Table II.

This method cannot be used, however, for palladiazo for values of n higher than 6 because of the complicated behaviour exhibited by the reagent in media of acidity greater than 1*N*.

Alternatively, we have calculated some ε_n and K_n values by a method proposed by Komar.[59,60] Each K_n and ε_n value is assessed by taking 3 absorbance measurements ($\bar{E}_{\mathrm{i}}$, $\bar{E}_{\mathrm{m}}$, $\bar{E}_{\mathrm{p}}$) at the same wavelength, made at 3 corresponding pH values ($\mathrm{pH_i}$, $\mathrm{pH_m}$, $\mathrm{pH_p}$) located within any of the isosbestic intervals exhibited by the system. Starting from the usual theory, after a number of simple transformations the following expressions are arrived at:

$$K_n = \frac{(\bar{E}_{\mathrm{i}}[\mathrm{H}]_{\mathrm{i}} - \bar{E}_{\mathrm{p}}[\mathrm{H}]_{\mathrm{p}})\,([\mathrm{H}]_{\mathrm{i}} - [\mathrm{H}]_{\mathrm{m}}) - (\bar{E}_{\mathrm{i}}\mathrm{H}_{\mathrm{i}} - \bar{E}_{\mathrm{m}}[\mathrm{H}]_{\mathrm{m}})\,([\mathrm{H}]_{\mathrm{i}} - [\mathrm{H}]_{\mathrm{p}})}{\{([\mathrm{H}]_{\mathrm{i}} - [\mathrm{H}]_{\mathrm{p}})\,(\bar{E}_{\mathrm{i}} - \bar{E}_{\mathrm{m}}) - ([\mathrm{H}]_{\mathrm{i}} - [\mathrm{H}]_{\mathrm{m}})\,(\bar{E}_{\mathrm{i}} - \bar{E}_{\mathrm{p}})\}} \tag{7}$$

$$\varepsilon_{n-1} = \frac{(\bar{E}_{\mathrm{i}}[\mathrm{H}]_{\mathrm{i}} - \bar{E}_{\mathrm{p}}[\mathrm{H}]_{\mathrm{p}})\,(\bar{E}_{\mathrm{i}} - \bar{E}_{\mathrm{m}}) - (\bar{E}_{\mathrm{i}}[\mathrm{H}]_{\mathrm{i}} - \bar{E}_{\mathrm{m}}[\mathrm{H}]_{\mathrm{m}})(\bar{E}_{\mathrm{i}} - \bar{E}_{\mathrm{p}})}{l \,.\, c_{\mathrm{L}}\{([\mathrm{H}]_{\mathrm{i}} - [\mathrm{H}]_{\mathrm{p}})(\bar{E}_{\mathrm{i}} - \bar{E}_{\mathrm{m}}) - ([\mathrm{H}]_{\mathrm{i}} - [\mathrm{H}]_{\mathrm{m}})(\bar{E}_{\mathrm{i}} - \bar{E}_{\mathrm{p}})\}} \tag{8}$$

$$\varepsilon_n = \frac{\bar{E}_{\mathrm{i}}\bar{E}_{\mathrm{m}}[\mathrm{H}]_{\mathrm{p}}([\mathrm{H}]_{\mathrm{i}} - [\mathrm{H}]_{\mathrm{m}}) + \bar{E}_{\mathrm{m}}\bar{E}_{\mathrm{p}}[\mathrm{H}]_{\mathrm{i}}([\mathrm{H}]_{\mathrm{m}} - [\mathrm{H}]_{\mathrm{p}}) - \bar{E}_{\mathrm{i}}\bar{E}_{\mathrm{p}}([\mathrm{H}]_{\mathrm{m}}([\mathrm{H}]_{\mathrm{i}} - [\mathrm{H}]_{\mathrm{p}})}{l \,.\, c_{\mathrm{L}}\{([\mathrm{H}]_{\mathrm{i}} - [\mathrm{H}]_{\mathrm{m}})(\bar{E}_{\mathrm{i}}[\mathrm{H}]_{\mathrm{i}} - \bar{E}_{\mathrm{p}}[\mathrm{H}]_{\mathrm{p}}) - ([\mathrm{H}]_{\mathrm{i}} - [\mathrm{H}]_{\mathrm{p}})(\bar{E}_{\mathrm{i}}[\mathrm{H}]_{\mathrm{i}} - \bar{E}_{\mathrm{m}}[\mathrm{H}]_{\mathrm{m}})\}} \tag{9}$$

$$\varepsilon_n = \frac{\bar{E}_{\mathrm{i}}(K_n + [\mathrm{H}]_{\mathrm{i}})}{K_n \,.\, c_{\mathrm{L}} \,.\, l} - \frac{[\mathrm{H}]_{\mathrm{i}} \,.\, \varepsilon_n}{K_n} \,. \tag{10}$$

The application of Komar's method to the case of palladiazo has been rather critical and restrictive for practical reasons; within a number of isosbestic intervals the absorbance values were so close that the relative errors were large (Table II). These difficulties arise when dissociation produces too small a chromogenic effect, for especially when the protolysis of the arsonic and sulphonic groups is involved.[24]

The K_1–K_6 values have also been calculated by Suk's simple graphical method,[61] the basis of which becomes clear upon taking logarithms for any of the identities expressed by equation (5).

$$\mathrm{pH} = \log \frac{(\bar{E} - \varepsilon_n \,.\, l \,.\, c_\mathrm{L})}{(c_\mathrm{L} \,.\, \varepsilon_{n-1} \,.\, l - \bar{E})} + \mathrm{p}K_n = y + \mathrm{p}K_n = \mathrm{p}K_n + \log\,[\mathrm{H}_{n-1}\mathrm{L}]/[\mathrm{H}_n\mathrm{L}]. \tag{11}$$

When the term $y = \log\,[(\bar{E} - \varepsilon_n \,.\, c_\mathrm{L} \,.\, l)/(c_\mathrm{L} \,.\, \varepsilon_{n-1} \,.\, l - \bar{E})]$ becomes zero (*i.e.*, when $[\mathrm{H}_{n-1}\mathrm{L}] = [\mathrm{H}_n\mathrm{L})$ the expression (11) simplifies to pH = pK. The value of y can be calculated from the ε_n and ε_{n-1} values obtained as already described. The results obtained by this method for K_1–K_6 are reproduced in Fig. 3, and included in the summary of results in Table VII.

Finally, the K_1–K_7 values have been calculated approximately by means of a very simple graphical method proposed by Buděšínský and Haas.[62] Starting from equation (2) it can readily be seen that K_n will become identical with [H] when

$$[\mathrm{H}_{n-1}\mathrm{L}] = [\mathrm{H}_n\mathrm{L}] = c_\mathrm{L}/2 \tag{12}$$

In this case the absorbance will be given by the expression

$$\bar{E} = \sum_{\mathrm{i}=n}^{\mathrm{i}=n-1} \bar{E}_\mathrm{i} = \frac{c_\mathrm{L} \,.\, (\varepsilon_{n-1} + \varepsilon_n) \,.\, l}{2}\,. \tag{13}$$

This treatment can be applied to the $\bar{E} = f(\mathrm{pH}, \lambda, c_\mathrm{L})$ functions (Fig. 1) if the curves exhibit flat portions ($\bar{E}$ = constant) over some pH intervals. Such a flat portion derives from the predominance of a single protolytic species, and if the absorbance

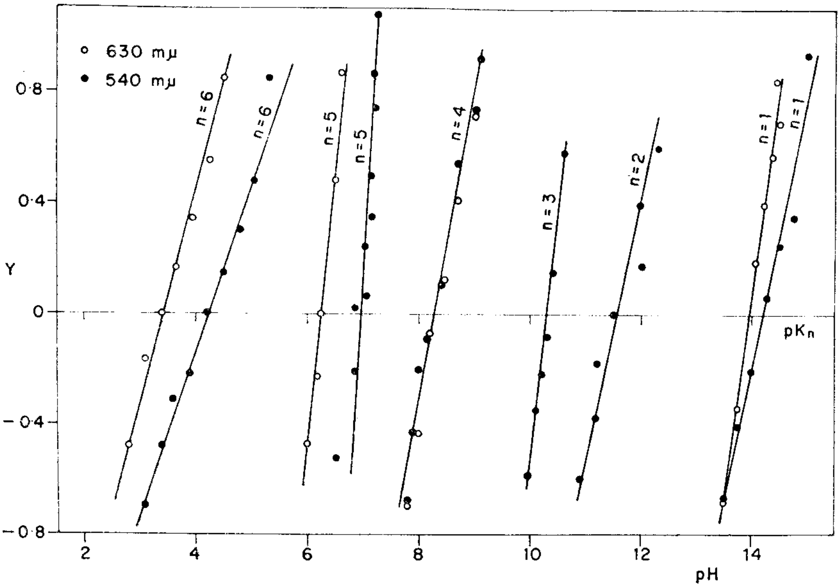

FIG. 3.—Graphical calculation of the K_1–K_6 instability constants of palladiazo in differently buffered media.

is ascribed to a pure species $[H_iL]$, the corresponding ε_i value can be calculated directly from $\bar{E} = \bar{E}_i = \varepsilon_i \,.\, l \,.\, [H_iL]$. When this condition holds for a number of successive equilibria, the pK_n values can be obtained from the pH values corresponding to the $\bar{E}$ values expressed by equation (13), which in turn are given by c_L and the ε_i values. The applicability of this method implies the fulfilment of certain requirements: the successive flat absorbance portions must correspond to true successive equilibrium steps; successive pK values must be sufficiently different ($\Delta pK \sim 1$–2); the chromogenic effects of the dissociation steps must bring about sufficiently strong spectral changes; sufficient experimental points must be used for the $\bar{E} = f(\text{pH}, \lambda, c_L)$ graphs. As a result of the number of these requirements, it is seldom possible to carry out the whole treatment of systems involving many equilibrium steps by exclusive application of this method. However, it may be very useful when additional comprehensive information about the protolytic features of the system is available (*i.e.*, establishment of the isosbestic intervals;[63] spectrophotometric variations, *etc*). In our case this method has proved very useful for calculation of the ε_7, ε_8 and pK_7 values.

Study of the protolytic equilibria in sodium hydroxide media

The absorbance *vs.* H_- functions in Fig. 1 clearly indicate that the last phenolic proton of palladiazo is very difficult to remove because of the formation of a hydrogen-bond between it and the two phenolate groups. The great stability of the chelate thus formed makes it quite impossible to attempt the study of the last deprotonation step by working with aqueous media of alkalinity in the pH range 11–13 although many authors[14,25,49,64–70] working on homologous reagents of the bis(azophenyl)chromotropic acid type have assumed that it is possible.

In Fig. 4 we reproduce the results obtained from the spectrophotometric investigation of the spectral variations exhibited by the reagent for increasing alkalinities. The originally pink palladiazo solutions (0·1*M* NaOH) turn successively purple (1*M* NaOH), lavender (5*M* NaOH), bluish (10*M* NaOH) and deep blue (NaOH > 12*M*) as the alkalinity of the medium increases within the range $13{\cdot}3 \leqslant \text{pH}, H_-\ H \leqslant 18{\cdot}3$. These changes are accompanied by a very strong bathochromic shift (555–635 nm) and a pronounced hyperchromic effect.

The alkalinity values in aqueous concentrated sodium hydroxide solutions must be calculated from the analytical concentration of the alkali (determined by acidimetric titration, with phenolphthalein or Methyl Red–Bromecresol Green indicators) through interpolation in the H_- alkalinity function, first determined by Schwarzenbach and Sulzberger[71] and defined by

$$H_- = pK_a - \log([HL]/[L^-]) \tag{14}$$

which is equivalent to

$$H_- = -\log(a_{H_3O^+} + f_{L^-}/f_{HL}) \tag{15}$$

(where pK_a is the negative logarithm of the thermodynamic dissociation constant of the acid indicator HL in water; $a_{H_3O^+}$ is the activity of the hydronium ion in solution and f_{HL} and f_{L^-} are the activity coefficients of the indicator and its conjugate base).

We have used the H_- values for solutions of pH > 13·5, as calculated by Schwarzenbach and Sulzberger,[71] which agree reasonably closely with those determined more recently by other authors.[72] The pK of the last deprotonation step, K_1, has been calculated graphically by a method first used by Heller and Schwarzenbach.[23]

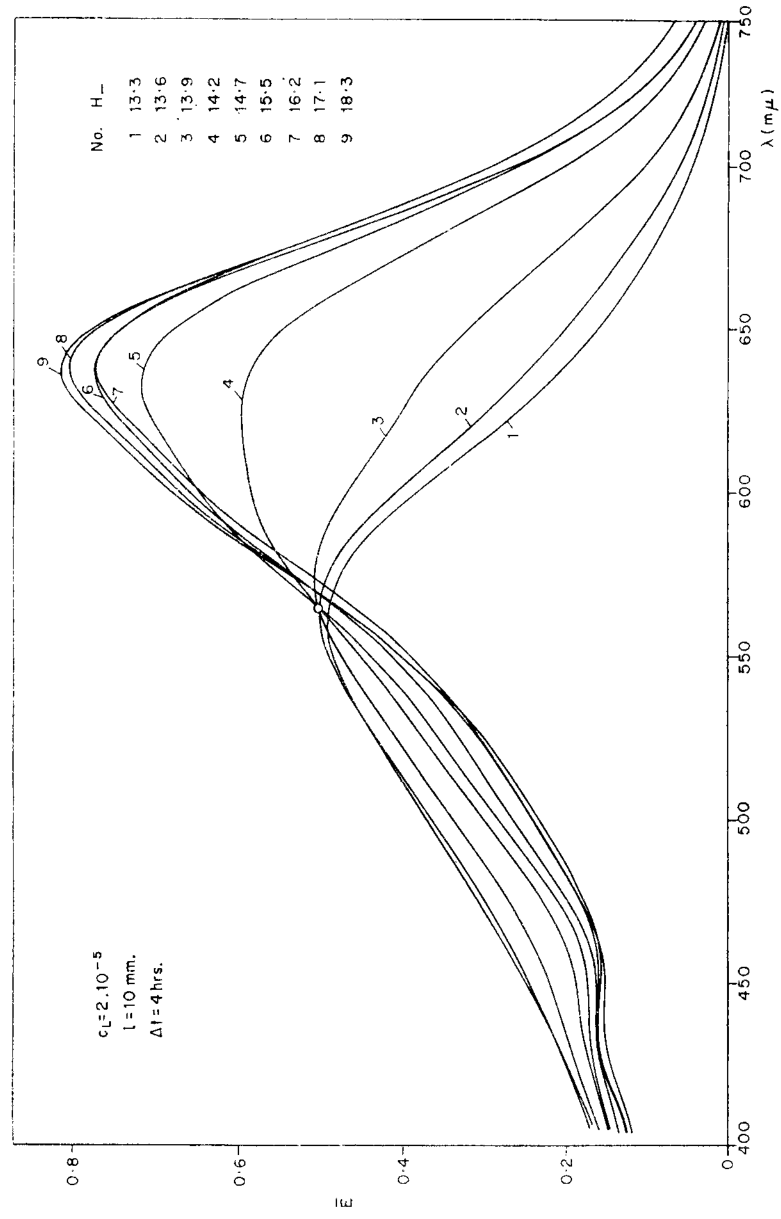

FIG. 4.—Absorption spectra of palladiazo in sodium hydroxide media.

From considerations similar to those used for deduction of equations (5) and (6), Heller and Schwarzenbach arrived at an expression which in our notation is

$$\frac{\varepsilon_0 \,.\, c_L}{\bar{E}} - \left[[\mathrm{H}] - \frac{\varepsilon_1 \,.\, [\mathrm{H}] \,.\, c_L}{\bar{E}}\right] \Big/ K_1 - 1 = 0, \tag{16}$$

Equation (16) is similar to an expression employed by Ågren[73] in connection with the determination of the stability constants of a number of phenolic acids by graphical means.

Plotting the term $c_L/\bar{E}$ *vs.* [H] . $(1 - \varepsilon_1 \,.\, c_L/\bar{E})$ for different pairs of values $\bar{E}$, H_{-} gives rise to a straight line which intersects with the abscissa at K_1 and with the ordinate at the point $1/\varepsilon_0$.

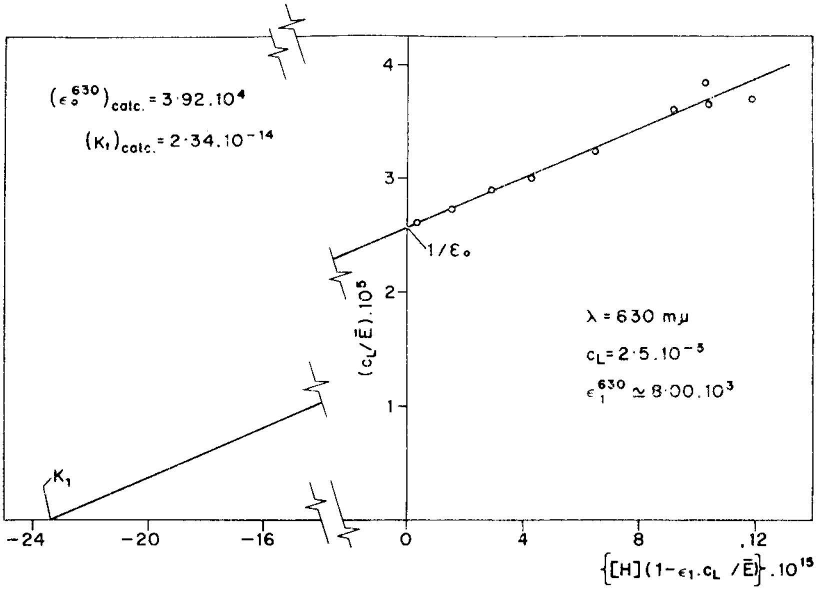

FIG. 5.—Graphical calculation of the last instability deprotonation constant of palladiazo in sodium hydroxide media.

In Fig. 5 we have reproduced the results obtained by application of this method to the absorbance measurements at 630 nm shown in Fig. 1 (the corresponding function at 540 nm proved unsatisfactory for the purpose because of the spectral changes at this wavelength, undergone by the reagent in concentrated sodium hydroxide solution; see Fig. 4). Extrapolation yields a value of $2\cdot 34 \times 10^{-14}$ for the last instability constant of palladiazo, which agrees well with the K_1 values found by other methods (Table II); the ε_0 value $3\cdot 92 \times 10^3$ l.mole^{-1} mm^{-1} also compares well with the value $4\cdot 00 \times 10^3$ calculated directly from the experimental results in Fig. 1.

The value of 800 l.mole^{-1}. mm^{-1} for ε_1 needed for equation (16) was obtained directly from the $\bar{E}_{630}$ *vs.* pH function (pH interval 11–12) in Fig. 1. This value for ε_1 is assumed to be sufficiently accurate in view of the good agreement between the ε_0 values obtained from Figs. 1 and 5.

It is worthy of note that the K_1 values of palladiazo and chromotropic acid indicate that the bisazo substitution of the chromotropic acid molecule brings about an approximately 100-fold decrease of the stability of the phenolic chelate. The extension of the

π-electron system which results from the introduction of the —N=N— group into the chromotropic acid molecule enhances the stability of the anion, which weakens the R–O · · · H · · · O–R′ phenolic hydrogen-bond and leads to a lowering of the pK. It is surprising that despite the huge amount of work which has been done in this field, and despite the conclusions reached by Heller and Schwarzenbach[23] this effect has rarely been recognized.[2,24,74]

The structure of the fully deprotonated $[L]^{8-}$ palladiazo molecule which is responsible for a very pronounced absorption band at 635 nm (Fig. 4) is most probably best described in terms of two limiting mesomeric structures in equilibrium. This equilibrium presupposes for the fully deprotonated palladiazo molecule a *trans-trans* electronic resonance structure as well as the absence of tautomeric intramolecularly hydrogen-bonded species. This structure is inferred from the following considerations.

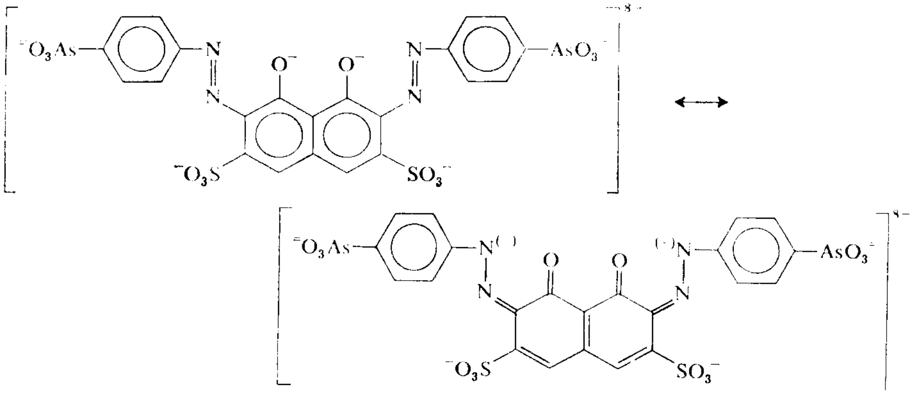

(*i*) We assume the symmetrical palladiazo molecule to be practically coplanar, exhibiting a unique chromophoric centre (very strong conjugation extent of the two azo groups; lack of steric hindrance).

(*ii*) Of the possible *trans-trans*, *cis-cis* and *cis-trans* stereoisomers we assume the *trans-trans* species to predominate over the others, in the light of the general conclusions reached during investigations of the isomeric properties of a number of azo and bisazo benzene and naphthalene derivatives,[39,40,41,57]

(*iii*) The high alkalinity of the medium implies the practical absence of hydroxy groups *o,o′*- to the azo groups, which rules out the establishment of the characteristic azo–quinonehydrozone tautomeric equilibrium[40] because of the lack of intramolecular hydrogen-bonds.

(*iv*) We assume that the structure of the fully deprotonated palladiazo molecule can be best illustrated in terms of the characteristic mesomeric electronic equilibrium found for the anions of deprotonated benzeneazonaphthols.[40]

Study of the protolytic equilibria in perchloric acid media

In media of increasing acidity the palladiazo reagent exhibits unexpectedly complicated behaviour: the reagent has a very low solubility over certain acidity ranges there are kinetically complicated phenomena related to precipitation and colloida; processes; amphoteric species are formed which give rise to a clearly defined point o minimum solubility of the reagent; anomalous absorption spectra depending on the overall reagent concentration, order of addition of reagents and acidity of the medium

The main features of these phenomena have been described in detail in a separate communication.[75]

The protolytic spectrophotometric investigation described so far has enabled us to determine the ε_n and K_n values of palladiazo up to the seventh protonation equilibrium step, which means that only the eighth step corresponding to the association of the first strongly acid $-SO_3H$ group remains to be investigated. For reasons similar to those explained in connection with the determination of the K_1 value in concentrated alkaline media, the protolytic features exhibited by the sulphonic acid groups cannot be investigated in aqueous media, even of low pH (< 1), but only in concentrated acid solutions.

In addition to the two sulphonic groups, the reagent has two $—N{=}N—$ groups which presumably undergo protonation in highly acidic media. Since the acidity in concentrated acid media of pH below the range 0·25–0·50 cannot be measured with electrodes, we are forced to use a function related to the analytical hydrogen ion concentration of the medium, as determined by alkalimetric titration, *e.g.*, with a mixed indicator for end-point detection.[76] As a rule, we used perchloric acid media to determine K_7 and K_8, and sulphuric acid media to investigate the protonation of the $—N{=}N—$ groups (as will be dealt with in a separate paper[77]).

The H_0 values used, defined by Hammett's acidity function,[78]

$$H_0 = pK_{HB^+} - \log [HB^+]/[B] = - \log (a_{H_3O^+} + f_B/f_{HB^+}) = - \log h_0 \qquad (17)$$

are those of Yates and Way[79] who have improved and extended the original acidity interval covered by Hammett and Deyrup.[78]

Interaction of palladiazo with perchloric acid

Palladiazo undergoes a number of visual colour changes as the acidity of the medium is increased. The palladiazo–perchloric acid solutions exhibit a pink colour in neutral or moderately acidic solutions, which becomes first more brilliant as the acidity increases up to $3{\cdot}6M$ $HClO_4$ then progressively purple ($4{\cdot}2M$ $HClO_4$), blue ($4{\cdot}8M$ $HClO_4$), bluish-green ($\leq 6{\cdot}4M$ $HClO_4$), and finally a brilliant emerald green ($11{\cdot}6M$ $HClO_4$ or $18M$ H_2SO_4, the most acidic media investigated). These colour transitions are readily reversible. Since concentrated perchloric acid is strongly oxidizing, special attention has to be paid to the behaviour exhibited by palladiazo in such media.

According to Budĕšínský[24] investigations involving bisazochromotropic acid derivatives in perchloric acid media should be carried out at low temperature (—5°). However, we have concluded that the palladiazo–$HClO_4$–H_2O system might be investigated at room temperature if the measurements are not unduly prolonged.

Figure 6 shows the results obtained at the three wavelengths of major interest (540; 630; 665 nm). From the analysis of Fig. 6 and other experimental evidence the following conclusions can be drawn.

(*i*) The 625–665 nm interval is the most useful for studying the interaction of the reagent with the acid.

(*ii*) As the overall reagent concentration increases, (by 30% at the $10^{-5}M$ level) the stability of the palladiazo solutions greatly increases.

(*iii*) The spectral changes are most spectacular within the H_0 interval -2 ± 1 as a result of the appearance of precipitation and colloidal phenomena, possible

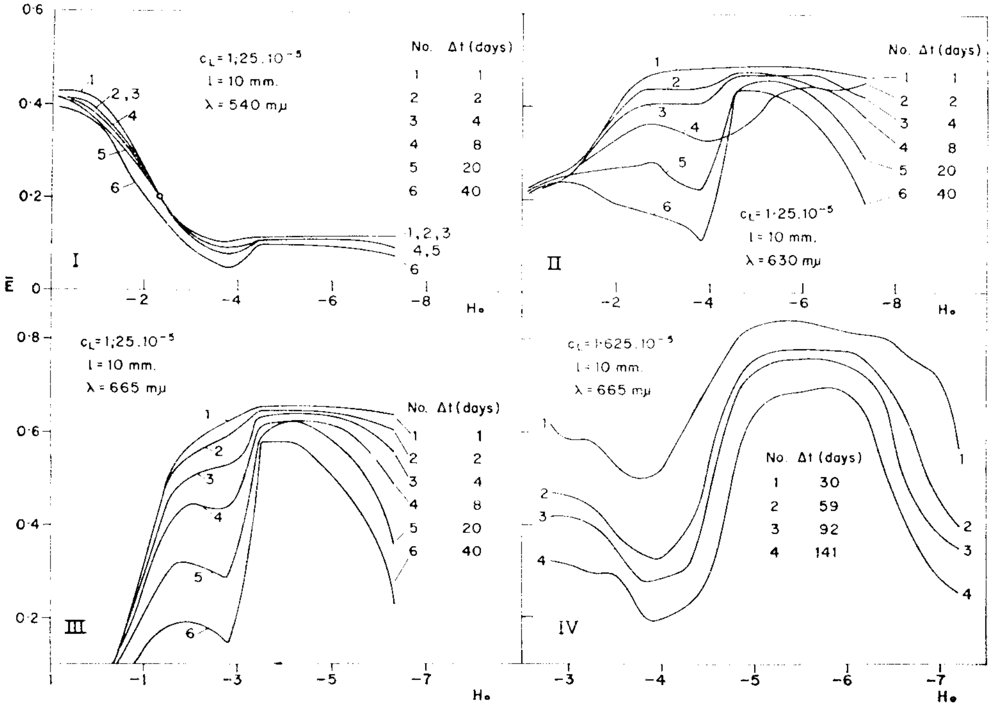

FIG. 6.—Spectral kinetic variations exhibited by the $\bar{E} = f(H_0, \lambda, c_L)$ function of palladiazo in perchloric acid media.

formation of amphoteric palladiazo hybrid species, a point of minimum solubility of the reagent (at $H_0 = -1·55$), *etc.* These phenomena have been dealt with elsewhere.[75]

(*iv*) Over a prolonged period (40 days), the original colours of the solutions faded, especially when the acidity was below $H_0 = -2·2$, the initial brilliant pink becoming very pale lilac and the original indigo and blue disappearing altogether. The greenish solutions ($-2·2 \leq H_0 \leq -3·1$) became very pale neutral-grey or slightly blue, and the emerald-green solutions ($-3·1 \leq H_0 \leq -3·8$) became much clearer and green or yellow-green in colour. The original emerald-green colour was kept only by solutions in the acidity range $-4·5 \leq H_0 \leq -5·3$, and at $H_0 > -5·3$ the original emerald green faded rapidly to very light yellowish-green.

Two series of palladiazo perchloric acid solutions were examined in detail spectrophotometrically after being aged for six months. The results are given in Table III, where only the spectrophotometric differences are considered. Additional information can be obtained by correlating Table III with Figs. 6 and 7. For conciseness no special discussions will be made here of the interesting and greatly varying characteristics shown by the stated hyperchromic and hypochromic effects. The wavelengths given do not necessarily include all the absorption bands exhibited by the solutions considered, but indicate the main spectral changes undergone during aging. The most probable explanations of the variations observed are briefly given in the remarks column of Table III.

The striking differences in behaviour exhibited by the two series of palladiazo solutions are indicative of the complicated nature of the interaction phenomena in the palladiazo-perchloric acid-water systems. The following hypotheses probably account for the nature of the products of the interaction.

(*i*) A change in the initial equilibria between the different stereoisomeric reagent species, caused by variation of the acidity conditions as a function of time, might give rise to the formation of increasing amounts of rose or slightly orange stereoisomeric species initially present in minor proportions. This conclusion is supported by the results of sorption experiments with palladiazo–perchloric acid solutions on activated silica columns.[80] In the case of azobenzene this type of isomeric interconversion has been clearly observed by Gerson and Heilbronner[81] and Schulte-Frohlinde.[82]

The formation of these rose or orange compounds, with absorption spectra showing a clearly hybridized main absorption band with maxima at 505 and 525 nm, occurs within the acidity interval $-1{\cdot}3 \leq H_0 \leq -2{\cdot}3$ which includes the point of minimum solubility[75] of the reagent (region of existence of the electrically neutral H_8L palladiazo species) at $H_0 = -1{\cdot}6 \pm 0{\cdot}1$ and is that over which there is maximum sorption of a rose palladiazo species (supposed to be an stereoisomer present in minor proportion in the starting palladiazo feed solutions) on activated silica columns.[80]

(*ii*) The formation of yellowish and strongly yellow solutions (maximum absorption wavelength 415–425 nm) we attribute to formation of palladiazo–perchloric acid addition compounds. This type of reaction has been reported by Layne *et al.*[83] for dialkyl-*N*-nitrosamines and perchloric acid, where adduct formation was shown to be accompanied by a general colour change. On the other hand, the reaction between different methoxyazobenzenes and perchloric acid has been shown[84] to lead normally to the formation of the corresponding salts of the protonated cationic azo structure (conjugate acid of the —N=N— group) and the ClO_4^- anion. However, the rather unexpected formation of an adduct of approximate 2:3 (azobenzene derivative: $HClO_4$) stoichiometry has been reported to occur in the case of the symmetrically substituted 4,4′-dimethoxy derivative.[84] In addition to the possible formation of palladiazo perchlorates and perchloric acid adducts we consider it highly possible that the initially formed palladiazo products are oxidized by the acid with the formation of cyclic structures, in a similar way to the formation of phenazones reported by Badger *et al.*[85] for the *cis*- and *trans*-isomers of azobenzene.

From the extreme complexity shown by the palladiazo-perchloric acid system, it is evident that more extensive investigation is needed before more definitive conclusions can be drawn as to the nature of the products of aging.

Isosbestic points and protolytic kinetics shown by palladiazo solutions in perchloric acid media

Because of the complicated interaction of the reagent with perchloric acid, the kinetic characteristics of the system had to be investigated before quantitative applications could be considered. Preliminary experiments (Table IV) revealed the presence of isosbestic points indicative of successive equilibria. The results obtained led to the following conclusions.

(*i*) The absence of isosbestic points 2 hr after preparation of the samples indicates that the protolytic equilibria are established very slowly, the more slowly as the overall reagent concentration becomes smaller.

(*ii*) The progressive appearance of isosbestic points indicates that several equilibira are established, with different kinetic characteristics.

(*iii*) The regularity of behaviour exhibited by the system can be inferred from the location of different isosbestic points at well-established wavelengths.

(*iv*) Quite apart from any disturbing effects which might be expected from the interaction of the reagent with the medium, a definite time period must be allowed to elapse before spectrophotometric measurements are made with the system.

(*v*) The system can be investigated quantitatively only at an overall reagent concentration of $c_L = 1{\cdot}25 \times 10^{-5}M$, despite the fact that this is far from being the most convenient one in terms of the kinetics and the aging phenomena.

From the facts above it is clear that a compromise in conditions has to be found for quantitative experiments, so that favourable kinetics are not offset by aging-reactions. The spectrophotometric and kinetic features of a series of palladiazo ($1{\cdot}25 \times 10^{-5}M$)-perchloric acid ($0{\cdot}5$–$11{\cdot}5M$) solutions were systematically investigated. The results are given in Table V and the absorption spectra recorded at the "kinetic optimum" time (*i.e.*, after 96 hr) are given in Fig. 7.

The information in Table V and Fig. 7 together with the theoretical implications discussed earlier have led us to a tentative interpretation of the protolytic features of the system and the main conclusions are summarized in Table VI. As a result of the several coexistent phenomena we do not rule out the possibility that some of the isosbestic points included in Table VI are kinetic in nature rather than corresponding to the true successive protolytic equilibria.

Assessment of the protonation constants of palladiazo in perchloric acid media

The complicated nature of the phenomena observed makes it advisable to treat the system quantitatively by methods which are not based on the use of the isosbestic points, because of the uncertainty as to their real origin and the observed disappearance and/or wavelength shifts of a number of them with passage of time.

Trial and error analytical or graphical methods based on the assumptions laid out in Table VI have been preferred, as a more convenient means of testing the validity of the theory. Within the acidity interval $-1 \leq H_0 \leq -3{\cdot}4$, the existence of the $[H_7L]^-$, $[H_8L]$ and $[H_9L]^+$ proton complex species is postulated; these are related to the instability constants K_8 and K_9 by the equations

$$K_8 = \frac{[H_7L][H]}{[H_8L]} \tag{18}$$

$$K_9 = \frac{[H_8L][H]}{[H_9L]}\,. \tag{19}$$

The overall palladiazo concentration is given by

$$c_L = [H_7L] + [H_8L] + [H_9L] \tag{20}$$

and the absorbance for a given H_0 value (λ constant) by

$$\bar{E} = \sum_{9}^{7} E_i = \varepsilon_7\,.\,[H_7L]\,.\,l + \varepsilon_8\,.\,[H_8L]\,.\,l + \varepsilon_9\,.\,[H_9L]\,.\,l. \tag{21}$$

Solving equations (18)–(21) with substitution of h_0 for [H] [since $H_0 = -\log h_0$ as

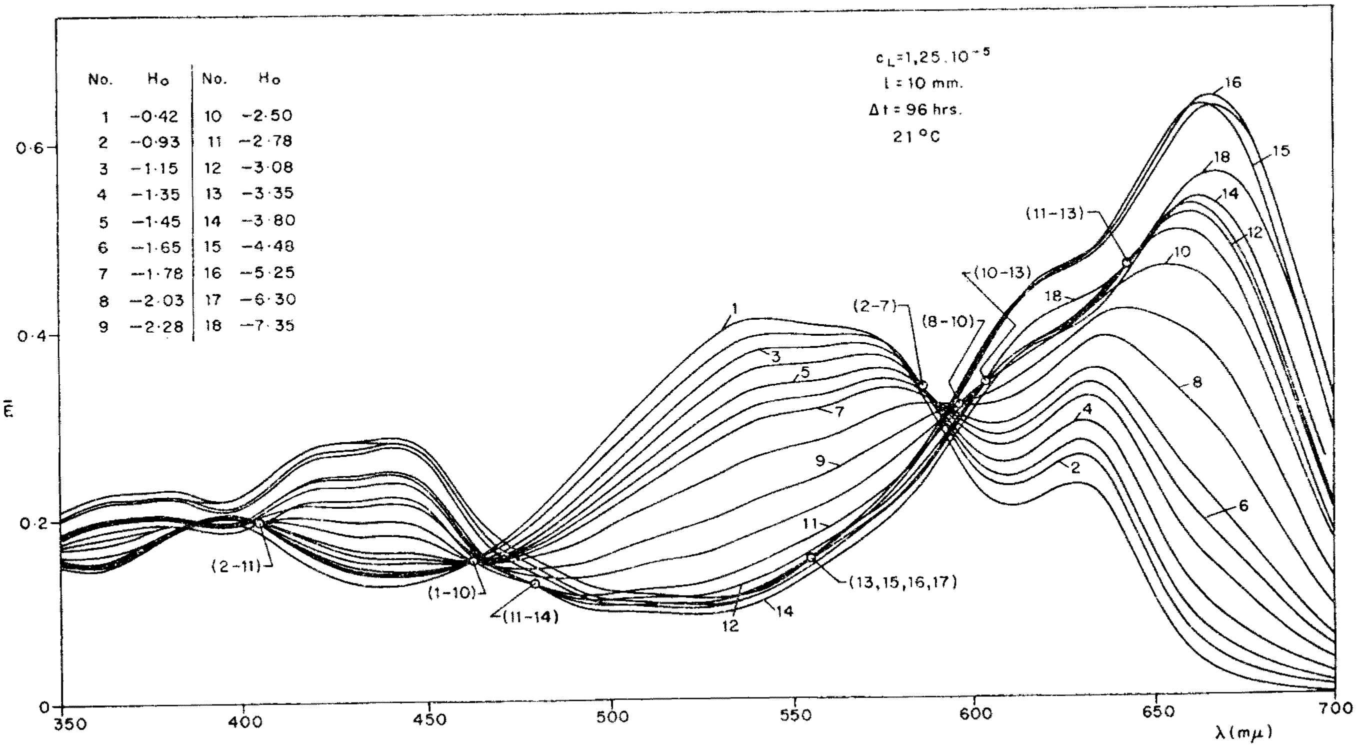

FIG. 7.—Absorption spectra and isosbestic points of palladiazo in perchloric acid media.

expressed by equation (17)] gives the final expression

$$\frac{1}{K_9} \cdot h_0^2(\varepsilon_9 \,.\, c_{\mathrm{L}} \,.\, \bar{E}) - K_8(\bar{E} - \varepsilon_7 \,.\, c_{\mathrm{L}}) + \varepsilon_8 \,.\, c_{\mathrm{L}} \,.\, h_0 - \bar{E} \,.\, h_0 = 0. \tag{22}$$

Equation (22) has been used by Körbl and Kakác[86] to solve a similar problem connected with the protolytic equilibria of Xylenol Orange and closely resembles an expression deduced by Schwarzenbach *et al.*[87] for calculation of the stability constants of some polyaminocarboxylic acids from potentiometric titrations (the main difference in this case is the use of the electroneutrality conditions instead of the absorbance additivity law).

Instead of solving equation (22) by analytical means (a very tedious proceeding unless a programming electronic calculating machine is used[86]), we have preferred a graphical procedure similar to that employed by Schwarzenbach *et al.*[87] by plotting for each set of absorbance–acidity values (E, H_0) a pair of values α, β, obtained from equation (22):

$$\alpha = \frac{\bar{E} \,.\, h_0 - \varepsilon_8 \,.\, c_{\mathrm{L}} \,.\, h_0}{h_0^2(\varepsilon_9 \,.\, c_{\mathrm{L}} - \bar{E})} \tag{23}$$

$$\beta = \frac{\bar{E} \,.\, h_0 - \varepsilon_8 \,.\, c_{\mathrm{L}} \,.\, h_0}{\bar{E} - \varepsilon_7 \,.\, c_{\mathrm{L}}} \,. \tag{24}$$

If the theoretical assumptions underlying this treatment (Table VI) are valid, then by means of (23) and (24) we will obtain a straight line for each pair of $\bar{E}$, H_0 values, and these lines will intersect at a point $\alpha_0 = 1/K_9$ and $\beta_0 = -K_8$. In addition, from a plot of the α and β values corresponding to the absorbance values measured within the acidity interval $-1 \leq H_0 \leq -3$ we will be able to draw conclusions concerning the acidity interval over which the three proton complex species considered can coexist, since outside this interval equation (22) will not hold.

In order to be able to apply equation (22) to calculate K_8 and K_9 we must know the values (for each wavelength setting) of ε_7, ε_8, ε_9 and h_0 [the latter can be readily calculated from the H_0 values by means of (17)]. The value ε_7 has been calculated directly from the absorbance *vs.* acidity function (540 nm, Fig. 1) from the flat absorbance curve over the acidity range $-1 \leq H_0 \leq 0$, since from the constancy of the function measured at 540 nm we conclude that only the $[H_7L]^-$ species is present over this acidity interval.

The value of ε_7 could not be calculated directly by this method from the measurements at 630 nm, since the sharp absorbance *vs.* acidity variations at this wavelength are indicative of the beginning of protonation of the first azo group (Figs. 1 and 7). Since the chromogenic effect from dissociation of the two $—SO_3H$ groups in bis(azophenyl)chromotropic acid derivatives has been shown as a rule to be very small[24] we have assumed tentatively that ε_8 (at 540 nm) is practically the same as ε_7 at 540 nm (Table VII), as inferred from the study carried out with sulphuric acid media.[77] The value of ε_9 has been calculated directly from the limiting absorbance of the $\bar{E} = f(H_0, \lambda)$ function (Fig. 1) as it becomes constant for increasing acidity ($H_0 \geq -4$).

The results obtained graphically are presented in Fig. 8, which confirms the satisfactory nature of the hypotheses made for the rather restricted acidity interval

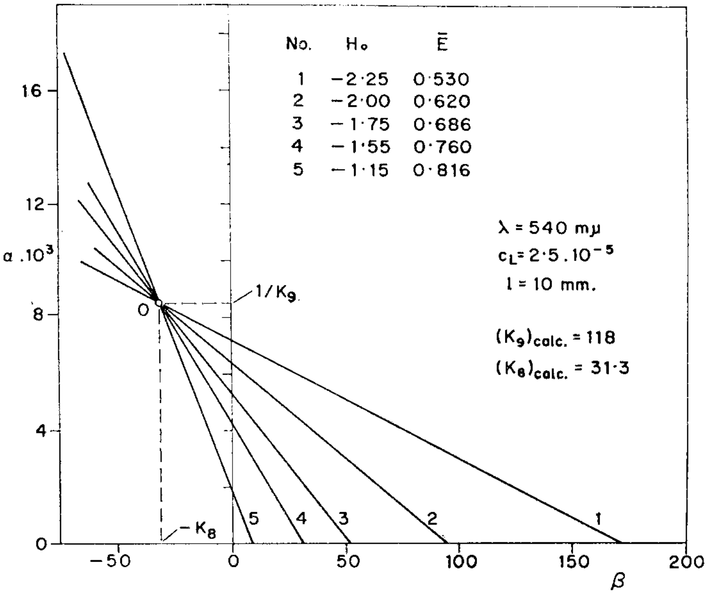

FIG. 8.—Graphical calculation of the K_8 and K_9 instability protonation constants of palladiazo.

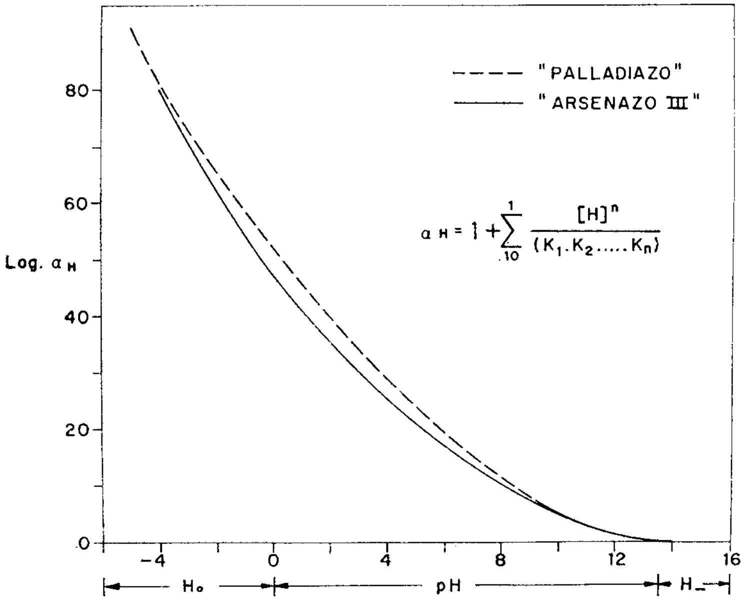

FIG. 9.—Graphical representation of the α_H functions of the structural isomers "palladiazo" and "arsenazo III".

$-1{\cdot}15 \le H_0 \le -2{\cdot}25$. It is possible, however, that the occurrence to some extent of the side-reactions might affect the apparent acidity limits of coexistence of the three proton complex species considered, and also affect the graphical solution of equation (22).

Finally, we have brought together in Table VII all the most significant results obtained for the protolytic dissociation of palladiazo. The K_n values have been used to calculate the palladiazo α_{H} function,[88] as defined by the expression

$$\alpha_{\mathrm{H}} = 1 + \sum_{n=10}^{n=1} \frac{[\mathrm{H}]^n}{\prod\limits_{n=10}^{n=1} K_n} . \tag{25}$$

This function is reproduced in Fig. 9 where we have also included the corresponding α_{H} function as calculated by Buděšínský[26] for arsenazo III. The similarity of both functions points very clearly to the fact that the acid properties of both structural isomers do not differ significantly as a result of bisarsonic substitution at the *o,o′*- or *p,p′*- positions of the bis(phenylazo)chromotropic acid molecule.

Acknowledgement—The authors express their warmest thanks to the Directorate of Chemistry and Isotopes of the Spanish Atomic Commission for the preparation of the diagrams as well as for the experimental facilities granted to carry out some important parts of this research.

Zusammenfassung—Das Reagens "Palladiazo" wurde in konzentrierter Perchlorsäure, verschiedenen wäßrigen Pufferlösungen und konzentrierten Natriumhydroxidlösungen eingehend spektrophotometrisch untersucht. K_1–K_{10}- und ε_1–ε_{10}-Werte, den Instabilitätskonstanten der beteiligten protolytischen Gleichgewichte und den molaren Extinktionskoeffizienten bei 540 und 630 nm der verschieden protonierten Spezies in dem System entsprechend, wurden mit Hilfe einer Reihe analytischer und graphischer spektrophotometrischer Methoden berechnet. Besondere Beachtung wird den komplizierten Erscheinungen bei der Einwirkung von Überchlorsäure auf das Reagens geschenkt: es wird gezeigt, daß Überchlorsäure die ursprüngliche Isomerenzusammensetzung des Reagens ändert. Ferner bilden sich durch Nebenreaktionen des Reagens mit dem Medium Anlagerungs- und/oder Oxidationsprodukte. Zum Vergleich werden alle auf mehreren Wegen erhaltenen Instabilitätskonstanten und molaren Extinktionskoeffizienten tabelliert.

Résumé—On a soumis le réactif "palladiazo" à une étude spectrophotométrique détaillée dans des solutions d'acide perchlorique concentré, de différents tampons aqueux et de soude concentrée. On a calculé les valeurs K_1–K_{10} et ε_1–ε_{10} correspondant aux constantes d'instabilité des équilibres protolytiques mis en jeu et aux coefficients d'absorption molaire à 540 et 630 nm des différentes espèces complexes protoniques du système par un certain nombre de méthodes spectrophotométriques analytiques et graphiques. On a porté une attention particulière à l'étude des phénomènes compliqués impliqués par l'interaction du réactif avec l'acide perchlorique, dont on a montré qu'il donne naissance à l'altération de la composition isomère initiale du réactif et à la formation de produits d'addition et/ou d'oxydation dérivés de réactions secondaires subies par le réactif avec le milieu. Toutes les constantes d'instabilité et les coefficients d'absorption molaire, que l'on a déterminés par plusieurs méthodes, sont mis en tableau pour comparaison.

REFERENCES

1. S. B. Savvin, *Dokl. Akad. Nauk SSSR*, 1959, **127**, 1231.
2. J. A. Pérez-Bustamante and F. Burriel-Martí, *Anal. Chim. Acta*, 1967, **37**, 49.

3. G. Popa, D. Negoin and G. Baiulescu, *Zh. Analit. Khim.*, 1959, **14**, 322.
4. J. A. Pérez-Bustamante, *Doctoral Thesis*, Madrid (1967).
5. J. A. Pérez-Bustamante, C. Morell García and F. Burriel-Martí, *Anal. Chim. Acta*, 1969, **44**, 95.
6. L. Bocanegra Sierra, *Doctoral Thesis*, Madrid (1969).
7. S. B. Savvin and Yu. M. Dedkov, *Zh. Analit. Khim.*, 1964, **19**, 21.
8. L. Sommer and M. Hniličková, *Collection Czech. Chem. Commun.*, 1957, **22**, 209.
9. L. Sommer and M. Cenek, *Chemist-Analyst*, 1967, **56**, 9.
10. H. Berger and K. H. Rohde, *Z. Chem.*, 1969, **9**, 178.
11. L. Sommer and M. Hniličková, *Folia Fac. Rer. Nat. Univ. Brno.*, 1964, **5**, 113.
12. S. B. Savvin and T. V. Petrova, *Zh. Analit. Khim.*, 1969, **24**, 177.
13. T. V. Petrova and S. B. Savvin, *ibid.*, 1969, **24**, 490.
14. A. I. Cherkesov and N. M. Alykov, *ibid.*, 1965, **20**, 1312.
15. S. B. Savvin and T. V. Petrova, *ibid.*, 1969, **24**, 177.
16. T. V. Petrova and S. B. Savvin, *ibid.*, 1969, **24**, 490.
17. S. B. Savvin, E. L. Kuzin, T. V. Petrova and N. Khakimkhodzhaev, *ibid.*, 1969, **24**, 1325.
18. S. B. Savvin, T. V. Petrova and N. Khakimkhodzhaev, *ibid.*, 1969, **24**, 1460.
19. L. Bocanegra Sierra, J. A. Pérez-Bustamante and F. Burriel-Martí (to be published).
20. S. B. Savvin, R. F. Propistsova and L. A. Okhanova, *Talanta*, 1969, **16**, 423.
21. *Idem*, *Zh. Analit. Khim.*, 1969, **24**, 1634.
22. J. A. Pérez-Bustamante and F. Burriel-Martí, *Anal. Chim. Acta*, 1967, **37**, 62.
23. J. Heller and G. Schwarzenbach, *Helv. Chim. Acta*, 1951, **34**, 1876.
24. B. Buděšínský, *Talanta*, 1969, **16**, 1277.
25. *Idem*, *Collection Czech. Chem. Commun.*, 1963, **28**, 2902.
26. *Idem*, *Z. Anal. Chem.*, 1965, **207**, 247.
27. J. A. Pérez-Bustamante and F. Burriel-Martí, *Inform. Quim. Anal.* (*Madrid*), 1968, **22**, 25.
28. *Idem*, *ibid.*, 1968, **22**, 31.
29. J. A. Pérez-Bustamante and R. Parellada Bellod, *An. Quím.*, 1968, **64B**, 213.
30. J. A. Pérez-Bustamante and F. Burriel-Martí (to be published).
31. A. K. Babko and T. Pilipenko, *Fotometricheskii Analiz*, Izdat Khimiya, Moscow, 1968.
32. R. Fernández Cellini and J. Alonso López, *An. Quím.*, 1956, **52B**, 163.
33. R. A. Robinson and R. H. Stokes, *Electrolyte Solutions*, Butterworths, London 1968.
34. B. Buděšínský and K. Haas, *Z. Anal. Chem.*, 1965, **210**, 263.
35. H. L. Schläfer and O. Kling, *Angew. Chem.*, 1956, **21**, 667.
36. O. Kling and H. L. Schläfer, *Z. Elektrochem.*, 1961, **65**, 142.
37. M. D. Cohen and E. Fischer, *J. Chem. Soc.*, 1962, 3044.
38. E. Kwiatkowskii, *Roczniki Chem.*, 1966, **40**, 177.
39. *Recent Advances in the Chemistry of Colouring Matters*, Spec. Publ. No. 4, pp. 1–27; 42–46. The Chemical Society, London, 1956.
40. H. Zollinger, *Die Chemie der Azofarbstoffe*, Birkhäuser Verlag, Basle-Stuttgart, 1958.
41. E. Fischer, *Fortschr. Chem. Forsch.*, 1967, **7**, 605.
42. W. R. Brode, J. H. Gould and G. M. Wyman, *J. Am. Chem. Soc.*, 1952, **74**, 4641.
43. L. A. Gribov, L. E. Kuzin and S. B. Savvin, *Zh. Analit. Khim.* 1967, **22**, 1790.
44. *Idem*, *ibid.*, 1968, **23**, 5.
45. *Idem*, *ibid.*, 1968, **23**, 490.
46. S. B. Savvin, R. F. Propistsova, Yu. G. Rozovskii and E. L. Kuzin, *Dokl. Akad. Nauk SSSR*, 1968, **181**, 613.
47. S. B. Savvin and E. L. Kuzin, *Talanta*, 1968, **15**, 913.
48. S. B. Savvin, T. V. Petrova and E. L. Kuzin, *Izv. Akad. Nauk SSSR, Ser. Khim.*, 1969, **2**, 290.
49. S. B. Savvin and R. F. Propistsova, *Zh. Analit. Khim.*, 1968, **23**, 653.
50. S. B. Savvin, *Usp. Khim.*, 1963, **32**, 195.
51. S. B. Savvin, R. F. Propistsova and R. V. Strel'nikova, *Zh. Analit. Khim.*, 1969, **24**, 31.
52. S. B. Savvin, R. F. Propistsova and T. G. Akimova, *ibid.*, 1969, **24**, 1231.
53. A. Okáč and L. Sommer, *Collection Czech. Chem. Commun.*, 1957, **22**, 433.
54. L. Sommer, *Bull. Soc. Chim. France*, 1959, 862.
55. M. Sakaguchi, A. Mizote, H. Miyata and K. Toei, *Bull. Chem. Soc. Japan*, 1963, **36**, 885.
56. J. A. Pérez-Bustamante and F. Burriel-Martí, unpublished results.
57. M. N. Inscoe, J. H. Gould and W. R. Brode, *J. Am. Chem. Soc.*, 1959, **81**, 5634.
58. A. A. Nemodruk, *Zh. Analit. Khim.*, 1967, **22**, 629.
59. N. P. Komar, *Dokl. Akad. Nauk SSSR*, 1950, **72**, 535.
60. *Idem*, *Tr. Inst. Kharkovsk. Univ.*, 1951, **8**, 51.
61. V. Suk, *Collection Czech. Chem. Commun.*, 1966, **31**, 3127.
62. B. Buděšínský and K. Haas, *Acta Chim. Acad. Sci. Hung.*, 1963, **39**, 7.

63. *Idem, Collection Czech. Chem. Commun.*, 1964, **29,** 1006.
64. B. Buděšínský, *Z. A ıal. Chem.*, 1963, **195,** 324.
65. B. Buděšínský and J. Gurovič, *Collection Czech. Chem. Commun.*, 1963, **28,** 1154.
66. A. E. Klygin and V. K. Pavlova, *Zh. Analit. Khim.*, 1959, **14,** 167.
67. A. I. Busev and G. E. Lunina, *ibid.*, 1966, **21,** 13.
68. A. F. Kuteinikov, *Zavodsk. Lab.*, 1962, **28,** 1179.
69. P. N. Palei, N. I. Udal'tsova and A. A. Nemodruk, *Zh. Analit. Khim.*, 1967, **22,** 1797.
70. H. Khalifa, M. A. Khater and A. A. El-Siraly, *Z. Anal. Chem.* 1968, **237,**, 111.
71. G. Schwarzenbach and R. Sulzberger, *Helv. Chim. Acta*, 1944, **27,** 348.
72. K. Bowden, *Chem. Revs.*, 1966, **66,** 119.
73. A. Ågren, *Acta Chem. Scand.*, 1955, **9,** 49.
74. S. B. Savvin and E. L. Kuzin, *Zh. Analit. Khim.*, 1967, **22,** 1058.
75. J. A. Pérez-Bustamante, F. Burriel-Martí, *Anal. Chim. Acta*, 1970, **51,** 277.
76. *Some laboratory methods currently used at the Royal Institute of Technology*, Stockholm, July 1959.
77. J. A. Pérez-Bustamante and F. Burriel-Martí, *Talanta*, to be published.
78. L. P. Hammett and A. J. Deyrup, *J. Am. Chem. Soc.*, 1932, **54,** 2721.
79. K. Yates and H. Wai, *ibid.*, 1964, **86,** 5408.
80. J. A. Pérez-Bustamante and F. Burriel-Martí (to be published).
81. F. Gerson, E. Heilbronner, A. van Been and B. M. Wepster, *Helv. Chim. Acta*, 1960, **43,** 1889.
82. D. Schulte-Frohlinde, *Annalen*, 1958, **612,** 131.
83. W. S. Layne, H. H. Jaffé and H. Zimmer, *J. Am. Chem. Soc.*, 1963, **85,** 1816.
84. Si-Jung Yeh and H. H. Jaffé, *J. Org. Chem.*, 1959, **24,** 717.
85. G. M. Badger, J. H. Seidler and B. Thomson, *J. Chem. Soc.* 1951, 3207.
86. J. Körbl and B. Kakác, *Collection Czech. Chem. Commun.*, 1958, **23,** 889.
87. G. Schwarzenbach, A. Willi and R. O. Bach, *Helv. Chim. Acta*, 1947, **30,** 1303.
88. A. Ringbom, *Complexation in Analytical Chemistry*, Interscience, New York, 1963.

Talanta, 1971, Vol. 18, pp. 213 to 218. Pergamon Press. Printed in Northern Ireland

EXTRACTION AND SEPARATION OF ^{137}Cs AND ^{86}Rb BY MEANS OF 4-t-BUTYL-2(α-METHYLBENZYL)PHENOL

J. Rais, J. Krtil and V. Chotívka
Institute of Nuclear Research, Řež by Prague, Czechoslovakia

(*Received* 9 *April* 1970. *Accepted* 27 *July* 1970)

Summary—The extraction of caesium-137 and rubidium-86 by a solution of 4-t-butyl-2(α-methylbenzyl)phenol in n-octane and tetrachloromethane has been investigated. The separation of rubidium and caesium has been performed by the Craig method and by reversed-phase extraction chromatography.

The extraction of rubidium and caesium by the substituted phenols, especially 4-s-butyl-2-(α-methylbenzyl)-phenol (BAMP), has received great attention. BAMP has been successfully used for the analytical estimation of caesium and rubidium,[1] for the extraction of caesium-137 from solutions of fission product wastes[2,3] and for the isolation of caesium and rubidium from minerals.[4] It has been suggested that caesium is extracted as a caesium phenolate solvated with additional molecules of the phenol. The distribution ratios increase generally in the sequence K < Rb < Cs and lithium and sodium are not appreciably extracted by BAMP.

The aim of this study was to find a method for the separation of rubidium and caesium which would be applicable to fission-product work, based on repeated extractions (Craig method) or reversed-phase extraction chromatography.

Rubidium and caesium have been separated in water–nitrobenzene by the Craig method in the presence of polyiodides[6] and by reversed-phase extraction chromatography as dipicrylaminates[7] and polyiodides.[8] Caesium-137 has been separated from other fission products on a Kel-F column with nitrobenzene and dipicrylaminates[9] and the separation of alkali metals by thin-layer chromatography with polyiodides has been achieved with nitrobenzene[10] and a mixture of nitromethane and benzene[11] as organic solvents.

Practically, it is of great interest to investigate the separation of caesium and rubidium by means of substituted phenols, because the separation factor q_{Cs}/q_{Rb} in the system water–nitrobenzene is approximately 5, whereas with substituted phenols values ranging from 12 to 21 can be reached.[12]

We have used 4-t-butyl-2(α-methylbenzyl)phenol (t-BAMP). Published results[12] suggest that its extraction behaviour will not be very different from BAMP, and the possibility of using it for reversed-phase extraction chromatography, with carbon tetrachloride as solvent and some graft copolymers as support, has been noted by Hornbeck.[13]

EXPERIMENTAL

Reagents

t-BAMP. The synthesis of t-BAMP was performed by arylalkylation of 4-t-butylphenol by styrene.[14,15] The t-BAMP was obtained as a nearly colourless oily liquid, b.p. = 180–5°, d_{25} = 1·004 g/ml, in good agreement with reported values.[15–17]

Radioisotopes. The following radioisotopes were used as tracers: ^{137}Cs, ^{86}Rb, ^{95}Zr–^{95}Nb, ^{144}Ce–^{144}Pr and ^{85}Sr. Their radiochemical purity was checked by β-absorption and γ-spectrometry. The β-emitters were counted by Geiger-Müller tube. ^{137}Cs and ^{86}Rb mixtures were estimated by a method based on differential absorption in aluminium foils.

All commercial reagents were of analytical-grade purity. Organic solvents were purified by distillation before use.

Procedures

Extraction experiments. Extractions were carried out in 10-ml glass centrifuge tubes. The ionic strength of the aqueous phase was maintained at $\mu = 1$, during the extraction into n-octane, with sodium hydroxide and nitrate. Three ml of the aqueous phase containing microamounts of rubidium-86 or caesium-137 were equilibrated with an equal volume of organic phase containing t-BAMP. Equilibrium was reached in less than 15 min for carbon tetrachloride extractions, but usually an equilibration time of 1 hr was allowed. The distribution ratios were calculated as

$$q = \frac{\text{activity per ml of organic phase}}{\text{activity per ml of aqueous phase}}\,.$$

Craig method for the separation of rubidium and caesium. Water and n-octane were mutually saturated beforehand at room temperature. The ionic strength of the aqueous phase was constant ($\mu = 1$), the concentration of t-BAMP in the initial organic phase was 0·5*M* and the pH of the aqueous phase was 12·67. The volumes of the organic and aqueous phases were 3 ml. A known amount of ^{86}Rb and ^{137}Cs was taken in tube (0) and evaporated to dryness. The organic and aqueous phase were added to tube (0) and after equilibration (30 min) and centrifugation the organic phase was quantitatively transferred into tube (1) where it was equilibrated with a fresh portion of aqueous phase. A fresh portion of the organic phase was added to the tube (0) and equilibrated. After equilibration the procedure was repeated as described. Ten transfers of the organic phase were accomplished during the experiment. After the last equilibration the aliquots of all organic and aqueous phases for radioactivity measurement of ^{137}Cs and ^{80}Rb were taken.

Reversed-phase extraction chromatography method. Ftoroplast-40 (perfluoropolyethylene of Soviet origin) was used as the supporting material. Some preliminary experiments have shown that styrenedivinylbenzene was not suitable as supporting material in the system used.

Two ml of 1*M* t-BAMP in carbon tetrachloride were added to 1·2–1·3 g of Ftoroplast-40 and shaken for 24 hr. Then the phases were separated. The saturated material was carefully transferred into a column of internal diameter 5 mm. The free volume of the column was estimated colorimetrically (solution of Methyl Red in 1*M* sodium hydroxide). All the solutions which were poured into the column were saturated beforehand with the solution of 1*M* t-BAMP in carbon tetrachloride for 2 hr. The flow-rate for sorption and elution, regulated by means of air pressure, was 3 drops/min which corresponds to 5 μl/mm^2/min in most cases. The drops were collected on aluminium dishes and evaporated and their β-activity was measured.

The break-through curves for microamounts of caesium were determined as follows. The [^{137}Cs]caesium chloride (tracer) was mixed with 1*M* alkali metal hydroxide and the solution was passed through the column. The effluent activity was compared with the activity of the initial solution.

The acidic solutions (2*M* nitric acid) of strontium-85, zirconium-95 or cerium-144 were neutralized with a mixture of sodium hydroxide and 0·01*M* EDTA to give a resulting solution 1*M* in sodium hydroxide. The mixture was heated for 15 min under an infrared source, then mixed with caesium-137 and transferred to the top of the column. The elution of Sr, Ce and Zr was effected by 200 drops of a mixture of 1*M* sodium hydroxide and 0·01*M* EDTA (saturated with t-BAMP) and the caesium-137 was then eluted by 100 drops of 0·1*M* sodium hydroxide.

RESULTS AND DISCUSSION

Batch experiments

Batch experiments were designed so as to give information on the extractive power of the reagent and the separation properties of the system water–n-octane. The dependence of the distribution ratio for rubidium (q_{Rb}) and caesium (q_{Cs}) on the pH of the aqueous phase and on the concentration of t-BAMP is shown in Figs. 1 and 2. The dependence of log q on pH is linear with a slope of unity. This is in accord with the idea that a caesium (rubidium) cation replaces one proton of the reagent and forms a phenolate in the organic phase. The extraction efficiency is greater for caesium than for rubidium, the separation factor for the pair Cs–Rb ($q_{\mathrm{Cs}}/q_{\mathrm{Rb}}$) being 17·4 for the whole range of pH studied (Fig. 1), which is more than three times that in the system water–nitrobenzene.

The dependence of the distribution ratio on the concentration of the reagent (on the logarithmic scale) is linear with a slope of 2·5 for both elements (Fig. 2). The supposition that the caesium phenolate is further solvated by molecules of the reagent in the organic phase seems quite reasonable in view of these results and this is in agreement with results obtained with BAMP.[5]

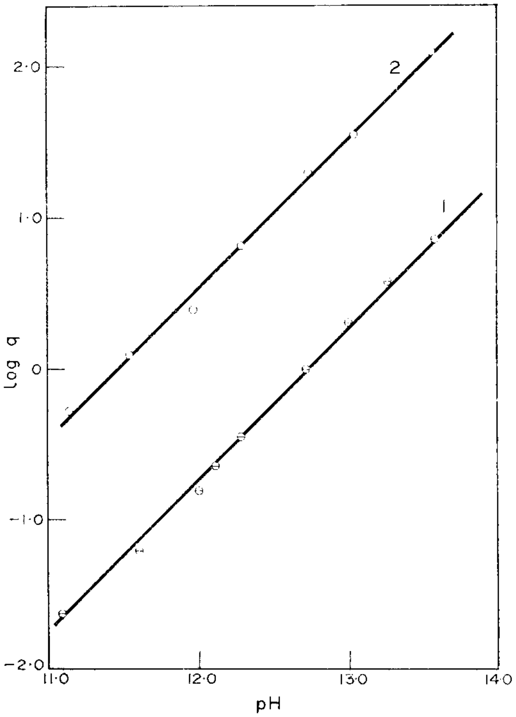

FIG. 1.—Dependence of the distribution ratio for caesium and rubidium on the pH of the aqueous phase.
1—^{86}Rb, *2*—^{137}Cs.
1*M* t-BAMP in n-octane, $\mu = 1$ (NaOH + NaNO$_3$), $v_a = v_0 = 3{\cdot}0$ ml.

The separation factor, if carbon tetrachloride was used for extraction instead of n-octane, was dependent on the concentration of sodium hydroxide in the aqueous phase. The following values were obtained for 0·1; 0·3; 0·5 and 1*M* sodium hydroxide (1*M* t-BAMP in carbon tetrachloride): 8·8; 8·8; 15·7; 15·9 (and distribution ratio q_{Cs}: 0·57; 1·48; 3·06 and 7·81, respectively). The distribution ratios from 1*M* aqueous ammonia were too low to be of practical importance.

Repeated extractions

The Craig method described in the experimental section was used for the separation of microamounts of rubidium and caesium. The theoretical distribution was calculated on the basis of the relationships given by Markov.[19] The amount of the species in both phases after *n* extractions is given by

$$C = \frac{A_{n,W} \cdot C_0 \cdot D^n}{(D+1)^W} \quad \text{and} \quad A_{n,W} = \frac{W!}{n!(W-n)!}$$

where n is the number of the tube (in our case 0,1,2 . . . 10), W is the total number of transfers (in our case 10), C is the total amount of the respective species (^{86}Rb, ^{137}Cs) in both phases of a given tube, C_0 is the initial amount of the substance introduced into tube (0) and D is the distribution ratio for a given species.

For D we have taken the values estimated from batch experiments ($q_{Cs} = 4{\cdot}0$ and $q_{Rb} = 0{\cdot}23$, see Fig. 2). The amounts of caesium and rubidium in separate tubes as found experimentally and calculated by the relationships above are in good agreement. The separation of both elements is good, as well as the efficacy of the separation, because the tubes (0), (1) and (2) contain ~70% of the rubidium in practically pure state and the tubes (8), (9) and (10) contain 68% of the caesium in pure form. It is obvious from the experiments performed that 11 tubes is quite sufficient for the separation of rubidium and caesium.

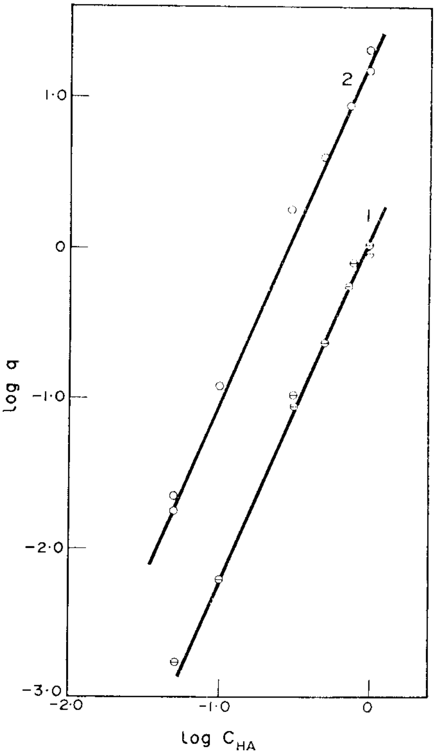

FIG. 2.—Distribution ratio for caesium and rubidium as a function of the amount of reagent.
1—^{86}Rb, *2*—^{137}Cs.
Extraction into n-octane, $\mu = 1$, pH = 12·69, $v_a = v_0 = 3{\cdot}0$ ml.

Reversed-phase extraction chromatography

It was found in the batch experiments that the separation factor q_{Cs}/q_{Rb} is dependent on the concentration of sodium hydroxide in the aqueous phase when extracting into t-BAMP in carbon tetrachloride. Therefore the amount of sodium hydroxide sufficient for quantitative separation of the two elements was determined.

The free volume (α_i) was in our case 0·17 ml and rubidium is always eluted in less than 1·2 ml. The separation of rubidium and caesium is good if the concentration of sodium hydroxide is equal to or greater than 0·5*M*.

It is interesting to compare the results of our dynamic experiments with some quantitative relations given by Trémillon.[20] For the position of the maximum of the respective peak (V_{Cs}, V_{Rb}) the relationship $(V_{Cs} - \alpha_i)/(V_{Rb} - \alpha_i) = q_{Cs}/q_{Rb}$ should apply. The calculated values 6 and 12 for 0·3*M* and 0·5*M* sodium hydroxide, respectively, agree relatively well with the values obtained from batch experiments (8·8 and 15·7). Moreover, the relationship $V_{Cs}/V_{Cs,0.37} = V_{Rb}/V_{Rb,0.37}$ holds ($V_{X,0.37}$ being the width of the peak in the region where the concentration of X is equal to 37% of its concentration at the maximum of the peak). Thus it is best to elute a mixture of rubidium and caesium with 0·5–0·6*M* sodium hydroxide or to perform the elution in two steps: (*i*) elution of rubidium by 1*M* sodium hydroxide in approximately 1·5 ml, (*ii*) subsequent elution of caesium by 0·1*M* sodium hydroxide. The use of n-octane instead of carbon tetrachloride as the solvent for BAMP should have the advantage of allowing a good separation of caesium and rubidium at lower pH of the aqueous phase (pH = 11–14, see Fig. 1).

From the break-through curves for microamounts of caesium and rubidium it is obvious that it is best to sorb caesium from 1*M* sodium hydroxide. We would expect still better sorption from 1*M* lithium hydroxide but caesium passes through the column in a volume of 1 ml. It does not seem that the competition of lithium *vs.* the organic phase could be responsible for this effect, and most probably the pH of 1*M* lithium hydroxide is not sufficient for the effective extraction of caesium. Rubidium is not retained on the column and is eluted in the first 1 ml of effluent. Thus, the caesium and rubidium can be well separated in this system by the method of frontal analysis.

We have also investigated the possibilities of the separation of caesium from some fission products by the elution method. The fission products were complexed beforehand with EDTA,[9] and caesium was eluted by 0·1*M* sodium hydroxide. We have not determined the separation factors attainable in the system, but from the results it can be concluded that caesium can be obtained in sufficient purity for practical purposes.

For the final separation of caesium (or rubidium) from the supporting solution of sodium hydroxide, extraction by nitrobenzene in the presence of dipicrylamine can be recommended. Dipicrylamine is dissolved directly in the alkaline aqueous phase and caesium is selectively extracted into nitrobenzene with a separation factor[21] near to 10^3.

Acknowledgement—The authors are indebted to Mrs. Kadlecová and Mr. Mencl for valuable aid in performing some experiments.

Zusammenfassung—Die Extraktion von Caesium-137 und Rubidium-86 durch eine Lösung von 4-t-Butyl-2—α-methylbenzyl)phenol in n-Oktan und Tetrachlormethan wurde untersucht. Die Trennung von Rubidium und Caesium wurde mit dem Craig-Verfahren und durch Extraktionschromatographie mit umgekehrten Phasen erreicht.

Résumé—On a étudié l'extraction du caesium-137 et du rubidium-86 par une solution de 4-*t*-butyl 2-(α-méthylbenzyl) phénol en *n*-octane et tétrachlorure de carbone. La séparation du rubidium et du caesium a été réalisée par la méthode de Craig et la chromatographie d'extraction à phases inversées.

REFERENCES

1. W. J. Ross and J. C. White, *Anal. Chem.*, 1964, **36,** 1998.
2. L. A. Bray, *U.S. At. Energy Comm. Rept.* BNWL-68, August 1965.
3. C. L. Richardson, *U.S. At. Energy Comm. Rept.*, HW-80686, 1963.
4. W. D. Arnold, D. J. Crouse and K. B. Brown, *Ind. Eng. Chem. Process Design Develop.*, 1965, **4,** 249.
5. B. Z. Egan, R. A. Zingaro and B. M. Benjamin, *Inorg. Chem.*, 1965, **4,** 1055.
6. E. M. Kuznetsova, N. A. Kresova and G. M. Panchenkov, *Zh. Fiz. Khim.*, 1967, **41,** 1041.
7. M. Kyrš and L. Kadlecová, *J. Radioanal. Chem.*, 1968, **1,** 103.
8. I. Akaza, *Bull. Chem. Soc. Japan*, 1966, **39,** 585.
9. C. Testa and C. Cesarano, *J. Chromatog.*, 1965, **19,** 594.
10. G. E. Janauer and R. C. Johnston, *Anal. Chem.*, 1965, **38,** 786.
11. G. E. Janauer, J. D. Carrano and R. C. Johnston, *Microchim. Acta*, 1968, 61.
12. G. S. Rodionova, V. V. Alekseyeva and V. V. Starostin, *Zh. Neorgan. Khim.*, 1970, **15,** 176.
13. R. F. Hornbeck, *J. Chromatog.*, 1967, **30,** 438.
14. *U.S. Patent* 2394754 (1946).
15. *U.S. Patent* 2849517 (1958).
16. Ng. Ph. Bun-Hoi, H. Le Bihan and F. Binon, *J. Org. Chem.*, 1952, **17,** 243.
17. A. A. Gadzibalaev and M. I. Archipov, *Izv. Vysshykh Uchebn. Zavedenii Khim. i Khim. Tekhnol.*, 1965, **8,** 469.
18. *U.S. Patent* 2276117 (1942).
19. V. K. Markov, *Tr. Komis. po Anal. Khim. Akad. Nauk SSSR Inst. Geochim. i. Analit. Khim.*, 1963, **14,** 99.
20. B. Trémillon, *Les séparations par les résines échangeuses d'ions*, Gauthier-Villars, Paris, 1965.
21. J. Rais, M. Kyrš and M. Pivoňková, *J. Inorg. Nucl. Chem.*, 1968, **30,** 611.

Talanta, 1971, Vol. 18, pp. 219 to 224. Pergamon Press. Printed in Northern Ireland

MICRODETERMINATION OF NITRATES AND NITRITES—III*

GASOMETRIC AND GRAVIMETRIC METHODS BASED ON REDUCTION WITH FORMIC ACID

W. I. Awad, S. S. M. Hassan and M. T. M. Zaki
Research Microanalytical Laboratories, Chemistry Department,
Faculty of Science, Ain Shams University, Cairo, U.A.R.

(*Received* 15 *May* 1970. *Accepted* 16 *June* 1970)

Summary—Simple microgasometric and gravimetric methods for the determination of the nitrate and nitrite groups are described. These are based on reduction with formic acid whereby one mole of nitrous oxide and four moles of carbon dioxide are simultaneously liberated per two moles of nitrate; two moles of nitrous oxide and six moles of carbon dioxide are liberated per seven moles of nitrite. Nitrous oxide is measured gasometrically and carbon dioxide gravimetrically. Results accurate to $\pm 0{\cdot}2\%$ absolute are obtained for both nitrate and nitrite.

LITTLE work has been reported on the use of organic reagents for gasometric and gravimetric determination of the nitrate group, apart from salicylic acid[1] and hydroquinone.[2]

Organic compounds such as nitron,[3] di(α-naphthylmethyl) amine,[4] α-phenyl-β-diethylaminoethyl-*p*-nitrobenzoate,[5] *N*-diethylbenzhydrylamine,[6] cinchonamine,[7] diphenylguanidine,[8] *p*-tolyl isothiourea,[8] 5-nitro-6-ethoxyquinoline,[9] and *N*- substituted α-naphthyl-methylamine[10] have been used to determine the nitrate group gravimetrically, but all have their limitations and give less accurated results when used on the microscale.

In the present work formic acid is used as an organic reductant for both the nitrate and nitrite groups. The nature of the reaction, advantages, limitations, and some possible interferences have been studied and microgasometric and gravimetric procedures are described.

EXPERIMENTAL

Apparatus

The gasometric measurements were made with the apparatus previously described.[2] The gravimetric measurements were made by using the apparatus shown in Fig. 1. It consists of a 25-ml reaction vessel (A), a 100 × 20 mm trap for moisture condensation (B), a 100 × 20 mm trap filled with 14–22 mesh anhydrone for moisture absorption (C), a Pregl absorption tube filled with a layer of 10–20 mesh manganese dioxide and a layer of anhydrone for nitric oxide absorption (D), a Pregl absorption tube filled with a layer of 14–22 mesh soda asbestos and a layer of anhydrone for carbon dioxide absorption (E), a guard-tube filled with alternate layers of soda asbestos and anhydrone (G), a small funnel (F), a Mariotte bottle, a stop-watch and a microburner.

The nitrogen used is purified by passage through a bell-chamber immersed in concentrated sulphuric acid contained in a cylindrical jar, and then through two U-tubes filled with anhydrone and soda asbestos respectively.

Reagents

All reagents were of analytical grade unless otherwise specified. The organic nitrates used were prepared according to standard methods. Cadmium nitrate tetrahydrate, bismuth nitrate pentahydrate, and lanthanum nitrate hexahydrate (commercial grade) were purified by several crystallizations. All the nitrate samples were $>99{\cdot}5\%$ pure (standard nitrometer method).

---

* Part II, Talanta, 1969, **16**, 1393.

Procedures

Gasometric determination of nitrates and nitrites. Introduce 3–5 mg of the nitrate into the reaction vessel, displace the air with carbon dioxide for 5 min till no air bubbles are collected in the nitrometer. Introduce 3 ml of formic acid through the funnel. Heat gently (~5 min), using a microburner, till no more gas bubbles are collected. Leave for 5 min and record the volume of nitrous oxide liberated. Carry out a blank experiment.

For nitrite determination, use the same procedure but insert a Pregl absorption tube filled with manganese dioxide between the reaction vessel and the nitrometer.

Calculate the nitrate and nitrite nitrogen-content according to the equation

$$\%\text{Nitrate or nitrite nitrogen} = F(V_1 - V_2)(P - p)/(273 + T)W$$

where V_1 ml is the volume of nitrous oxide, V_2 is the blank, P is the observed atmospheric pressure, p the vapour pressure of potassium hydroxide solution at $T°$ (the average temperature of the room and of the solution in the nitrometer), W mg is the sample weight, and F equals 45·02 and 78·61 for nitrate and nitrite respectively if the pressures are measured in mmHg (the practical measurement) and the corresponding factors are 33·77 and 56·46 for pressures measured in mbar.

Gravimetric determination of nitrates and nitrites. Weigh 3–8 mg of nitrate or nitrite sample into the reaction vessel (A) (Fig. 1). Connect the vessel to traps (B), (C) and tube (D). Adjust the rate of nitrogen flow to 20–25 ml/min and sweep for 10 min. Wipe and weigh the carbon dioxide absorption tube (E) and connect it to tube (D). Add 5 ml of formic acid through the funnel (F). Heat gently for 3 min. Sweep out the gaseous reaction products for 10 min. Disconnect the carbon dioxide absorption tube (E) and close it tightly with its cone and socket. Leave the tube in the balance room for 5 min; meanwhile weigh the next sample. Rewipe and reweigh the tube, using the same weighing schedule. Carry out a blank experiment. Calculate the nitrate and nitrite nitrogen-content from the equation

$$\text{Nitrate or nitrite nitrogen} = FW_1/W\%$$

where W_1 mg is the weight of carbon dioxide, W mg is the sample weight and F equals 15·91 and 37·12 for nitrate and nitrite respectively.

RESULTS AND DISCUSSION

Gasometric determination of nitrates and nitrites

Determination of the nitrate group. Formic acid reduces the nitrate group to nitrous oxide according to the equation[11]

$$6HCOOH + 2KNO_3 \rightarrow 2HCOOK + N_2O + 4CO_2 + 2H_2O$$

The reduction product of the nitrate group is proved to be pure nitrous oxide, since it is still recovered quantitatively when a trap of iron(II) solution or manganese dioxide is inserted between the reaction vessel and the nitrometer, and is therefore not nitric oxide or nitrogen dioxide. That it is not nitrogen is shown by passing the gaseous reduction products through a trap containing hydroiodic acid; iodine is liberated.[12]

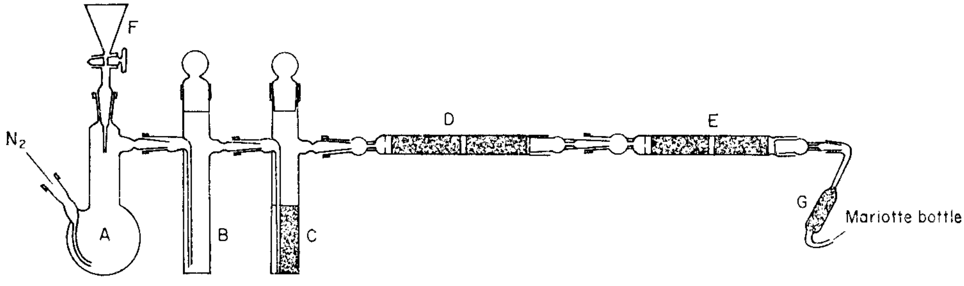

FIG. 1.—Apparatus for gravimetric determination of nitrates and nitrites (for description, see text).

Since nitrous oxide shows no solubility in alkaline solutions and known volume of the gas was unaltered when kept overnight over 50% potassium hydroxide solution, the reaction is used for the gasometric microdetermination of nitrates.

The action of formic acid on other nitrogen groups (*e.g.*, amide, azo, nitro, amine, oxime, and ammonium ions) gives no gaseous products. The presence of acetamide, Methyl Red, nitrobenzoic acid, *p*-aminophenol, α-benzoinoxime, and ammonium acetate does not affect the results for potassium nitrate, and the error was ±0.2% absolute. Inorganic oxidants such as potassium dichromate, permanganate, or periodate, ammonium metavanadate, sodium tungstate and potassium perchlorate do not interfere with the reaction.

Some nitrate samples are satisfactorily analysed by reduction with anhydrous formic acid (*cf.* Table I). The mean absolute error is ±0.1%. Similar results are also obtained by using acid of 70% concentration, but less accurate results are obtained by using more dilute acid. Nitrate esters (*e.g.*, P.E.T.N.) and nitramines (*e.g.*, nitroguanidine) are not reduced under these conditions.

TABLE I.—MICROGASOMETRIC DETERMINATION OF SOME NITRATE SAMPLES BY REDUCTION WITH FORMIC ACID

Sample	Nitrate-nitrogen, %	
	Calculated	Found
Potassium nitrate	13·85	13·8
		13·8
		13·9
Barium nitrate	10·71	10·6
		10·7
		10·8
Silver nitrate	8·24	8·2
		8·2
		8·3
Bismuth nitrate pentahydrate	8·67	8·6
		8·6
		8·8
Cadmium nitrate tetrahydrate	9·08	9·0
		9·1
		9·1
Lanthanum nitrate hexahydrate	9·70	9·7
		9·6
		9·6
Guanidine nitrate	11·47	11·4
		11·4
		11·5

Other reducing acids such as oxalic, tartaric and citric acids were also tried both in the presence of hydrochloric acid and as saturated solutions. No gaseous products were obtained, and the nitrate-nitrogen was quantitatively recovered as nitrous oxide after addition of formic acid, indicating that the nitrate group was unaffected by these acids. However, ascorbic acid in 6*M* hydrochloric acid reduced potassium nitrate to nitric oxide; the average recovery was only 70%.

Determination of the nitrite group. Reduction of sodium nitrite in acidic media with mercury, iron(II) and hydroquinone was tried. The mean average recoveries obtained were 100, 86 and 93% respectively with these reagents (Table II). Although satisfactory results were obtained with the mercury–sulphuric acid procedure, this method has its limitations in presence of aromatic substances, because of nitrosation of the aromatic moiety in preference to reduction of the nitrate group.[2]

It was found that sodium nitrite reacts with anhydrous formic acid according to the equation

$$7NaNO_2 + 13HCOOH \rightarrow 7HCOONa + 6CO_2 + 9H_2O + 3NO + 2N_2O$$

Compounds containing an aromatic moiety do not interfere. The presence of nitric oxide is confirmed by the brown fumes formed on exposure of the gaseous reduction products to air and by the reaction with iron(II) solution. The nitrous oxide is indicated by the liberation of iodine from hydriodic acid after the nitric oxide has been absorbed in a trap of granular manganese dioxide. Reduction of sodium nitrite with anhydrous formic acid and collection of the liberated gas over 50% potassium hydroxide solution, with a manganese dioxide trap inserted between the reaction vessel and the nitrometer, showed that the volume of gas obtained was two-fifths of that obtained without the trap. This indicates that nitrous and nitric oxide are liberated in ratio of 2:3. This can be explained on the basis that two reactions proceed simultaneously:

$$4NaNO_2 + 8HCOOH \rightarrow 4HCOONa + 4CO_2 + 6H_2O + 2N_2O$$

$$3NaNO_2 + 5HCOOH \rightarrow 3HCOONa + 2CO_2 + 3H_2O + 3NO$$

The recovery of two moles of nitrous oxide per seven moles of the nitrite, after absorption of the nitric oxide, constitutes the basis of the gasometric procedure. The results obtained by reduction of sodium nitrite with anhydrous formic acid show a mean absolute error of ±0·1% (Table II).

Reduction with dilute formic acid (70% v/v) is not quantitative and proceeds according to the first route only, since the gas liberated is pure nitrous oxide.

Gravimetric determination of nitrates and nitrites

The use of nitron. Gravimetric microdetermination of nitrate (*e.g.*, potassium nitrate) by precipitation with nitron proved to be unsuccessful. The average recovery is 81%. The solubility product of nitron nitrate was found to be $1{\cdot}2 \times 10^{-7}$ at 25°. The accuracy is independent of pH over the range 0·5–5.

TABLE II.—MICROGASOMETRIC DETERMINATION OF SODIUM NITRITE (20·29% N) BY REDUCTION WITH IRON(II), HYDROQUINONE, MERCURY AND FORMIC ACID

Reductant	Nitrite-nitrogen, found, %	Recovery %
Iron(II)–hydrochloric acid	17·7	87
	17·4	86
	17·0	84
Hydroquinone–hydrochloric acid	18·7	92
	18·9	93
	18·8	93
Mercury–sulphuric acid	20·3	100
	20·3	100
	20·3	100
Formic acid	20·2	100
	20·2	100
	20·2	100

Precipitation from solutions containing 5 mg of potassium nitrate per ml, in a filter beaker,[13] cooling, filtration and washing with 5 ml of cold water (5°) gave results correct within ±0·7% absolute but the use of this precipitant on the micro scale suffers from many difficulties; (*i*) several carefully controlled operations are needed, including precipitation, filtration washing and drying; (*ii*) solubility of the precipitate; (*iii*) poor precision and accuracy.

The use of formic acid. Carbon dioxide is an oxidation product of formic acid with both nitrates and nitrites. Four and six moles of carbon dioxide are liberated per two moles of nitrate and seven moles of nitrite respectively. The carbon dioxide is dried over anhydrone then swept with pure nitrogen gas into a previously weighed absorption tube containing soda asbestos. In the nitrite determination an additional trap of granular manganese dioxide is used to absorb the nitric oxide gas liberated.

TABLE III.—MICROGRAVIMETRIC DETERMINATION OF SOME NITRATE AND NITRITE SAMPLES USING FORMIC ACID

Sample	Nitrate or nitrite nitrogen, %	
	Calculated	Found
Barium nitrate	10·71	10·7 10·7 10·7
Silver nitrate	8·24	8·3 8·3 8·2
Cadmium nitrate tetrahydrate	9·08	9·1 9·1 9·0
Bismuth nitrate pentahydrate	8·67	8·6 8·8 8·7
Lanthanum nitrate hexahydrate	9·70	9·8 9·7 9·8
Urea nitrate	11·38	11·2 11·4 11·3
Sodium nitrite	20·29	20·3 20·3 20·2

Gravimetric analysis of different nitrate samples shows a mean absolute error of 0·04%. For sodium nitrite the mean absolute error is ±0·1% (Table III). However, this method is not applicable to nitrite or nitrate samples in presence of inorganic oxidants such as potassium dichromate, permanganate, periodate or perchlorate, ammonium metavanadate and sodium tungstate. Organic compounds containing a nitrogen function (*e.g.*, acetamide, Methyl Red, nitrobenzoic acid, *p*-aminophenol, α-benzoinoxime and ammonium acetate) do not interfere.

Zusammenfassung—Einfache mikrogasometrische und gravimetrische Methoden zur Bestimmung von Nitrat- und Nitritgruppen werden beschrieben. Sie beruhen auf Reduktion mit Ameisensäure, wobei für zwei Mol Nitrat ein Mol Distickstoffmonoxid und vier Mol Kohlendioxid zugleich frei werden; auf sieben Mol Nitrit entstehen zwei Mol Distickstoffmonoxid und sechs Mol Kohlendioxid. Distickstoffmonoxid wird gasometrisch, Kohlendioxid gravimetrisch gemessen. Sowohl für Nitrat als auch für Nitrit werden auf ±0,2% absolut genaue Ergebnisse erhalten.

Résumé—On décrit des méthodes microgazométrique et gravimétrique simples pour la détermination des groupes nitrate et nitrite. Elles sont basées sur la réduction au moyen d'acide formique, par laquelle une mole de protoxyde d'azote et quatre moles de gaz carbonique sont libérées simultanément pour deux moles de nitrate; deux moles de protoxyde d'azote et six moles de gaz carbonique sont libérées pour sept moles de nitrite. On mesure le protoxyde d'azote gazométriquement et le gaz carbonique gravimétriquement. On obtient des résultats exacts à ±0,2% absolu tant pour le nitrate que pour le nitrite.

REFERENCES

1. S. Ohashi and H. Makishima, *Bull. Chem. Soc. Japan*, 1956, **29**, 700.
2. W. I. Awad and S. S. M. Hassan, *Talanta*, 1969, **16**, 1393.
3. M. Busch, *Ber.*, 1905, **38**, 861.
4. H. Rupe and F. Becherer, *Helv. Chim. Acta.*, 1923, **6**, 674.
5. C. S. Marvel and V. Du Vigneaud, *J. Am. Chem. Soc.*, 1924, **46**, **2661**.
6. A. Ogata and M. Konishi, *J. Pharm. Soc. Japan*, 1934, **54**, 546.
7. M. Arnaud, *Compt. Rend.*, 1884, **97**, 174.
8. F. Arndt, *Annalen*, 1911, **384**, 322.
9. M. C. Grimaux, *Compt. Rend.*, 1895, **121**, 749.
10. R. Hutton, S. Salam and W. Stephen, *J. Chem. Soc.*, *A* 1966, 1573.
11. J. Mellor, *A Comprehensive Treatise on Inorganic and Theoretical Chemistry*, Vol VIII, p. 397. Longmans, London, 1947.
12. A. Quartaroli, *Gazz. Chim. Ital.*, 1911, **41**, 53, 64.
13. A. Vogel, *A Text Book of Quantitative Inorganic Analysis*, 2nd Ed., p. 826. Longmans, London, 1957.

Talanta, 1971, Vol. 18, pp. 225 to 228. Pergamon Press. Printed in Northern Ireland

SHORT COMMUNICATIONS

Solvent extraction and spectrophotometric determination of palladium(II) with 7-iodo-8-hydroxyquinoline-5-sulphonic acid

(*Received* 19 *May* 1969. *Revised* 10 *March* 1970. *Accepted* 20 *April* 1970)

7-IODO-8-HYDROXYQUINOLINE-5-SULPHONIC ACID (Ferron) was introduced as an analytical reagent by Yoe,[1] for the colorimetric determination of iron(III). None of the metal-Ferron complexes is soluble in non-polar organic solvents, so it was initially believed[2] that they could not be extracted from water. Later it was reported[3] that the iron(III) complex can be extracted with pentanol. Recently, a method has been developed[4] for the extraction and spectrophotometric determination of vanadium(V) with Ferron as reagent and n-butanol as solvent.

In this paper, a similar method for palladium(II) is described.

EXPERIMENTAL

Reagents

Palladium perchlorate solution. Prepared from palladium chloride by the method of Burger and Dyrssen,[5] and standardized gravimetrically with dimethylglyoxime and diluted to the desired concentration.

Ferron solution. 0·005*M*.

Procedure

Transfer an aliquot containing 25–215 μg of palladium to a separating funnel along with 2·5 ml of 0·005*M* Ferron. If interfering ions are present, use more reagent solution. Dilute to 25 ml, make 0·2*M* in perchloric acid and extract with two 10-ml portions of n-butanol for 2 min each. Combine the extracts in a 25-ml flask, make up to the mark with n-butanol, and read the absorbance at 430 nm against a reagent blank similarly prepared. Prepare a calibration curve similarly.

RESULTS AND DISCUSSION

The absorption spectra of Ferron and its palladium(II) complex (extracted into *n*-butanol) are shown in Fig. 1. The system adheres to Beer's law over a wide range of palladium concentration; the smallest amount of palladium that could be determined was 2·5 ppm. The molar absorptivity is 958 $\text{l.mole}^{-1}.\text{mm}^{-1}$.

The effect of acidity on the extraction is shown in Fig. 2, and it is seen that maximum extraction (95%) occurs at $[H^+] = 0{\cdot}15\text{–}0{\cdot}30M$ and therefore 0·2*M* perchloric acid was used as the aqueous medium. The degree of extraction falls at lower acidity because of dissociation of a proton from the sulphonic acid group. Similar results were obtained when hydrochloric, nitric and sulphuric acids were used to regulate the acidity, showing that the variation is a function only of hydrogen ion concentration.

Maximum extraction of palladium was achieved when the reagent concentration was at least four times that of the palladium. No salting-out agent was found which would improve the degree of extraction. A second extraction gave an overall recovery of ~99%, the first extraction giving a recovery of 95%.

Interferences

The results in Table I show the effect of various ions on the extraction of 133 μg of palladium. The tolerance limit was set at the amount required to cause a ±2% error in the determination of palladium. Excess of a large number of anions such as chloride, phosphate, oxalate, citrate and tartrate does not interfere.

Among the reported extractive procedures[6] those using 1-nitroso-2-naphthol and 2-nitroso-1-naphthol as reagents, appeared to be the best on the basis of sensitivity and there is no interference by the platinum metals though base metals interfere. In the case of the present reagent the sensitivity is quite high and many of the base metals do not interfere.

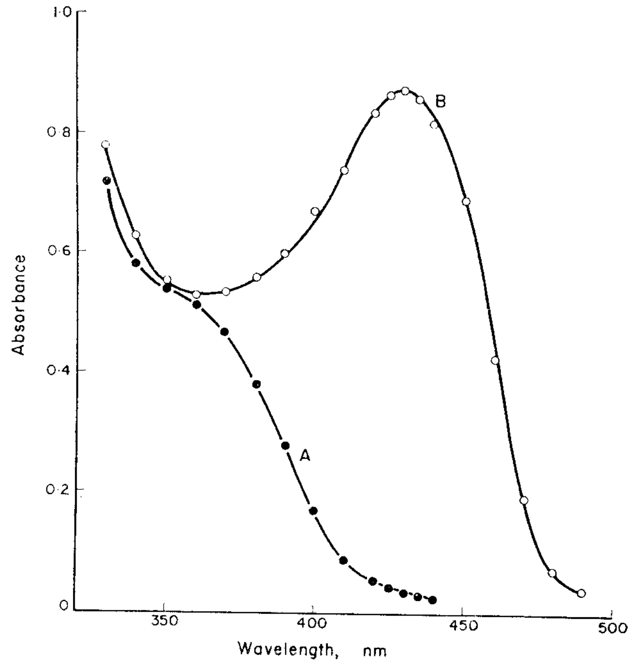

FIG. 1.—Absorption spectra of Ferron(*A*) and Pd-Ferron complex (*B*) in n-butanol. [Pd] = $1{\cdot}0 \times 10^{-4}M$; [Ferron] = $5{\cdot}0 \times 10^{-4}M$; $[H^+] = 0{\cdot}2M$ $HClO_4$.

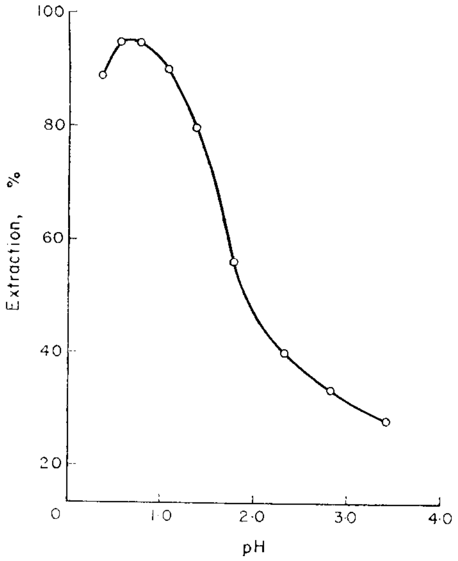

FIG. 2.—Effect of pH on the extraction of palladium.

TABLE I.—INTERFERENCES

Foreign ion	Added as	Tolerance limit, *mg*
Fe(III)	$Fe_2(SO_4)_3$	nil
Co(II)	$Co(NO_3)_2.6H_2O$	10·2
Ni(II)	$NiSO_4.6H_2O$	12·5
Ru(III)	$RuCl_3$	1·0*
Rh(III)	$RhCl_3$	10·3
Os(VIII)	OsO_4	0·02
Ir(III)	$IrCl_3$	2·6*
Pt(IV)	H_2PtCl_6	4·0
V(V)	NH_4VO_3	nil
Cr(III)	$Cr(NO_3)_3.9H_2O$	1·0
Mo(VI)	$(NH_4)_6Mo_7O_{24}.4H_2O$	<0·005
W(VI)	$Na_2WO_4.2H_2O$	13·0
EDTA	Disodium salt	0·8

* In presence of more reagent, larger amounts can be tolerated.

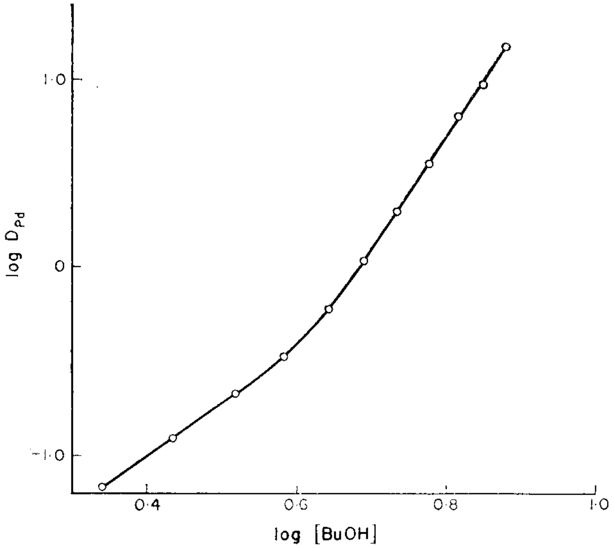

FIG. 3.—Effect of n-butanol concentration on extraction of palladium. [Pd] = 1·0 × $10^{-4}M$; [Ferron] = 5·0 × $10^{-4}M$. Butanol diluted with benzene.

Composition of the extracted species

The ratio of palladium(II) to Ferron in the extracted species was determined by the method of continuous variations modified for a two-phase system by Irving and Pierce.[7] The curves obtained indicated the formation of a 1:2 palladium-Ferron complex, which was confirmed by the mole-ratio method[8] modified for extraction, and corresponds to the composition in an acidic aqueous phase.[9]

In Fig. 3, the logarithm of the distribution ratio of palladium (log D_{Pd}) is plotted against log of the butanol concentration (with benzene as diluent) for fixed Ferron concentration and acidity. As the butanol concentration is increased the slope of the curve increases from ~3 and reaches ~6 when the concentration of butanol is >50%. This shows that the ratio of palladium to butanol in the extracted species is 1:6. Therefore, the composition of the extracted species appears to be Pd:Ferron: butanol = 1:2:6. This ratio has been confirmed for several concentrations of palladium.

Palladium(II) has a co-ordination number of 4 and Ferron forms 5-membered chelate rings. Thus it is believed that at high enough acidity a neutral palladium-IHS complex is formed which is extractable. However, this species would be highly hydrophilic because of the sulphonic acid group, which has to be rendered hydrophobic before considerable extraction can occur. For this purpose, the addition of six n-butanol molecules is apparently required.

Acknowledgement—The work was supported by the Council of Scientific and Industrial Research, New Delhi, India. The authors are thankful for the award of a fellowship to TS.

Chemical Laboratories
University of Allahabad
Allahabad, India

Tej Singh
Arun K. Dey

Summary—An extractive spectrophotometric procedure has been developed for the determination of palladium (II) at microgram levels. The palladium(II) chelate of 7-iodo-8-hydroxyquinoline-5-sulphonic acid is extracted into n-butanol. Extraction is maximal (95%) from $0.2M$ perchloric acid. Beer's law is valid at 430 nm over a wide range of palladium concentration from 2.5 ppm. The molar absorptivity is 958 $1.mole^{-1}.mm^{-1}$. The system can tolerate a large excess of Co(II), Ni(II), Rh(III), Pt(IV), Cr(III), W(VI), chloride, phosphate, citrate and tartrate. Small quantities of Ru(III), Ir(III) and EDTA do not interfere, but serious interference is caused by Fe(III), V(V), Mo(VI) and Os(VIII).

Zusammenfassung—Ein spektrophotometrisches Extraktions-verfahren zur Bestimmung von Palladium(II) im Mikrogrammbereich wurde entwickelt. Das Palladium(II)-Chelat der 7-Jod-8-hydroxychinolin-5-sulfonsäure wird in n-Butanol extrahiert. Die Extraktion ist am vollständigsten (95%) aus $0,2M$ Überchlorsäure. Das Beersche Gesetz gilt bei 430 nm von 2,5 ppm an in einem großen Konzentrationsbereich. Der molare Extinktionskoeffizient beträgt 958 $1\ mol^{-1}\ mm^{-1}$. Das System ist unempfindlich gegen einen großen Überschuß von Co(II), Ni(II), Rh(III), Pt(IV), Cr(III), W(VI), Chlorid, Phosphat, Citrat und Tartrat. Kleine Mengen Ru(III), Ir(III) und EDTA stören nicht, ernsthafte Störungen werden dagegen durch Fe(III), V(V), Mo(VI) und Os(VIII) verursacht.

Résumé—On a élaboré une technique spectrophotométrique par extraction pour le dosage du palladium (II) à l'échelle du microgramme. On extrait le chélate du palladium (II) avec l'acide 7-iodo 8-hydroxyquinoléine 5-sulfonique en *n*-butanol. L'extraction est maximale (95%) à partir d'acide perchlorique $0,2M$. La loi de Beer est suivie à 430 nm dans un large domaine de concentration en palladium à partir de 2,5 p.p.m. Le coefficient d'absorption molaire est 958 $1\ .\ mole^{-1}\ .\ mm^{-1}$. Le système peut tolérer un grand excès de Co(II), Ni(II), Rh(III), Pt(IV), Cr(III), W(VI), chlorure, phosphate, citrate et tartrate. De petites quantités de Ru(III), Ir(III) et EDTA n'interfèrent pas, mais Fe(III), V(V), Mo(VI) et Os(VII) causent une gêne sérieuse.

REFERENCES

1. J. H. Yoe and F. H. Wirsing, *J. Am. Chem. Soc.*, 1932, **54**, 1866.
2. F. Feigl, *Chemistry of Specific, Selective and Sensitive Reactions*, Academic Press, New York, 1949.
3. E. B. Sandell, *Colorimetric Determination of Traces of Metals*, Interscience, New York, 1959.
4. N. Kurmaiah, D. Satyanarayana and V. P. R. Rao, *Anal. Chim. Acta*, 1966, **35**, 484.
5. K. Burger and D. Dyrssen, *Acta Chem. Scand.*, 1963, **17**, 1489.
6. F. E. Beamish, *The Analytical Chemistry of Noble Metals*, p. 429. Pergamon, Oxford, 1966.
7. H. Irving and T. B. Pierce, *J. Chem. Soc.*, 1959, 2565.
8. J. H. Yoe and A. L. Jones, *Ind. Eng. Chem., Anal. Ed.*, 1944, **16**, 111.
9. J. N. Mathur and S. N. Banerji, *J. Indian Chem. Soc.*, 1967, **44**, 513.

Talanta, 1971, Vol. 18, pp. 228 to 230. Pergamon Press. Printed in Northern Ireland

Spectrophotometric determination of traces of antimony

(*Received* 3 *March* 1970. *Accepted* 26 *April* 1970)

In a previous paper[1] a simple and selective method for spectrophotometric determination of traces of arsenic(III) was described, based on extraction of arsenic(III) iodide into carbon tetrachloride and subsequent reaction with 8-mercaptoquinoline (HTOx). An analogous reaction can be used for antimony(III).

Addition of HTOx to antimony(III) iodide in carbon tetrachloride causes the instantaneous formation of a yellow 1:1 complex with maximum absorbance at 390 nm.

$$SbI_3 + HTOx = SbI_2TOx + HI$$

The addition of acetone (5% v/v) increase the solubility as well as the molar absorptivity of the complex (mean value 610 l.mole^{-1}.mm^{-1}).

Procedure

Transfer 5 ml of the solution to be analysed (containing 0–100 µg of antimony, pH 1–13) and 4 ml of 10*M* sulphuric acid into a 50-ml separatory funnel. After cooling, add 10 ml of carbon tetrachloride, 1 ml of 0·5*M* potassium iodide and shake immediately for 30 sec. Separate the organic extract and centrifuge it for 1 min (2500 rpm). Transfer 8 ml of the extract into a 10-ml volumetric flask, add 1·5 ml of 0·005*M* 8-mercaptoquinoline solution in carbon tetrachloride and 0·5 ml of acetone. Measure the absorbance immediately in a 10-mm cell at 390 nm against a blank. Prepare a calibration curve (which should be linear up to 100 µg of antimony) from standard antimony(III) solution, using the procedure given.

Results

The procedure described was used for the determination of antimony(III) in the presence of an excess of other metals. The results obtained are summarized in Table I. Selenium(IV) and vanadium(V) do not interfere if solid ascorbic acid is added before the potassium iodide. In the presence of copper and iron(III), iodine is evolved, which interferes in the determination; in this case, antimony is extracted as described and then stripped into 6 ml of 1*M* sulphuric acid. To the separated aqueous phase, 3 ml of 10*M* sulphuric acid, 10 ml of carbon tetrachloride and 1 ml of 0·5*M* potassium iodide are added and antimony extracted and determined as above.

TABLE I.—DETERMINATION OF 100 µg OF ANTIMONY IN THE PRESENCE OF OTHER METALS

Other metals, *mg*		Sb found, *µg*	Other metals, *mg*		Sb found, *µg*
Mn	2·1	102	W(VI)	5	105
Ag	3·2	105	Zn	1·2	104
Hg	4	104	Te(IV)	1·4	105
In	4	99	Zr	3·2	104
La	2·8	99	Cr(III)	9	106
Ga	2·4	102	Bi	5·2	94
Ge	7·2	104	V(V)*	1·8	98
Mo(VI)	1·8	98	Se(IV)*	1	106
Ti	5	96	Cu†	2·4	98
Co	2	98	Fe(III)†	1	95
Ni	2	104	As(III)§	0·07	105
Cd	3·4	100		0·3	104
U(VI)	4·8	105		0·5	112
Al	2·2	100			

* Before the addition of KI 0·5 g of solid ascorbic acid was added.

† The antimony extracted was stripped into dilute sulphuric acid and the extraction repeated.

§ KI concentration 0·01*M*.

The procedure is simple and rapid, and repeated extraction greatly increases the selectivity of the method.

Laboratory of Analytical Chemistry
J. Heyrovský Polarographic Institute
Czechoslovak Academy of Science
Praha 1, *Jilská* 16, *Czechoslovakia*

VÊRA STARÁ

Summary—Antimony(III) is extracted into carbon tetrachloride from 4*M* sulphuric acid that is 0.05*M* in potassium iodide. 8-Mercaptoquinoline and acetone are added to the organic extract and the absorbance of the complex formed is measured at 390 nm. Repeating the extraction procedure greatly increases the selectivity of the method.

Zusammenfassung—Antimon(III) wird aus 0,05*M* Kaliumjodid enthaltender 4*M* Schwefelsäure in Tetrachlorkohlenstoff extrahiert. Zum organischen Extrakt werden 8-Mercaptochinolin und Aceton gegeben und die Extinktion des gebildeten Komplexes bei 390 nm gemessen. Eine Wiederholung des Extraktionsschritts erhöht die Selektivität des Verfahrens erheblich.

Résumé—On extrait l'antimoine(III) en tétrachlorure de carbone à partir d'acide sulfurique 4*M* qui est 0,05*M* en iodure de potassium. On adjoute de la 8-mercaptoquinoléine et de l'acétone à l'extrait organique et mesure l'absorption du complexe formé à 390 nm. La répétition de la technique d'extraction accroît grandement la sélectivité de la méthode.

REFERENCE

1. V. Stará and J. Starý, *Talanta*, 1970, **17**, 341.

Talanta, 1971, Vol. 18, pp. 230 to 234. Pergamon Press. Printed in Northern Ireland

Colorimetric determination of pyrogallol and 2,6-dimethoxyphenol with diphenylpicrylhydrazyl

(*Received* 1 *June* 1970. *Accepted* 2 *July* 1970)

PHENOLS have been determined colorimetrically with a variety of reagents such as titanium sulphate,[1] osmium tetroxide,[1] and the free radical diphenylpicrylhydrazyl,[2,3,4] or DPPH. In contrast, specific methods for very reactive phenols such as pyrogallol are not numerous although it is possible to determine this phenol selectively by condensation with vanillin.[5]

The intensely purple DPPH has been investigated to some extent[4] in these laboratories as a selective colorimetric reagent for hydroquinone and pyrocatechol (catechol). It has the structure

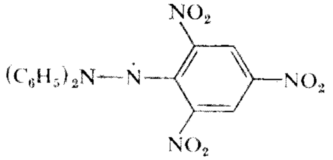

The advantages of this reagent are its intense absorption bands, its ability to react with phenols at vastly different rates, and its "clean" one-electron reduction to the corresponding diphenylpicrylhydrazine.

We were interested in extending our studies of DPPH to the colorimetric determination of the phenol that would react at the highest possible rate with DPPH. It might then be possible to determine this phenol in the presence of all other phenols. Since it has been found[6,7] that the *ortho* substitution of electron-donating groups (with little steric hindrance) on phenols increases the rate of reaction of DPPH with such phenols, we chose the trihydric phenol pyrogallol and its ether, 2,6-dimethoxyphenol, for initial study. (A recent kinetic study[8] indicates that pyrogallol does indeed react very rapidly with oxidants such as DPPH.) Since monohydric phenols react very slowly with DPPH,[9] it appeared that pyrogallol and 2,6-dimethoxyphenol might well be determined colorimetrically in the presence of at least monohydric phenols by use of DPPH.

The stoichiometry of the oxidation of pyrogallol and 2,6-dimethoxyphenol is complicated. It has been suggested that the latter is oxidized by periodate[10,11] to a mixture of products, two benzoquinones, and a β-naphthoquinone:

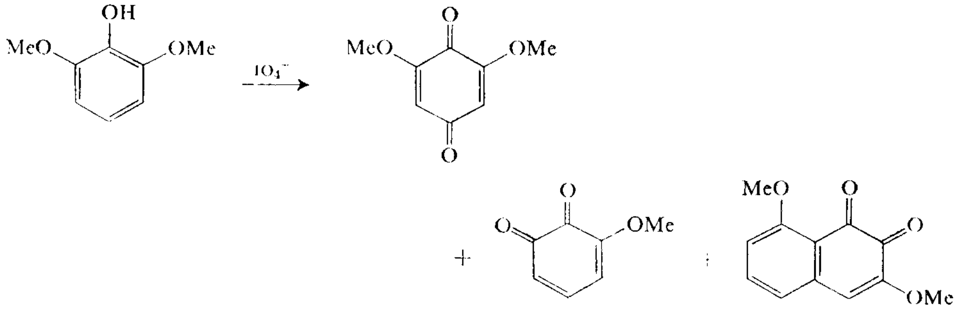

It is also possible that the *o*-benzoquinone can be oxidized to a *cis*,*cis*-muconic acid, as suggested[4] for the second step for the oxidation of catechol (pyrocatechol). Thus the oxidation of either phenol can be expected to involve more than a two-electron charge, and probably at least a four-electron charge.

The absorption spectrum of DPPH reported by Proll and Sutcliffe[12] shows two absorption bands at 330 nm ($\varepsilon = 1{\cdot}65 \times 10^4$ l.mole^{-1}.mm^{-1}) and at 520 nm ($\varepsilon = 1{\cdot}20 \times 10^4$). Since the reduction product of DPPH, diphenylpicrylhydrazine, also absorbs strongly at 330 nm, the 520-nm band was chosen for colorimetric measurement. However, since there is a slow photochemical decomposition of DPPH to the hydrazine,[12,13] measurements were made at 540 instead of 520 nm to avoid errors arising from a slight absorption by the diphenylpicrylhydrazine at 520 nm.

The analytical technique used by Blois[2] and our laboratories[4] was chosen for this study. The calibration curve is a plot of the absorbance of the unreacted DPPH *vs.* the concentration of phenol, and is thus the reverse of a normal Beer's law calibration curve.

EXPERIMENTAL

Reagents

2,2-Diphenyl-1-picrylhydrazyl (DPPH) was obtained from Eastman (White Label grade) and was used as received. Ethanolic solutions of DPPH ($1 \times 10^{-4}M$) were prepared by first adding 1–5 ml of acetone (enough to dissolve the DPPH) and then the appropriate solvent. Pyrogallol (1,2,3-trihydroxybenzene) was a Matheson reagent; it was necessary to prepare this phenol solution daily to avoid decomposition. 2,6-Dimethoxyphenol was Eastman White Label grade. Catechol (pyrocatechol), ninhydrin (1,2,3-indantrione monohydrate) and vanillin were all Matheson reagents. Hydroquinone (Baker Grade) and phloroglucinol (practical grade) were from Baker. The *p*-methoxybenzene was from Ansul. Resorcinol was reagent grade from Merck and the salicylic acid was reagent grade from Allied Chemical. All phenols and inferent solutions were $2{\cdot}5 \times 10^{-4}M$. When absolute ethanol was used as the solvent, it was first dried over "Drierite" for at least 24 hr.

Procedure

The time studies of 2,6-dimethoxyphenol and pyrogallol reactions with DPPH were made by adding 50 ml of $1 \times 10^{-4}M$ DPPH to 4 ml of $2{\cdot}5 \times 10^{-4}M$ of the respective phenol and then diluting to 100 ml with either 95% or absolute ethanol. Absorbance readings were taken at 540 nm.

Calibration curves were made for solutions in both absolute and 95% ethanol by adding 50 ml of $1{\cdot}28 \times 10^{-4}M$ DPPH to 2, 4, 6, 8 and 10 ml of $2{\cdot}5 \times 10^{-4}M$ solutions of each phenol and then diluting to 100 ml with the appropriate solvent. Absorbance readings were taken at 540 nm after 1 hr or, in the case of absolute 2,6-dimethoxyphenol, after 2 hr.

Interference studies were made by adding 2, 4, 6, 8 and 10 ml of solution of the interfering substances to 6 ml of 2,6-dimethoxyphenol solution, or 1, 2, 3, 4 and 5 ml of solution of the interfering substance to 3 ml of pyrogallol solution, then adding 50 ml of $1 \times 10^{-4}M$ DPPH solution, and diluting to 100 ml. Readings were taken at 540 nm at the times mentioned above for the calibration curve.

RESULTS AND DISCUSSION

The relative rates of the four selected DPPH–phenol reactions are shown in Table I. It can be seen that pyrogallol does react more rapidly than pyrocatechol (catechol) or hydroquinone, the two phenols

TABLE I.—RATES OF DPPH OXIDATIONS

Phenol, $1 \times 10^{-5}M$	Amount of 4-electron reaction with $5{\cdot}0 \times 10^{-5}M$ DPPH, %							
	Time, *min* 10	30	50	70	90	120	140	180
Absolute ethanol as solvent								
Pyrogallol	64	82	88	91	92	97	99	100
2,6-Dimethoxyphenol	10	23	40	47	53	61	63	70
95% Ethanol as solvent								
Pyrogallol	80	86	89	91	94	95	96	97
2,6-Dimethoxyphenol	38	45	53	58	66	74	82	92

TABLE II.—DETERMINATION OF PYROGALLOL AND 2,6-DIMETHOXYPHENOL IN THE PRESENCE OF VARIOUS INTERFERENCES

Mole ratio of interferent pyrogallol or 2,6-dimethoxyphenol	Interferent	Found ($\times 10^{-5}M$) 95% EtOH	absolute EtOH
Pyrogallol ($0{\cdot}5 \times 10^{-5}M$)		(One hour reaction in both)	
1:1	Catechol	2·13	1·41
1·67:1		2·13	3·00
1:1	Hydroquinone	1·80	0·96
1·67:1		1·80	1·27
1:1	Ninhydrin	0·71	0·72
1·67:1		0·84	0·69
1:1	*p*-Methoxybenzene	0·74	0·77
1·67:1		0·80	0·72
1:1	Phloroglucinol	—	0·68
1·67:1		—	0·75
1:1	Resorcinol	0·57	0·87
1·67:1		0·60	0·81
1:1	Salicylic acid	0·89	0·80
1·67:1		0·91	0·77
1:1	Vanillin	0·55	0·74
1·67:1		0·57	0·69
2,6-Dimethoxyphenol ($1{\cdot}50 \times 10^{-5}M$)		(One hour reaction)	(two hour reaction)
1:1	Catechol	7·09	2·64
1:1	Hydroquinone	5·54	2·51
1:1	Ninhydrin	1·59	1·64
1·67:1		1·68	1·61
1:1	*p*-Methoxybenzene	1·42	1·43
1·67:1		1·48	1·40
1:1	Phloroglucinol	—	1·53
1:1	Resorcinol	1·41	1·42
1·67:1		1·47	1·55
1:1	Salicylic acid	1·73	1·48
1·67:1		1·58	1·33
1:1	Vanillin	1·50	1·47
1·67:1		1·49	1·63

which have been thus far found[3] to react at the highest rate with DPPH. In 10 min, pyrocatechol completes 45% of a *two-electron* reaction in absolute ethanol[4] whereas pyrogallol completes 64% of a *four-electron* reaction in absolute ethanol. It was therefore decided to pursue further colorimetric studies for the purpose of establishing whether a selective method for pyrogallol could be devised. Although 2,6-dimethoxyphenol reacted much more slowly, it was also investigated further.

It is also obvious from Table I that the water in 95% ethanol enhances the rate of the oxidation of pyrogallol and 2,6-dimethoxyphenol. It appears as though the reaction is an overall four-electron oxidation which occurs very rapidly at first and then decreases to a much slower rate. It is difficult to follow the rate and thus establish the stoichiometry because after the first hour or two the decomposition of DPPH is quite significant.[12]

The preparation of calibration curves for both 95% and absolute ethanol media was investigated, but suitable times at which to measure the absorbance had to be chosen. The times chosen corresponded to those at which the reaction rates had decreased sufficiently so that absorbance did not change measurably within 5 min either side of the time of measurement. A time of 60 min was chosen for pyrogallol in both solvents and also for 2,6-dimethoxyphenol in 95% ethanol, but 120 min was chosen for this phenol in absolute ethanol.

The determination of pyrogallol and 2,6-dimethoxyphenol in the presence of various phenols and phenyl ethers as interferents was then studied. The results are shown in Table II. It was found that those compounds with the lowest reaction rates did not interfere appreciably and that the determinations are more accurate when absolute ethanol is used than with 95% ethanol. Thus pyrogallol can be determined fairly accurately in the presence of comparable amounts of ninhydrin, *p*-methoxybenzene, salicylic acid, and vanillin. It can be predicted that other phenols that are equally reactive towards DPPH such as phenol itself, *p*-bromophenol, *p*-nitrophenol and *p*-phenylphenol,[3] should interfere no more than these phenols in the determination of pyrogallol. Unfortunately, both hydroquinone and pyrocatechol (catechol) react too rapidly and interfere seriously. As expected, the results for $0{\cdot}75 \times 10^{-5}M$ pyrogallol are very high when equal amounts of either of these phenols are present.

Since 2,6-dimethoxyphenol reacts more slowly than pyrogallol, it is to be expected that the interferents listed in Table II will cause more error in its determination than in the determination of pyrogallol. This is true for compounds such as ninhydrin and *p*-methoxyphenol. It does not always appear to be true for every concentration of salicylic acid and resorcinol. No explanation is offered for this.

As has been found by Blois,[2] aromatic amines such as *p*-aminophenol, thiol functions such as those in mercaptans and proteins, and other good reducing agents such as ascorbic acid interfere by reacting rapidly with DPPH. Aldehyde groups such as that in glucose are apparently not oxidized by DPPH, nor are unsaturated carbon–carbon bonds.

Department of Chemistry,
Wayne State University,
Detroit,
Michigan 48202,
U.S.A.

George H. Schenk
Nancy K. Swieczkowski

Summary—A colorimetric study was made of the reactions of the free radical 2,2-diphenyl-1-picrylhydrazyl (DPPH) and the phenols pyrogallol and 2,6-dimethoxyphenol. Both of these phenols were colorimetrically determined by use of DPPH, in the presence of various interferents. It was shown that the determination of pyrogallol and 2,6-dimethoxyphenol was more accurate when absolute ethanol was used than with 95% ethanol. It was also shown that the best results were obtained when the ratio of phenol to interferent was no greater than 1:1.

Zusammenfassung—Die Reaktionen des freien Radikals 2,2-Diphenyl-1-pikrylhydrazyl (DPPH) und der Phenole Pyrogallol und 2,6-Dimethoxyphenol wurden kolorimetrisch untersucht. Beide Phenole wurden in Gegenwart verschiedener störender Substanzen mit DPPH kolorimetrisch bestimmt. Es wurde gezeigt, daß die Bestimmung von Pyrogallol und 2,6-Dimethoxyphenol bei Verwendung von absolutem Äthanol genauer war als mit 95% Äthanol. Außerdem wurde gezeigt, daß die besten Ergebnisse erzielt wurden, wenn das Verhältnis von Phenol zu störender Substanz nicht größer war als 1:1.

Résumé—On a effectué une étude colorimétrique des réactions du radical libre 2,2-diphényl-1-picrylhydrazyle (DPPH) et des phénols pyrogallol et 2,6-diméthoxyphénol. On a déterminé ces deux phénols colorimétriquement en utilisant le DPPH, en la présence de diverses interférences. On a montré que le dosage des pyrogallol et 2,6-diméthoxyphénol est plus précis lorsqu'on utilise l'éthanol absolu qu'avec l'éthanol à 95%. On a aussi montré que les meilleurs résultats sont obtenus lorsque le rapport du phénol à la substance interférente n'est pas plus grand que 1:1.

REFERENCES

1. F. D. Snell and C. T. Snell, *Colorimetric Methods of Analysis, Vols. I, III*, Van Nostrand, New York, 1965.
2. M. S. Blois, *Nature*, 1958, **181**, 1199.
3. G. J. Papariello and M. A. M. Janish, *Anal. Chem.*, 1966, **38**, 21.
4. G. H. Schenk and D. J. Brown, *Talanta*, 1967, **14**, 257.
5. D. J. W. Grant and J. C. Patel, *Anal. Biochem.*, 1969, **28**, 139.
6. J. C. McGowan and T. Powell, *J. Chem. Soc.*, 1961, 2160.
7. P. Venker and H. Herzmann, *Naturwiss.*, 1960, **47**. 133.
8. H. Rein and O. Ristaw, *Z. Phys. Chem. Leipzig*, 1968, **239**, 115.
9. J. S. Hogg, D. H. Lohmann, and K. E. Russell, *Can. J. Chem.*, 1961, **39**, 1588.
10. E. Adler, R. Magnusson, B. Berggren, and H. Thomeluis, *Acta Chem. Scand.*, 1960, **14**, 515.
11. W. I. Taylor and A. R. Battersby, *Oxidative Coupling of Phenols*, Dekker, p. 57. New York, 1967.
12. P. J. Proll and L. H. Sutcliffe, *Trans. Faraday Soc.*, 1963, **59**, 2090.
13. A. Suzuki, M. Takahasi and K. Shiomi, *Bull. Chem. Soc. Japan*, 1963, **36**, 998; *Chem. Abstr.*, 1964, **60**, 389*h*.

Talanta, 1971, Vol. 18, pp. 234 to 237. Pergamon Press. Printed in Northern Ireland

Determination of zinc in copper by atomic-fluorescence flame spectroscopy

(*Received* 22 *June* 1970. *Accepted* 20 *July* 1970)

SINCE the theory[1] and description[2] of the application of atomic-fluorescence flame spectroscopy to trace element detection and determination first appeared, the technique has been considerably improved, so that now it may be used for the investigation of many elements. The improvements have been mainly in primary light sources (high-intensity hollow-cathodes[3] and electrodeless discharge tubes[4]) and flames (*e.g.*, separated flames[5] and high-temperature flames[6]). Limits of detection for many elements in demineralized water are similar to or better than those obtained by atomic-absorption spectroscopy.[4]

To date, however, the majority of the published investigations have involved the determination of elements in demineralized water, with interference effects being investigated with ions in approximately 1000-fold excess. Practical applications have been limited to the determination of trace metals in hydrocarbon fuels[7,8] and silicon in low alloy steels.[9] The object of this communication is to further show the practical usefulness and possible limitations of atomic-fluorescence flame spectroscopy, by considering the determination of trace (ppm level) quantities of zinc in copper. Results are compared with those from atomic-absorption spectroscopy.

The presence of zinc impurities in copper can render the copper unsuitable for electronic tube and valve applications. The British Standard Specification (B.S. 3839:1955) states that for oxygen-free, high-conductivity copper for electronic valves and semi-conductor devices the zinc content should be less than 0·0025%. In the present investigation, copper from several different sources has been investigated for the presence of zinc impurities, by spraying a fairly concentrated copper solution, premixed with air and fuel, directly into a flame and determining the zinc content by atomic-fluorescence spectroscopy. The minimum concentration of zinc in copper that could be determined in this way was approximately 10^{-5}%, the limitation being set by the scatter of primary radiation from within the flame producing a signal that prevented the amplifier from being used on maximum gain.

EXPERIMENTAL

Apparatus

The apparatus used in this investigation has been described previously.[10] Ground-state atoms, produced in an air–acetylene flame, were irradiated with radiation from a Philips zinc vapour-discharge lamp. The fluorescence radiation was collected by a condensing lens and focussed onto a photomultiplier, in front of which was placed a narrow-band interference filter centered on the zinc resonance wavelength. This filter greatly attenuated wavelengths other than the zinc resonance wavelength emitted by the flame. The signal from the photomultiplier was fed into a phase-sensitive, lock-in a.c. amplifier, the output from which was displayed on a pen recorder. The air–acetylene flame was supported on a burner-spray chamber combination from a Unicam S.P. 90 flame photometer.

Atomic-absorption measurements were made on a Unicam S.P. 90 flame photometer using a 100-mm path-length air–acetylene flame.

Procedure

The copper samples, in the form of sheet or turnings, were repeatedly washed in isopropanol and demineralized water. Standard sample solutions of zinc in the presence of copper were prepared by dissolving 0·5 g of copper (Sample A), assumed to contain no zinc, in 5 ml of concentrated nitric acid, adding known concentrations of zinc, as an aqueous solution of zinc chloride, and diluting the mixture with demineralized water to 50 ml to obtain concentrations of 0·001–0·2 ppm of zinc and 10^4 ppm of copper in solution. Solutions of copper, suspected of containing zinc, were also prepared by dissolving 0·5 g of the sample to be analysed in 5 ml of concentrated nitric acid and diluting to 50 ml to obtain a concentration of 10^4 ppm of copper in solution. These solutions, premixed with air and fuel, were sprayed directly into the air–acetylene flame.

The optimum fluorescence signal:noise ratio was obtained under the following conditions: lamp current 0·5 A; air flow-rate 5·00 l/min; acetylene flow-rate 0·80 l/min; aspiration rate 3·10 ml/min; time constant 1 sec; photomultiplier voltage 1·00 kV. Except for a hollow-cathode lamp current of 5·0 mA and a 100-mm long flame, identical conditions were used for atomic-absorption measurements.

RESULTS AND DISCUSSION

The presence of copper at concentrations in excess of 10 ppm in solution produced a scatter signal from within the flame, indistinguishable from the zinc fluorescence signal. Investigation of the flame conditions showed that the largest fluorescence signal:scatter signal ratio was obtained with the maximum sample aspiration rate. The presence of 10^4 ppm of copper did not affect the fluorescence signal from a given concentration of zinc.

In Fig. 1, curve *a* shows the scatter signal from 10^4 ppm of copper (Sample A), curve *b* the fluorescence signal from various concentrations of zinc, and curve *c* the combined fluorescence and scatter signals from solutions containing various concentrations (0·001–0·2 ppm) of zinc and 10^4 ppm of copper (Sample A). The zinc content of the various copper samples was determined by comparing the combined scatter and fluorescence signals obtained from 10^4-ppm concentrations of the sample with curve *c*. Five determinations were made for each sample. The concentrations of zinc impurity found in the various samples are listed in Table I. These values are relative to Sample A, assumed to contain no zinc.

Table I.—Zinc content of various samples of copper, detected by atomic-absorption and fluorescence flame spectroscopy

Copper sample	Zinc content % A.F.S.	A.A.S.
A (electrolytic)	0 (assumed)	0 (assumed)
B (vacuum-melted)	0·00003	none found
C (electrolytic)	0·00006	none found
D (vacuum-melted)	0·0011	0·0011

Atomic-absorption measurements were made in a similar manner: the calibration curve for solutions containing 0·001–0·2 ppm of zinc and 10^4 ppm of copper (Sample A) was obtained with use of maximum scale expansion and the signals from the various copper samples were compared with this curve.

The limit of detection (the solution concentration giving signal:noise = 2) for zinc in demineralized water was 10^{-5} ppm. A solution containing 10^4 ppm of copper produces a scatter signal equivalent to the fluorescence signal from 0·01 ppm of zinc. This scatter signal could not be completely backed-off when the present amplifier was used, so the maximum gain of the amplifier could not be used. The practical limit of detection for zinc in the presence of 10^4 ppm of copper with this apparatus was that concentration of zinc giving a fluorescence signal just detectable above the scatter signal from 10^4 ppm of copper, *i.e.*, 10^{-3} ppm of zinc (Fig. 1), equivalent to 0·1 part of zinc in 10^6 parts of copper.

To investigate scatter in further detail, solutions containing, independently, various concentrations in the range 10^2–10^5 ppm of Na (as the chloride, fluoride, bromide, iodide, sulphate and carbonate), Hg(II) (as the chloride), Cu (as the analytical-grade nitrate) and Cu (as the nitrate from Sample A) were sprayed into the air–acetylene flame. When irradiated with 213·9-nm zinc radiation all these solutions produced straight-line log-log plots of scatter signal *vs.* element concentration. The gradients of these curves were identical, the scatter signal being approximately proportional to the square root of the element concentration. This is at variance with results obtained by Smith *et al.*,[11] who, using a total-consumption burner and 324·8-nm copper radiation, obtained scatter curves indicating an approximately direct proportionality between the scatter signal and element concentration. Scatter signals of different magnitude were obtained from the same concentrations of sodium from various sodium compounds.

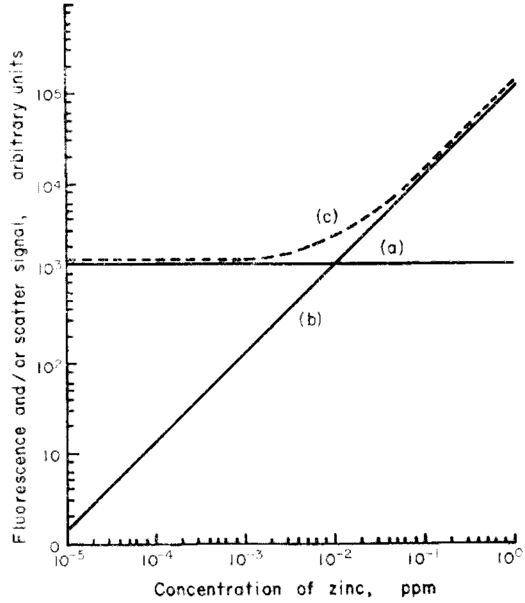

FIG. 1.—(*a*) Scatter signal from 10^4 ppm of copper (Sample A); (*b*) fluorescence calibration curve for zinc in demineralized water; (*c*) combined fluorescence and scatter signal for various concentrations of zinc in the presence of 10^4 ppm of copper (Sample A).

As identical scatter curves were obtained for copper from the two sources indicated, and the gradients were similar to those obtained from the scatter curves for elements containing no zinc, the assumption that Sample A contains little or no zinc seems justified.

The limit of detection for the determination of zinc in copper by atomic-fluorescence spectroscopy could be improved by altering the backing-off facilities in the amplifier or reducing the scatter signal. The scattering of primary radiation from within the flame has been recognized as a possible disadvantage to the application of atomic-fluorescence spectroscopy to trace element determination.[12] In a simple flame system, the sample solution enters the flame from the spray chamber as small droplets, the solvent is evaporated to give salt particles, and the particles are thermally dissociated into atoms.[13] In such a system primary radiation could be scattered by (*a*) droplets, (*b*) incompletely vaporized salt particles[11] or (*c*) molecular aggregates of combustion products formed in the flame.[14] Scattering by droplets is unlikely because spraying demineralized water into the flame produced no scattering signal. It is probable that the formation of combustion products would take place in the secondary reaction zone of the flame. However, the scatter signal from a solution of 10^4 ppm of copper, as the nitrate, was unchanged when the primary reaction zone of the flame was viewed after separation of the air–acetylene flame in a manner similar to that described by Hobbs *et al.*[5] This suggests that the major source of scatter is the incomplete decomposition of compound entering the flame, and that scatter could be reduced by using a hotter flame. The investigation of scatter is being continued.

The results above show that atomic-fluorescence flame spectroscopy enables traces of zinc to be determined in copper at levels above $10^{-5}\%$ with a simple apparatus and little sample preparation. The technique is shown to be more sensitive than atomic-absorption spectroscopy (Table I). It is suggested, in agreement with Smith *et al.*[11] that scatter from particles within the flame should not be a serious limitation to the practical application of the technique for trace metal determination in a matrix other than demineralized water. By improving the backing-off facilities of the amplifier, choosing a compound of the matrix element, where possible, that produces minimum scatter, and optimizing the flame conditions and aspiration rate, it should be possible to reduce the scatter signal to a tolerable level.

Central Research Laboratories
General Electric Company Ltd.
Hirst Research Centre
Wembley, England

P. D. WARR

Summary—The application of atomic-fluorescence flame spectroscopy to the determination of trace quantities of zinc in copper is described. A limit of detection of $10^{-5}\%$ zinc in copper has been established. The scatter of primary radiation from within the flame determined the limit of detection, but it is suggested that scatter is not a serious limitation to the practical application of the technique.

Zusammenfassung—Die Anwendung der Atomfluoreszenz-Flammenspektroskopie auf die Bestimmung von Spurenmengen Zink in Kupfer wird beschrieben. Eine Nachweisgrenze von $10^{-5}\%$ Zink in Kupfer wurde ermittelt. Die Nachweisgrenze war bestimmt durch die Streuung von Primärstrahlung in der Flamme; es wird aber darauf hingewiesen, daß die Streuung für die praktische Anwendung des Verfahrens keine ernsthafte Einschränkung bedeutet.

Résumé—On décrit l'application de la spectroscopie de flamme de fluorescence atomique au dosage de zinc à l'état de traces dans le cuivre. On a établi une limite de détection de $10^{-5}\%$ de zinc dans le cuivre. La dispersion de la radiation primaire de l'intérieur de la flamme a déterminé la limite de détection, mais l'on suggère que la dispersion n'est pas une limitation sérieuse à l'application pratique de la technique.

REFERENCES

1. J. D. Winefordner and T. J. Vickers, *Anal. Chem.*, 1964, **36**, 161.
2. J. D. Winefordner and R. A. Staab, *ibid.*, 1964, **36**, 165.
3. J. V. Sullivan and A. Walsh, *Spectrochim. Acta*, 1965, **21**, 721.
4. K. E. Zacha, M. P. Bratzel, Jr., J. D. Winefordner and J. M. Mansfield, Jr., *Anal. Chem.*, 1968, **40**, 1733.
5. R. S. Hobbs, G. F. Kirkbright, M. Sargent and T. S. West, *Talanta*, 1968, **15**, 997.
6. D. N. Hingle, G. D. Kirkbright and T. S. West, *Analyst*, 1968, **93**, 522.
7. D. H. Cotton and D. R. Jenkins, *International Atomic Absorption Spectroscopy Conference*, Sheffield, July 1969.
8. V. Sychra and J. Matousek, *International Atomic Absorption Spectroscopy Conference*, Sheffield July, 1969.
9. G. F. Kirkbright, A. P. Rao and T. S. West, *Anal. Letters*, 1969, **2**, 465.
10. P. D. Warr, *Talanta*, 1970, **17**, 543.
11. R. Smith, R. C. Elser and J. D. Winefordner, *Anal. Chim. Acta*, 1969, **48**, 35.
12. D. C. Manning and P. Heneage, *At. Absorption Newsletter*, 1967, **6**, 124.
13. G. M. Hieftje and H. V. Malmstadt, *Anal. Chem.*, 1968, **40**, 1860.
14. C. Veillon, J. M. Mansfield, M. L. Parsons and J. D. Winefordner, *ibid.*, 1966, **38**, 204.

Talanta, 1971, Vol. 18, p. i. Pergamon Press. Printed in Northern Ireland

PAPERS RECEIVED

Stability constants of aluminium fluoride complexes: P. RAGHUNATH AGARWAL and EDGARD C. MORENO. (28 *September* 1970)

Structure, bonding, and fluorescence of bivalent metal chelates of *o,o*'-dihydroxyazobenzene: J. KNOECK and J. A. BUCHHOLZ. (30 *November* 1970)

Behaviour of ferroin indicator in iron(II)–dichromate titration—a critical study—II: K. SRIRAMAM. (2 *December* 1970)

Determination of boron and nitrogen in boron nitride: L. SANFORD ERICKSON and FRANK J. CONRAD. (3 *December* 1970)

Spectrophotometric study of the determination of copper with ammonium 1-pyrrolidinecarbodithioate: R. W. LOOYENGA and D. F. BOLTZ. (3 *December* 1970)

The rapid analysis of fertilizers by the direct-reading thermometric method: ISTVAN SAJÓ and B. SIPOS. (4 *December* 1970)

Thermodynamic proton-ligand stability constant of *N*-phenyl-*m*-methylbenzohydroxamic acid: Y. K. AGARWAL and S. G. TANDON. (4 *December* 1970)

Reductimetric determinations with thioglycollic acid: H. ALFARO J. and OSWALD PLATTEAU V. (7 *December* 1970)

A review of the use of basic dyes in the determination of anions, particularly as a means of determining antimony, thallium and gallium: A. G. FOGG, C. BURGESS and D. THORBURN BURNS. (7 *December* 1970)

Amperometric complex-formation titration of traces of thorium: F. FREESE, R. OOSTERVINK and G. DEN BOEF. (9 *December* 1970)

The stability of plutonium sulphate tetrahydrate, an analytical standard: A ten-year evaluation: CHARLES E. PIETRI and W. ALBERT WENZEL. (9 *December* 1970)

On the melting point of 2,9-dimethyl-1,10-phenanthroline: KEIHEI UENO, MIKIHIKO SAITO and SHUICHI IWANO. (14 *December* 1970)

Chitosan for the collection from sea-water of naturally occurring zinc, cadmium, lead and copper: RICCARDO A. A. MUZZARELLI and LÁSZLÓ SIPOS. (15 *December* 1970)

The solubility of lead(II) tartrate and the amperometric titration of tartrate with lead(II): E. BOTTARI and M. VICEDOMINI. (15 *December* 1970)

Talanta, 1971, Vol. 18, p. iii. Pergamon Press. Printed in Northern Ireland

PUBLICATIONS RECEIVED

Techniques and Methods of Polymer Evaluation, Vol. 2, Thermal Characterization Techniques: Eds. PHILIP E. SLADE, JR. and LLOYD T. JENKINS. Pp. x + 371. £8·90.

The first volume in this series of review articles on evaluation of polymers dealt mainly with differential thermal analysis and thermogravimetric analysis. This second volume is also concerned with thermal characterization techniques but of a more specialized nature. These include differential scanning calorimetry, pyrolysis–gas chromatography for polymer identification, stress-strain temperature relations, torsional braid analysis, thermal conductivity and electrothermal analysis of polymers. The references in most chapters go to 1967. It is a useful book, particularly for those interested in practical applications. The chapter on pyrolysis–gas chromatography is somewhat overshadowed by Volume 3 in the series which deals exclusively with this technique.

Electroanalytical Chemistry, Volume 4: ED. ALLEN J. BARD. Marcel Dekker, New York, 1970. Pp. 327. $18.75; £8·90.

Three aspects of the study of electrode reactions are discussed in rigorous mathematical terms, with the mathematical relationships frequently illustrated in graphical form, showing the effect of changing important parameters. This certainly helps the average reader to appreciate the point of the argument. In all three chapters due attention is paid to practical details such as the instrumentation required, and examples from the recent literature are quoted. The topics covered are "Sine wave methods in the study of electrode processes" by Margaretha Sluyters-Rehbach and Jan H. Sluyters, "Theory and practice of electrochemistry with thin-layer cells" by A. T. Hubbard and F. C. Anson, and "Application of controlled potential coulometry to the study of electrode reactions" by A. J. Bard and K. S. V. Santhanam. A good starting point for the research worker who wants to use one of these techniques.

Masking and Demasking of Chemical Reactions: D. D. PERRIN. Wiley-Interscience Inc., New York, 1970. Pp. 211. $12.95.

Most of us have quite large funds of chemical information which can sometimes be recalled in time of need. This book is indeed a treasury of such useful information, and a reading will, I am sure, both remind the analyst of things which he thought he once knew and also tell him much more. For this reviewer several current problems were solved in a few hours, and he is more than grateful to Dr. Perrin for writing such a book. Eleven chapters deal with aspects of complexation reactions in different branches of analytical chemistry (titrimetry, spectrophotometry, electroanalytical chemistry, etc.) and each includes a selection of useful references—by no means complete, but that would be out of the question in such a book. Chapters on Industrial and Biological Applications present a rather different picture, and apart from being interesting reading, will be of direct use to those concerned with the analysis of related materials. A most welcome addition to the laboratory bookshelf.

Electrochemical Reactions in Nonaqueous Systems: CHARLES K. MANN and KAREN K. BARNES. Marcel Dekker, New York, 1970. Pp. 560. $34.50; £16·40.

The size of this book and the immense amount of electrochemical data, mainly for organic compounds, which it contains are a indication of the activity in this field at present. Research workers interested in organic electrochemistry will find this an easy to use and valuable reference book both for its discussions on reaction mechanisms and for its very extensive complications of half-wave potentials. There is one chapter dealing with organometallic compounds, and also one on inorganic compounds.

SUMMARIES FOR CARD INDEXES

Role of solution equilibria in atomic-absorption spectroscopy: P. E. THOMAS and W. F. PICKERING, *Talanta*, 1971, **18**, 127. (Department of Chemistry, University of Newcastle, N.S.W. 2308.)

Summary—The interference effects observed in a series of absorption studies using nitrous oxide/acetylene or air/acetylene flames are interpreted in terms of the nature of the chemical species present in solution. The elements studied include Nb, Ta, Ti, Y, V, W and Ni, and species shown to influence the atomic absorption include hydrofluoric, phosphoric and sulphuric acids, the ions of Ca, K, Al, Fe and Mn, and compounds such as EDTA and ammonium acetate.

Reaktionsstufen-Coulometrie—I. Theoretische Prinzipien: PETER GRÜNDLER and HEINZ HOLZAPFEL, *Talanta*, 1971, **18**, 139. (Sektion Chemie der Karl-Marx-Universität, 701 Leipzig, D.D.R.)

Summary—Differences in the kinetic behaviour of two substances in solution are exploited to allow the determination of both with a common titrant generated coulometrically at constant current. Concentration-time curves for the case of two oxidants in admixture are derived theoretically, and the necessary conditions to be met by the rate constants for the two substances in order to satisfy analytical requirements, and also the effect of amperometric indication on the shape of the experimental curves, are discussed.

Reaktionsstufen-Coulometrie—II. Analytische Untersuching von Stoffgemischen: PETER GRÜNDLER and HEINZ HOLZAPFEL, *Talanta*, 1971, **18**, 147. (Sektion Chemie der Karl-Marx-Universität, 701 Leipzig, D.D.R.)

Summary—Mixtures of cerium(IV) and chlorate, and of hypochlorite and chlorate have been analysed by titration with titanium(III) generated coulometrically at a mercury cathode in acidic chloride solution. The concentration-time curves were recorded with amperometric or biamperometric indication respectively. The rate of reduction of chlorate was modified by the addition of a large amount of strong electrolyte. Loss of chlorine during the titration of hypochlorite was avoided by using a closed electrolysis cell.

РОЛЬ РАВНОВЕСИЙ РАСТВОРЕНИЯ В АТОМНО-АБСОРБЦИОННОЙ СПЕКТРОСКОПИИ:

P. E. Thomas and W. F. Pickering, *Talanta*, 1971, **18**, 127.

Резюме—Обнаруженные в изучении абсорьции помехи, пользуясь пламенами закиси азота (ацетилена или воздуха) ацетилена, истолкованы на основе природы классов химических соединений присутствующих в растворе. Изученные элементы включают Nb, Ta, Ti, Y, V, W и Ni, а соединения влияющие на атомную абсорбцию включают фтороводородную, фосфорную и серную кислоты, ЭДТА и ацетат аммония, и ионы Ca, K, Al, Fe и Mn.

КУЛОНОМЕТРИЯ С ПРИМЕНЕНИЕМ СТУПЕНЕЙ РЕАКЦИЙ—I. ТЕОРЕТИЧЕСКИЕ ОСНОВЫ:

Peter Gründler and Heinz Holzapfel, *Talanta* 1971, **18**, 139.

Резюме—Разници между кинетическим поведением двух веществ в растворе использованы для определения обоих с тем же, кулонометрическим путем произведенным титрованным раствором при константном токе. Теоретическим путем разработаны кривы перемены концентрации с временем и условия констант скорости реакции обоих веществ, необходимые для применения метода в анализе. Изучено влияние амперометрической индикации на форму экспериментальных кривых.

КУЛОНОМЕТРИЯ С ПРИМЕНЕНИЕМ СТУПЕНЕЙ РЕАКЦИЙ—II. АНАЛИЗ СМЕСЕЙ ВЕЩЕСТВ:

Peter Gründler and Heinz Holzapfel, *Talanta* 1971, **18**, 147.

Резюме—Смеси церия(IV) и хлората и смеси гипохлорита и хлората анализированы титрованием с титаном(III), образованным кулонометрическим путем на ртутном катоде в кислом растворе хлорида. Кривые перемены концентрации с временем записаны с применением амперометрической или биамперометрической индикации, соответственно. Скорость восстановления хлората изменена добавлением раствору большего количества сильного электролита. Потери хлора при титровании гипохлорита избегнуты использованием замкнутой ячейки для электролиза.

Molecular emission characteristics of various fluorides in a low-temperature diffusion flame: R. M. Dagnall, B. Fleet, T. H. Risby and D. R. Deans, *Talanta*, 1971, **18**, 155. (Chemistry Department, Imperial College of Science and Technology, London, S.W. 7, U.K.)

Summary—A capillary burner supporting a nitrogen/hydrogen diffusion flame has been evaluated as a possible means of detection for several volatile fluorides after their gas-chromatographic separation. The fluorides of As, B, C, Ge, I, Mo, P, Re, S, Sb, Se, Si, Te and W were formed by the reaction of the element with chlorine trifluoride, and the intense molecular emission given by each was recorded. An attempt was made to identify the emitting species.

Massenspektrometrische Untersuchungen zur Elementaranalyse organischer Verbindungen—I. Einlaßsystem zur Analyse von Gasgemischen in großen Temperatur- und Druckbereichen: Walter Walisch and Ottokar Jaenicke, *Talanta*, 1971, **18**, 165. (Institut für Organische Chemie, Universität des Saarlandes, 66 Saarbrücken, B.R.D.)

Summary—It has been shown that a single-stage, viscous inlet system ensures under certain conditions accurate proportionality between the partial pressures of the components in a sample at normal pressure and the corresponding ion currents. The main condition is that the viscosity of the mixture does not change with the composition; this is nearly always the case when one of the components is present in large excess as carrier gas. An equation has been derived which describes the behaviour of this "quantitative" inlet system. Experimental testing has confirmed the validity of this inlet equation and demonstrates, moreover, the wide range of application of this simple and rapid inlet system, consisting usually of a quartz capillary.

Massenspektrometrische Untersuchungen zur Elemenaranalyse Organischer Verbindungen—II. Bestimmung von Verbrennungsprodukten im Trägergasstrom durch Peakintegration: Ottokar Jaenicke and Walter Walisch, *Talanta*, 1971, **18**, 175. (Institut für Organische Chemie, Universität des Saarlandes, 66 Saarbrücken, B.R.D.)

Summary—The organic sample is ignited in the oxygen carrier gas in an empty "jet" tube. The products of combustion flow at constant speed past the inlet capillary which is linked to the mass spectrometer. The output voltage from the mass spectrometer, set at the mass of one combustion product, is fed to an integrator. The integral measured is proportional to the amount of the combustion product. If combustion of the element under consideration yields a single product, the amount of this element in the organic compound can be calculated from the peak integral and the weight of sample. Several elements can be determined simultaneously by using a mass spectrometer with several collectors. The control data quoted show that the procedure is fundamentally suitable for elementary analysis but that the reproducibility is not quite good enough.

ХАРАКТЕРИСТИКИ МОЛЕКУЛЯРНОЙ ЭМИССИИ РАЗЛИЧНЫХ ФТОРИДОВ В ДИФФУЗИОННОЙ ПЛАМЕНИ НИЗКОЙ ТЕМПЕРАТУРЫ:

R. M. Dagnall, B. Fleet, T. H. Risby and D. R. Deans, *Talanta*, 1971, **18**, 155.

Резюме—Испытана капиллярная горелка для диффузионной пламени азота-водорода для обнаружения некоторых летучих фторидов после их газо-хроматографического разделения. Фториды As, B, C, Ge, I, Mo, P, Re, S, Sb, Se, Si, Te и W образованы реакцией элемента с трифторидом хлора и записана интенсивная молекулярная эмиссия этих соединений. Сделана попытка идентифицировать испускающие соеднения.

ПРИМЕНЕНИЕ МЕТОДА МАСС-СПЕКТРОМЕТРИИ В ИССЛЕДОВАНИИ ЭЛЕМЕНТАРНОГО АНАЛИЗА ОРГАНИЧЕСКИХ СОЕДИНЕНИЙ:—I. СИСТЕМА ВВЕДЕНИЯ ДЛЯ АНАЛИЗА СМЕСЕЙ ГАЗОВ В ШИРОКОМ ДИАПАЗОНЕ ТЕМПЕРАТУР И ДАВЛЕНИЙ:

Walter Walisch and Ottokar Jaenicke, *Talanta*, 1971, **18**, 165

Резюме—Показано что одноступеньчатая вязкая система обеспечивает при известных условиях точную пропорциональность парциальных давлений компонентов образца при нормальном давлении и соответствующих ионных токах. Главное условие системы что вязкость смеси не надо изменяться с составом; это условие удоволено в большинстве случаев, когда один из компонентов присутствует в большом избытке в качестве газа носителя. Выведено уравнение выражающее поведение этой «количественной» системы введения пробы. Опыты подтвердили обоснованность этого уравнения и показали применимость в широком диапазоне этой несложной и быстрой системы введения, состоящейся обычно из кварцевого капилляра.

ПРИМЕНЕНИЕ МЕТОДА МАСС-СПЕКТРОМЕТРИИ В ИССЛЕДОВАНИИ ЭЛЕМЕНТАРНОГО АНАЛИЗА ОРГАНИЧЕСКИХ СОЕДИНЕНИЙ—II. ОПРЕДЕЛЕНИЕ ПРОДУКТОВ СЖИГАНИЯ В ГАЗЕ-НОСИТЕЛЕ ПУТЕМ ИНТЕГРАЦИИ ПИКОВ:

Ottokar Jaenicke and Walter Walisch, *Talanta*, 1971, **18**, 175.

Резюме—Органическую пробу сжигают в кислороде (газеносителе) в пустой «струйной» трубке. Продукты сжигания протекают с константной скоростью мимо капиллярного впуска, соединенного с масс-спектрометром. Выходное напряжение из масс-спектрометра, установленное на массу одного из продуктов сжигания подают на интегратор. Измеренный интеграл пропорционален количеству продукта сжигания. Если сжигание исследованного элемента дает только один продукт, количество этого элемента в органическом соединении можно рассчитать из интеграла пика и навески пробы. Применение масс-спектрометра с рядом коллекторов позволяет определять одновременно несколько элементов. Приведенные данные показывают что этот метод в основе применимый в элементарном анализе, но что воспроизводимость не удовлетворяет требованиями.

Spectrophotometric determination of the protolytic dissociation constants of the new chromogenic reagent "Palladiazo"—I. Investigations with sodium hydroxide, perchloric acid and different aqueous buffer solutions: J. A. Pérez-Bustamante and F. Burriel-Martí, *Talanta*, 1971, **18**, 183. (Consejo Superior de Investigaciones Científicas, Departamento de Química Analítica, Universidad de Madrid, Facultad de Ciencias, Ciudad Universitaria, Madrid—3, Spain.)

Summary—The "palladiazo" reagent has been subjected to a detailed spectrophotometric investigation in concentrated perchloric acid, different aqueous buffers and concentrated sodium hydroxide solutions. K_1–K_{10} and ϵ_1–ϵ_{10} values corresponding to the instability constants of the protolytic equilibria involved and to the molar absorptivities at 540 and 630 nm of the different proton complex species of the system have been calculated by a number of analytical and graphical spectrophotometric methods. Special attention has been paid to the study of the complicated phenomena implied by the interaction of the reagent with perchloric acid, which has been shown to give rise to alteration of the initial isomeric composition of the reagent and to the formation of addition and/or oxidation products derived from side-reactions undergone by the reagent with the medium All the instability constants and molar absorptivities, which have been determined by several methods, are tabulated for comparison.

Extraction and separation of ^{137}Cs and ^{86}Rb by means of 4-t-butyl-2-(α-methylbenzyl)phenol: J. Rais, J. Krtil and V. Chotívka, *Talanta*, 1971, **18**, 213. (Institute of Nuclear Research, Řež near Prague, Czechoslovakia.)

Summary—The extraction of caesium-137 and rubidium-86 by a solution of 4-t-butyl-2(α-methylbenzyl)phenol in n-octane and tetrachloromethane has been investigated. The separation of rubidium and caesium has been performed by the Craig method and by reversed-phase extraction chromatography.

Microdetermination of nitrates and nitrites—III. Gasometric and gravimetric methods based on reduction with formic acid: W. I. Awad, S. S. M. Hassan and M. T. M. Zaki, *Talanta*, 1971, **18**, 219. (Research Microanalytical Laboratories, Chemistry Department, Faculty of Science, Ain Shams University, Cairo, U.A.R.)

Summary—Simple microgasometric and gravimetric methods for the determination of the nitrate and nitrite groups are described. These are based on reduction with formic acid whereby one mole of nitrous oxide and four moles of carbon dioxide are simultaneously liberated per two moles of nitrate; two moles of nitrous oxide and six moles of carbon dioxide are liberated per seven moles of nitrite. Nitrous oxide is measured gasometrically and carbon dioxide gravimetrically. Results accurate to $\pm 0{\cdot}2\%$ absolute are obtained for both nitrate and nitrite.

СПЕКТРОФОТОМЕТРИЧЕСКОЕ ОПРЕДЕЛЕНИЕ ПРОТОЛИТИЧЕСКИХ КОНСТАНТ ДИССОЦИАЦИИ НОВОГО ХРОМОГЕННОГО РЕАГЕНТА «ПАЛЛАДИАЗО»—I. ИЗУЧЕНИЕ С ИСПОЛЬЗОВАНИЕМ ГИДРООКИСИ НАТРИЯ, ХЛОРНОЙ КИСЛОТЫ И РАЗЛИЧНЫХ ВОДНЫХ БУФФЕРНЫХ РАСТВОРОВ:

J. A. PÉREZ-BUSTAMANTE and F. BURRIEL-MARTÍ, *Talanta*, 1971, **18**, 183.

Резюме—Реагент «палладиазо» подвергнут тщательному спектрофотометрическому изучению в концентрированной хлорной кислоте, в различных водных буфферных растворах и в концентрированных растворах гидроокиси натрия. Величины K_1–K_{10} и ε_1–ε_{10}, соответствующие константами неустойчивости и молярными коэффициентами поглощения при 540 и 630 нм различных родов протонных комплексов системы вычислены с применением ряда аналитических и графических спектрофотометрических методов. Особое внимание придано изучению сложных явлений, вызванных взаимодействием реагента с хлорной кислотой. Показано что эта кислота изменяет первоначалный изомерный состав реагента и приводит образованию продуктов присоединения и/или окисления в результате побочных реакций реагента с средой. Все определенные различными методами константы неустойчивости и молярные коэффициенты поглощения приведени для сравнения в форме таблицы.

ЭКСТРАКЦИЯ И РАЗДЕЛЕНИЕ ^{137}Cs и ^{86}Rb 4-ТРЕТ-БУТИЛ-2-(α-МЕТИЛБЕНЗИЛ) ФЕНОЛОМ:

J. RAIS, J. KRTIL and V. CHTIVKA, *Talanta*, 1971, **18**, 213.

Резюме—Изучена экстракция цезия-137 и рубидия-86 раствором 4-трет-бутил-2(α-метилбензил) фенола в н-октане и тетрахлорметане. Разделение рубидия и цезия проведено методом Крейга и методом экстракционной хроматографии с обратной фазой.

МИКРООПРЕДЕЛЕНИЕ НИТРАТОВ И НИТРИТОВ—III. ГАЗОМЕТРИЧЕСКИЕ И ВЕСОВИЕ МЕТОДЫ ОСНОВАНЫ НА ВОССТАНОВЛЕНИИ МУРАВЬИННОЙ КИСЛОТОЙ:

W. I. AWAD S. S. M. HASSAN and M. T. M. ZAKI, *Talanta*, 1971, **18**, 219.

Резюме—Описаны несложные микрогазометрические и весовие методы определения нитрат- и нитритгруппы. Методы основаны на восстановлении муравьинной кислотой, при чём выделяются одновременно один моль закиси азота и четыре моля двуокиси углерода из двух молей нитрата. Два моля закиси азота и шесть молей двуокиси углерода выделяются из семь молей нитрита. Закись азота измеряют газометрическим путем, а двуокись углерода—весовым методом. Точность результатов полученных для нитрата и нитрита ±0,2 % абс.

Solvent extraction and spectrophotometric determination of palladium(II) with 7-iodo-8-hydroxyquinoline-5-sulphonic acid: TEJ SINGH and ARUN K. DEY, *Talanta*, 1971, **18**, 225. (Chemical Laboratories, University of Allahabad, Allahabad, India.)

Summary—An extractive spectrophotometric procedure has been developed for the determination of palladium (II) at microgram levels. The palladium(II) chelate of 7-iodo-8-hydroxyquinoline-5-sulphonic acid is extracted into n-butanol. Extraction is maximal (95%) from 0.2*M* perchloric acid. Beer's law is valid at 430 nm over a wide range of palladium concentration from 2.5 ppm. The molar absorptivity is 958 $1.mole^{-1}.mm^{-1}$. The system can tolerate a large excess of Co(II), Ni(II), Rh(III), Pt(IV), Cr(III), W(VI), chloride, phosphate, citrate and tartrate. Small quantities of Ru(III), Ir(III) and EDTA do not interfere, but serious interference is caused by Fe(III), V(V), Mo(VI) and Os(VIII).

Spectrophotometric determination of traces of antimony: VĚRA STARÁ, *Talanta*, 1971, **18**, 228. (Laboratory of Analytical Chemistry, J. Heyrovský Polarographic Institute, Czechoslovak Academy of Science, Praha 1, Jilská 16, Czechoslovakia.)

Summary—Antimony(III) is extracted into carbon tetrachloride from 4*M* sulphuric acid that is 0.05*M* in potassium iodide. 8-Mercaptoquinoline and acetone are added to the organic extract and the absorbance of the complex formed is measured at 390 nm. Repeating the extraction procedure greatly increases the selectivity of the method.

Colorimetric determination of pyrogallol and 2,6-dimethoxyphenol with diphenylpicrylhydrazyl: GEORGE H. SCHENK and NANCY K. SWIECSKOWSKI, *Talanta*, 1971, **18**, 230. (Department of Chemistry, Wayne State University, Detroit, Michigan 48202, U.S.A.)

Summary—A colorimetric study was made of the reactions of the free radical 2,2-diphenyl-1-picrylhydrazyl (DPPH) and the phenols pyrogallol and 2,6-dimethoxyphenol. Both of these phenols were colorimetrically determined by use of DPPH, in the presence of various interferences. It was shown that the determination of pyrogallol and 2,6-dimethoxyphenol was more accurate when absolute ethanol was used than with 95% ethanol. It was also shown that the best results were obtained when the ratio of phenol to interferent was no greater than 1:1.

Determination of zinc in copper by atomic-fluorescence flame spectroscopy: P. D. WARR, *Talanta*, 1971, **18**, 234. (The General Electric Company Limited, Central Research Laboratories, Hirst Research Centre, Wembley, England.)

Summary—The application of atomic-fluorescence flame spectroscopy to the determination of trace quantities of zinc in copper is described. A limit of detection of 10^{-5}% zinc in copper has been established. The scatter of primary radiation from within the flame determined the limit of detection, but it is suggested that scatter is not a serious limitation to the practical application of the technique.

ЭКСТРАКЦИОННО-СПЕКТРОФОТОМЕТРИЧЕСКИЙ МЕТОД ОПРЕДЕЛЕНИЯ ПАЛЛАДИЯ(II) С ИСПОЛЬЗОВАНИЕМ 7-ИОДО-8-ОКСИХИНОЛИН-5-СУЛЬФОНОВОЙ КИСЛОТЫ:

Tej Singh and Arun K. Dey, *Talanta*, 1971, **18**, 225.

Резюме—Разработан экстракционно-спектрофотометрический метод определения микрограммовых количеств палладия(II). Хелат палладия(II) с 7-иодо-8-оксихинолин-5-сульфоновой кислотой экстрагируют н-бутанолом. Максимальную экстракцию (95%) получают из 0,2М хлорной кислоты. Закон Бера почитается при 430 нм в широком диапазоне концентраций палладия от 2,5 мкг/мл. Молярное поглощение равно 958 л.моль$^{-1}$.мм$^{-1}$. Система позволяет большие избыткд Co(II), Ni(II), Rh(III), Pt(IV), Cr(III), W(VI), хлорида, фосфата, цитрата и тартрата. Небольшие количества Ru(III), Ir(III) и ЭДТА не влияют на определение, но Fe(III), V(V), Mo(VI) и Cs(VIII) сильно мешают определению.

ОПРЕДЕЛЕНИЕ СЛЕДОВ СУРЬМЫ СПЕКТРОФОТОМЕТРИЧЕСКИМ МЕТОДОМ:

Vera Stara, *Talanta*, 1971, **18**, 228.

Резюме—Сурьму(III) экстрагируют тетрахлорметаном из 4М раствора серной кислоты содержащего 0,05М иодида калия. Органическому экстракту добавляют 8-меркаптохинолин и ацетон и измеряют светопоглощение образованного комплекса при 390 нм. Повторение экстракции сильно повышает селективность метода.

КОЛОРИМЕТРИЧЕСКОЕ ОПРЕДЕЛЕНИЕ ПИРОГАЛЛОЛА И 2,4-ДИМЕТОКСИФЕНОЛА С ИСПОЛЬЗОВАНИЕМ ДИФЕНИЛПИКРИЛГИДРАЗИЛА:

George H. Schenk and Nancy K. Swiecskowski, *Talanta*, 1971, **18**, 230.

Резюме—Изучены колориметрическим методом реакции свободного радикала 2,2-дифенил-1-пикрилгидразила (ДФПГ) с пирогаллолом и 2 6-диметоксифенолом. Оба фенола определены колориметрическим методом с использованием дФПГ, в присутствии разных мешающих веществ. Показано что определение пирогаллола и 2,6-диметоксифенола точнее в присутствии абсолютного спирта чем в присутствии 95%-ного спирта. Самые лучшие результаты получены когда отношение фенола к мешающем веществу не превышало 1:1.

ОПРЕДЕЛЕНИЕ ЦИНКА В МЕДИ МЕТОДОМ АТОМНО-ФЛУОРЕСЦЕНТНОЙ СПЕКТРОСКОПИИ:

P. D. Warr, *Talanta*, 1971, **18**, 234.

Резюме—Описано применение метода атомно-флуоресцентной спектроскопии в определении следовых количеств цинка в меди. Получена чувствительность 10^{-5}% цинка в меди. Чувствительность определена рассеянием первичного излучения из пламени, но выражено мнение что рассеяние не представляет собой серьезное ограничение для применения метода в практике.

ELECTROCHIMICA *Acta*

Editor-in-Chief: DR T P HOAR, Cambridge

Electrochimica Acta is published by Pergamon Press Ltd under the auspices of the International Committee for Electrochemical Thermodynamics and Kinetics (CITCE).

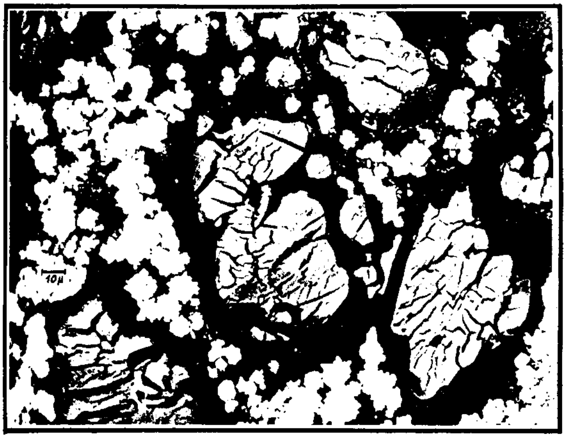

Microphotograph of a DSK working layer.

Executive Editorial Board:
DR T P HOAR
University of Cambridge, England
PROFESSOR J O'M BOCKRIS
University of Pennsylvania, USA
PROFESSOR N IBL
Swiss Federal Institute of Technology, Zurich, Switzerland
PROFESSOR P Van RYSSELBERGHE
Stanford University, USA
PROFESSOR G VALENSI
Faculté des Sciences de Poitiers, France

This is an international journal of pure and applied electrochemistry, publishing papers on every aspect of this subject. More than two hundred papers are presented each year, either in the form of original reports or as serious, critical reviews. Electrochimica Acta thus provides a comprehensive up-to-date coverage of current activity throughout the rapidly expanding field of electrochemistry.

The following papers appear in Volume 14 Number 10 of Electrochimica Acta:
H B URBACH and R J BOWEN:
Behaviour of the oxygen-peroxide couple on platinum
I FRIED and E SHAMIR:
A unified mathematical treatment of diffusion-controlled voltammetric processes
A WINSEL:
Flow rate and pressure drop of gas mixtures and electrolyte in gas-diffusion electrodes
C WAGNER:
Current yield during electrolysis of metal salt solutions with cations in different valency states
R D COWLING and A C RIDDIFORD:
The anodic behaviour of cobalt in alkaline solutions
T IWASITA and M C GIORDANO:
Kinetics of the bromine-tribromide-bromide redox processes on platinum electrodes in acetonitrile solutions

Published monthly

Please write now for full details of subscription rates, a free inspection copy and information on other related Pergamon publications.

Pergamon Press
OXFORD · NEW YORK · LONDON · PARIS · SYDNEY

Volume 18, No. 2   February 1971

Contents

Short Communications

Talanta Annual Subscription Rates (including postage)

$10 (£3.50.)—*Bona fide* students

$90 (£36)—Multiple-reader institutions

Private individuals whose departmental libraries subscribe, may obtain this journal for their pe
use at a reduced rate of $25 (£8) per annum.

Printed in Northern Ireland at The Universities Press, Belfast